GEAEP-66

JPL NO 3950

A CONCEPTUAL DESIGN STUDY OF A HIGH TEMPERATURE SOLAR THERMAL RECEIVER

FINAL REPORT

Contract No. 955455

January 4, 1980

Prepared for

JET PROPULSION LABORATORY
CALIFORNIA INSTITUTE OF TECHNOLOGY
Pasadena, California 91103

GENERAL ELECTRIC
ADVANCED ENERGY DEPARTMENT
EVENDALE OPERATIONS
CINCINNATI, OHIO 45215

FINAL REPORT

A CONCEPTUAL DESIGN STUDY OF A HIGH TEMPERATURE SOLAR THERMAL RECEIVER

by

CS ROBERTSON, CL EHDE, LE STACY, SS ABUJAWDEH
R. NARAYANAN, LR McCREIGHT, A. GATTI, AND HW RAUCH, SR.

for

JET PROPULSION LABORATORY
CALIFORNIA INSTITUTE OF TECHNOLOGY
PASADENA, CALIFORNIA 91103

M.L. PEELGREN
PROGRAM MANAGER

CONTRACT NO. 955455

JANUARY 4, 1980

GENERAL ELECTRIC
ADVANCED ENERGY DEPARTMENT
EVENDALE OPERATIONS
CINCINNATI, OHIO 45215

"This work was performed for the Jet Propulsion Laboratory, California Institute of Technology sponsored by U.S. Department of Energy through an agreement with the National Aeronautics and Space Administration."

ABSTRACT

A conceptual design has been made for a solar thermal receiver capable of operation in the 1095-1650°C (2000-3000°F) temperature range. This receiver is designed for use with a two-axis parabaloidal concentrator in the 25 to 150 kW_{th} power range, and is intended for industrial process heat, Brayton engines, or chemical/fuels reactions. Three concepts were analyzed parametrically. One was selected for conceptual design. Its key feature is a helical coiled tube of sintered silicon nitride which serves as the heat exchanger between the incident solar radiation and the working fluid. A mechanical design of this concept was prepared, and both thermal and stress analysis performed. The analysis showed good performance, low potential cost in mass production, and adaptability to both Brayton cycle engines and chemical/fuels production.

TABLE OF CONTENTS

Page No.

Page No.

LIST OF FIGURES

LIST OF TABLES

SECTION I

SUMMARY

The objective of this program was to conduct studies and analyses resulting in a recommended conceptual design of an advanced solar receiver for industrial processes and high temperature applications. This receiver design is intended for potential use with two-axis paraboloidal concentrators in the 25-150 kW_t input power range. Potential applications include advanced Brayton cycle engines, chemical transport, and fuels or chemical production.

At the inception of the program, a parametric analysis of three promising concepts was made. All utilized ceramic materials in order to meet the goals of high efficiency and potential low cost in mass production while operating in the 1095-1650°C (2000-3000°F) temperature range with air, helium, or nitrogen as working fluids. The first concept utilized a coiled tube heat exchanger made of sintered silicon nitride located in an annulus between a ceramic cylinder on the inside and the insulation on the outside. The ceramic cylinder forms the receiver cavity and receives the solar flux. The second concept uses a ceramic matrix much like an automotive gas turbine rotary regenerator as the heat exchanger. This matrix is located in a pressurized cavity and the solar flux enters through a fused silica window. The third concept resembles the first with the exception of the heat exchanger, which now consists of a ceramic tube and header design. The parametric analysis resulted in preliminary performance calculations, materials selections, weight, cost, and size data, and an assessment of the capability for short-term thermal energy storage.

At the conclusion of the parametric analysis the first concept using the helical coiled tube heat exchanger was selected for conceptual design. A Brayton cycle application was selected using air at three atmospheres pressure, 1371°C (2500°F) exit gas temperature, and a power level of 58 kW. Detailed thermal analysis was performed using two-dimensional finite element techniques. A mechanical design and supporting stress analysis was made, including mechanical drawings. At the conclusion of the conceptual design effort, a complete receiver configuration, backed by supporting analysis, was prepared. The supporting analysis included transient and off-design performance. This work validated the performance and suitability of the design.

An estimate of the unit production cost in large quantities was made, including the processes and equipment needed to produce the helical coiled tube. The potential for low cost in mass production was shown.

It was concluded that this concept provides an attractive, efficient, and low cost approach to a high temperature receiver. The basic

simplicity of the design leads to operational ease and low maintenance. The receiver can be adapted to direct chemical reactions. The only component not commercially available is the helical coiled tube. Only the size of this part is beyond the present state-of-the-art. The material and processes exist in smaller sizes.

It is recommended that a feasibility demonstration of the fabricability of the silicon nitride helical coiled tube be made. Following a successful demonstration, a full size receiver should be designed, built, and tested.

SECTION II

INTRODUCTION

A. OBJECTIVES

The objective of this contract was to conduct studies and analyses resulting in a recommended conceptual design of a solar receiver for industrial processes and high temperature applications. This receiver design is intended for potential use with a two-axis paraboloidal concentrating collector in the 25-150 kW_t power range. Potential applications include advanced Brayton cycle engines, chemical transport, and chemical production.

The use of solar energy for such high temperature applications requires the development of solar receivers which make use of advanced technology to achieve the goals of high efficiency and potentially low-cost mass producibility. The temperature requirements of this contract, between 1095°C (2000°F) and 1650°C (3000°F), are well above the capability of current concepts. This temperature range, as well as the use of air, nitrogen, or helium above atmospheric pressure tend to eliminate many useful lower-temperature concepts and materials from serious considerations. Metallic materials for use at these temperatures, when applicable, tend to be expensive, not readily available, and hard to machine. Conversely, it appears that by making use of ceramic materials receivers can be designed which will meet the technical and cost objectives.

Prior work had identified approximately a dozen different receiver concepts which were evaluated for suitability for this program. An attractive concept was identified, along with two potential alternates. In this program these three concepts were investigated. Their performance and potential for low-cost mass producibility was determined. One of these concepts was chosen to be the subject of a thorough conceptual design study. Operational and performance requirements associated with this design were characterized. Finally, production cost estimates were prepared.

The program was organized into five tasks.

- Task 1 - Parametric Analysis
- Task 2 - Conceptual Design
- Task 3 - Receiver Operation and Performance Requirements
- Task 4 - Production Cost Estimates
- Task 5 - Documentation and Briefings

B. SCOPE

The parametric analysis task involved three distinct concepts, which were evaluated over the range of parameters shown in Table 2-1.

Table 2-1. Guidelines and Constraints

- Designed for Use With a Two-Axis Paraboloidal Tracking Concentrator
- Design Boundaries:

- Working Fluids:	Helium, Nitrogen and Air
- Receiver Outlet Temperature	1200-1650°C (2200-3000°F)
- Inlet-Outlet Temperature Rise:	110-333°C (200-600°F)
- Pressure Level:	2-8 Atmosphere
- Pressure Drop:	Less than 4% $\Delta P/P$
- Power Level:	25-150 kW
- Flux Distributions:	Characteristic of High Performance Collectors, i.e., 1-2 mrad Slope Error

- Design Goals:

- High Performance:	High Efficiency
- Low Cost:	Potential for Low Cost in Mass Production

At the end of this task, one of the concepts was selected for conceptual design.

Directions were given by JPL to design the receiver for use with an advanced Brayton cycle engine. Table 2-2 shows these requirements.

Table 2-2. Design Point Requirements and Analysis Results

DESIGN REQUIREMENTS

Working fluid	Air
Inlet gas temperature	950°C (1750°F)
Exit gas temperature	1370°C (2500°F)
Pressure level	0.31 MPa (45 psia)
Mass flow rate	0.113 kg/sec (0.25 lb/sec)
Maximum pressure drop	4% $\Delta P/P$
Concentrator slope error	2 mrad

The resulting concept was analyzed for thermal performance, mechanical drawings were prepared, and stress analysis of the design performed. A limited amount of effort was spent determining the concepts applicability to chemical reactions and fuels production. Receiver operations and operational requirements were determined.

The suitability for low-cost mass production was evaluated, and production cost estimates prepared. Key design features leading to low cost were described.

The end result of this program was a conceptual design of a potentially low-cost receiver with relatively high performance in the high temperature range required.

C. CONCEPTS EVALUATED

Three concepts were selected for evaluation in the parametric analysis task. These included the most attractive one identified in earlier work as well as two other attractive concepts. It was the intent of this work to analyze them in sufficient detail to allow an intelligent choice between them for further conceptual design.

1. Helical Coiled Tube Concept

Figure 2-1 shows an early version of this concept. The key feature is the use of a single helical coiled tube of high temperature ceramic. This tube acts as the pressure containing heat exchanger. It requires only two joints to connect to the external equipment, and is simple in shape for good mechanical strength. An opaque sleeve of high temperature ceramic located inside the helix performs two important functions. First, it serves to protect the helix from direct solar insolation and thus reduce the thermal shock on the helix. Since the sleeve does not have to be gas-tight or support pressure loads, it can be designed solely to withstand thermal shock. Second, this sleeve provides a small amount of thermal energy storage. The remainder of the receiver is constructed out of insulation, ceramic support forms, and sheet metal.

2. Matrix Heat Transfer Concept

The second concept evaluated is shown in Figure 2-2. Its key feature is the use of a honeycomb type matrix as the heat exchanger. This component is much like the ceramic rotary regenerators being developed for automotive gas turbines. The use of this concept above atmospheric pressure requires two additional features which characterize this concept. One is a transparent window to allow the solar flux to enter the pressurized gravity. The other is the pressurization of the entire cavity and insulation to allow the pressure stress to be carried by a cool outer steel vessel.

3. Tube and Header Concept

The third concept, shown in Figure 2-3, uses a heat exchanger composed of two toroidal headers connected by many hairpin-shaped smaller tubes. It is similar to the first concept except for the different style of heat exchanger.

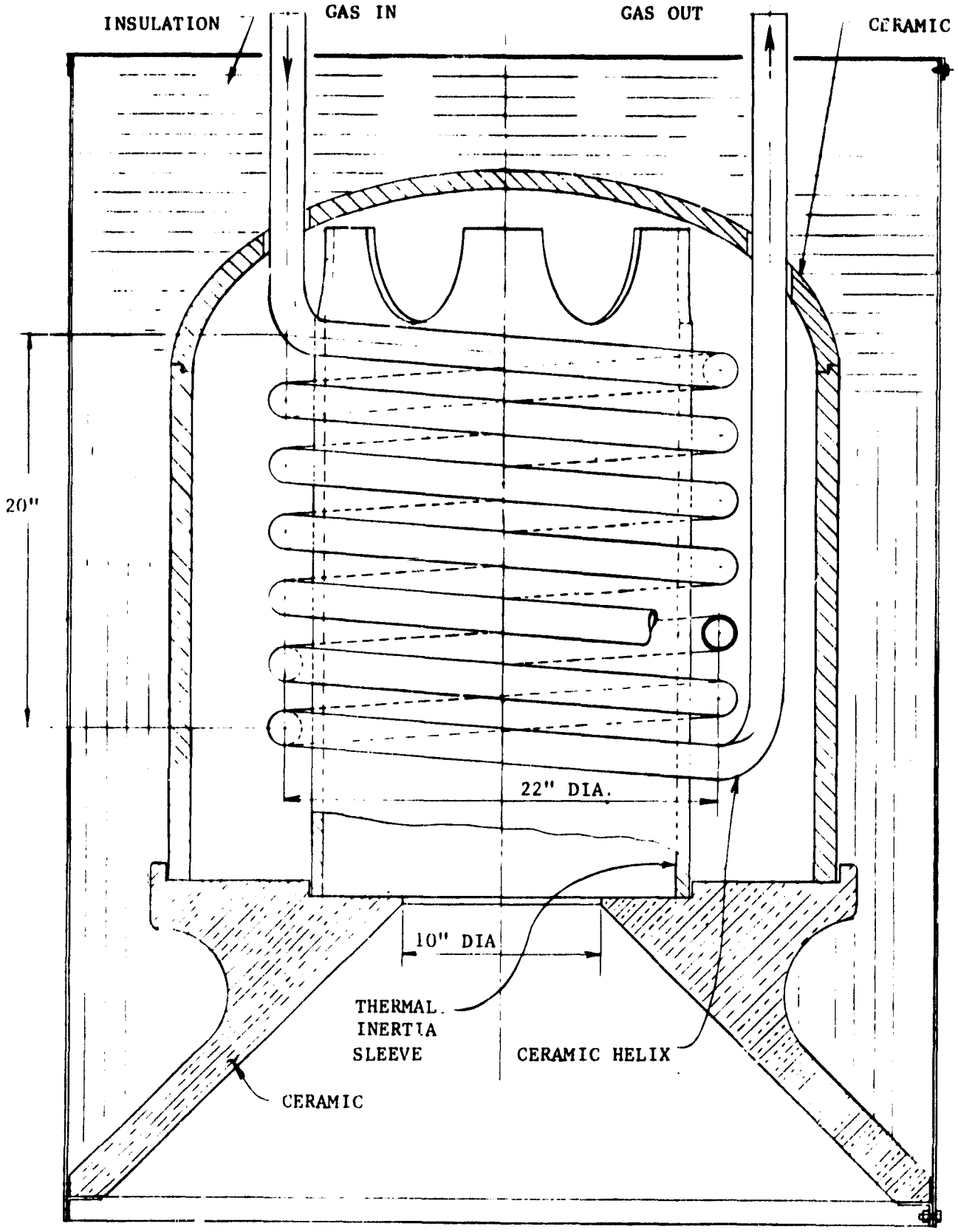

Figure 2-1. Helical Coiled Tube Concept

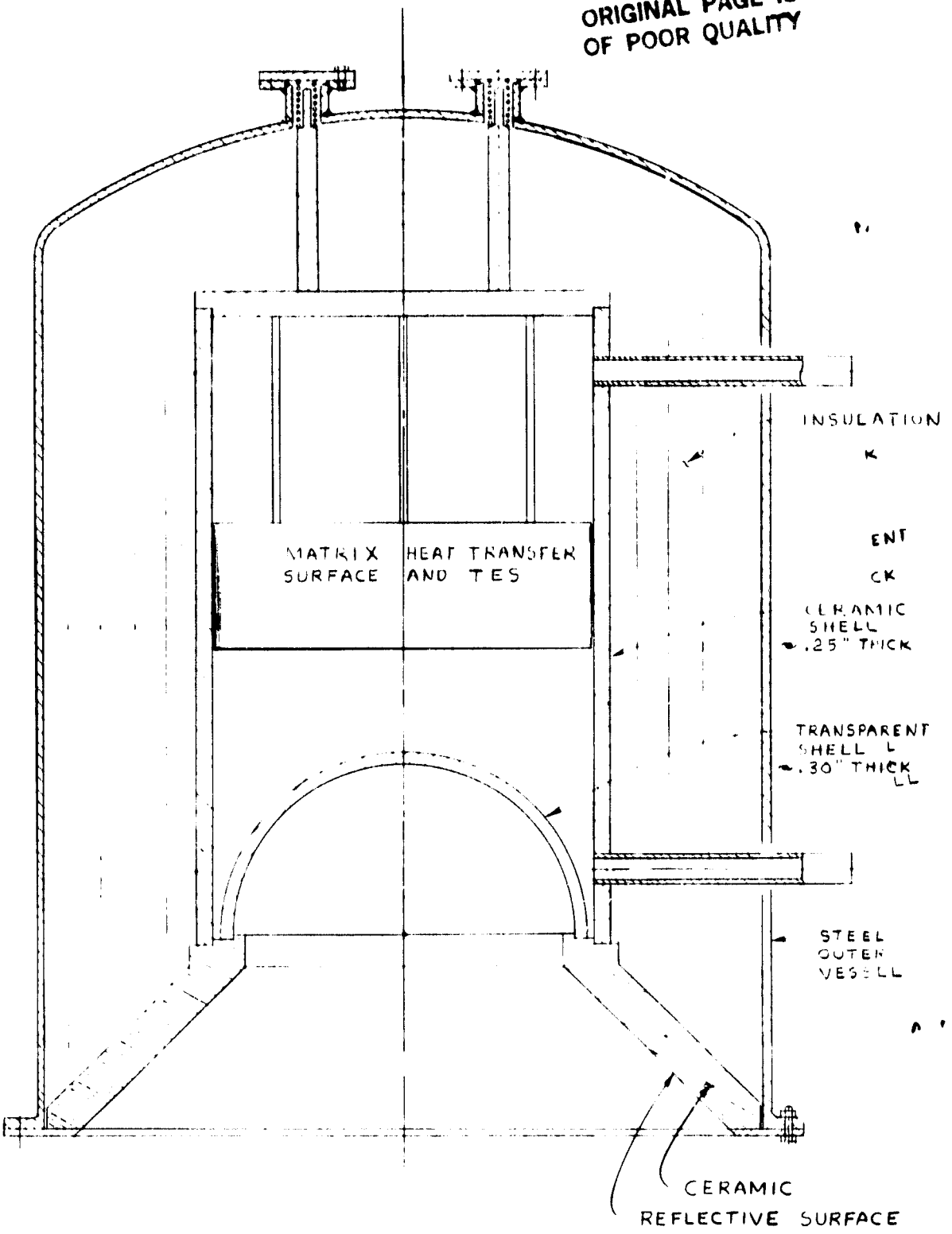

Figure 2-2. Matrix Heat Transfer Concept

ORIGINAL PAGE IS
OF POOR QUALITY

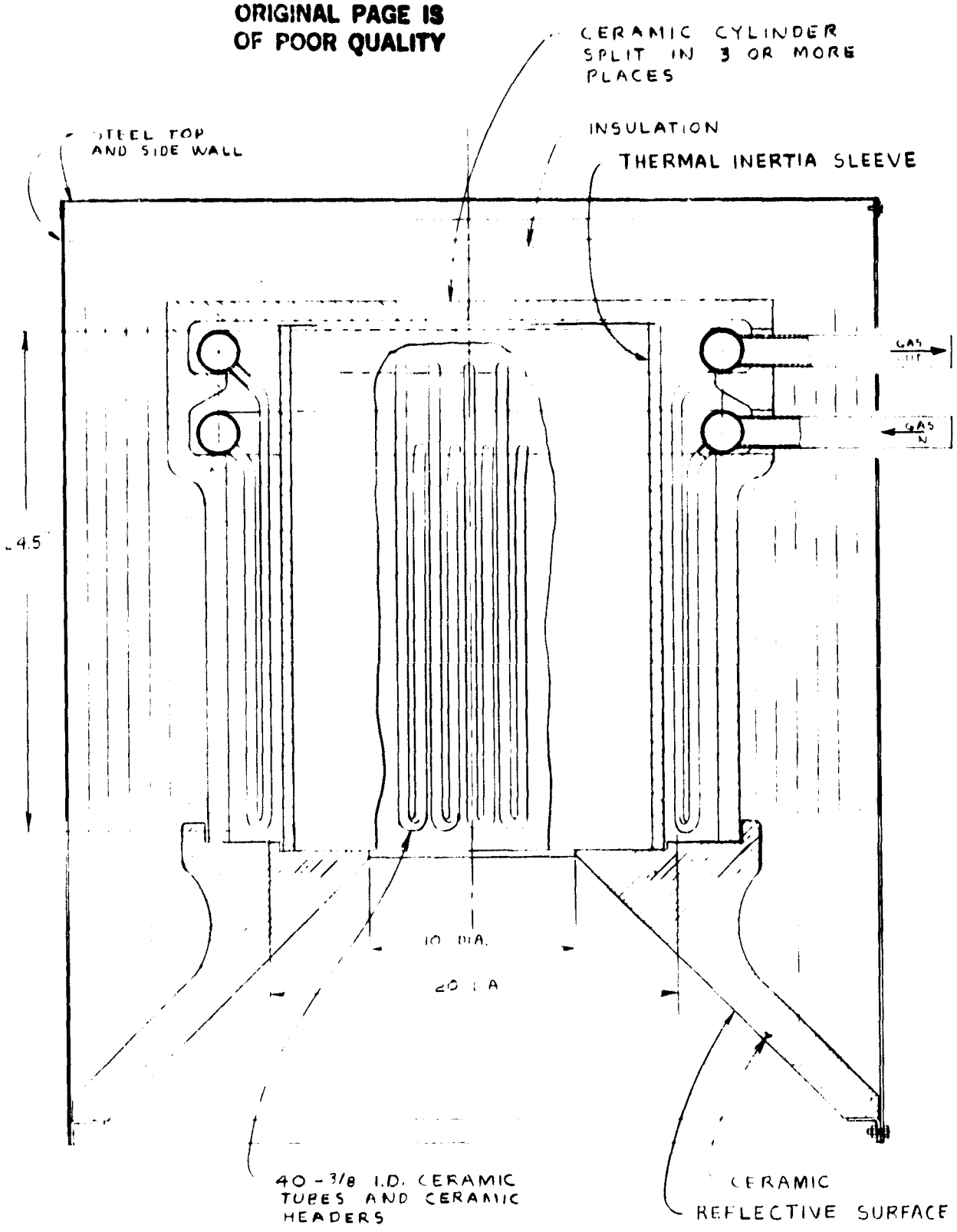

Figure 2-3. Tube and Header Concept

SECTION III

PARAMETRIC ANALYSIS

A. OBJECTIVES

The major objective of this task was to conduct a parametric analysis of the various concepts and design options so as to characterize the system performance for comparison and optimization purposes. The range of parameters investigated was shown in Table 2-1, and involves the operation of the receiver at above atmospheric pressures at temperatures above 1200°C (2200°F).

The results of this task were:

- Preliminary receiver performance calculations showing thermal efficiency, pressure drop, and temperatures of key components.
- Materials selections for key components, based on suitability, availability in required forms, and potential for low cost in mass production.
- Weight, cost, and size of the concepts on a parametric basis.
- An assessment of thermal energy storage feasibility for periods of up to 3 minutes.

Three concepts were evaluated in sufficient detail to determine the advantages and disadvantages of each. At the completion of the task, an evaluation was made to guide the selection of the one concept to be carried into conceptual design.

B. CONCEPTS STUDIED

As discussed in the Introduction, three concepts were studied. Additional engineering sketches were made, and several options investigated. Based on this work, three designs were analyzed. This section of the report describes each in enough detail so that the remainder of the discussion of results will be clear.

1. Helical Coiled Tube Concept (Concept No. 1)

Figure 3-1 shows a cross section of the helical coiled tube concept. The dimensions shown are only for reference, since they are varied during the parametric analysis. Solar radiation impinges on the ceramic thermal inertia sleeve which reradiates to the helix, thus providing a small amount of thermal energy storage and reducing thermal shock to the helix. The helical coil acts as the primary heat exchanger. It contains

ORIGINAL PAGE IS
OF POOR QUALITY

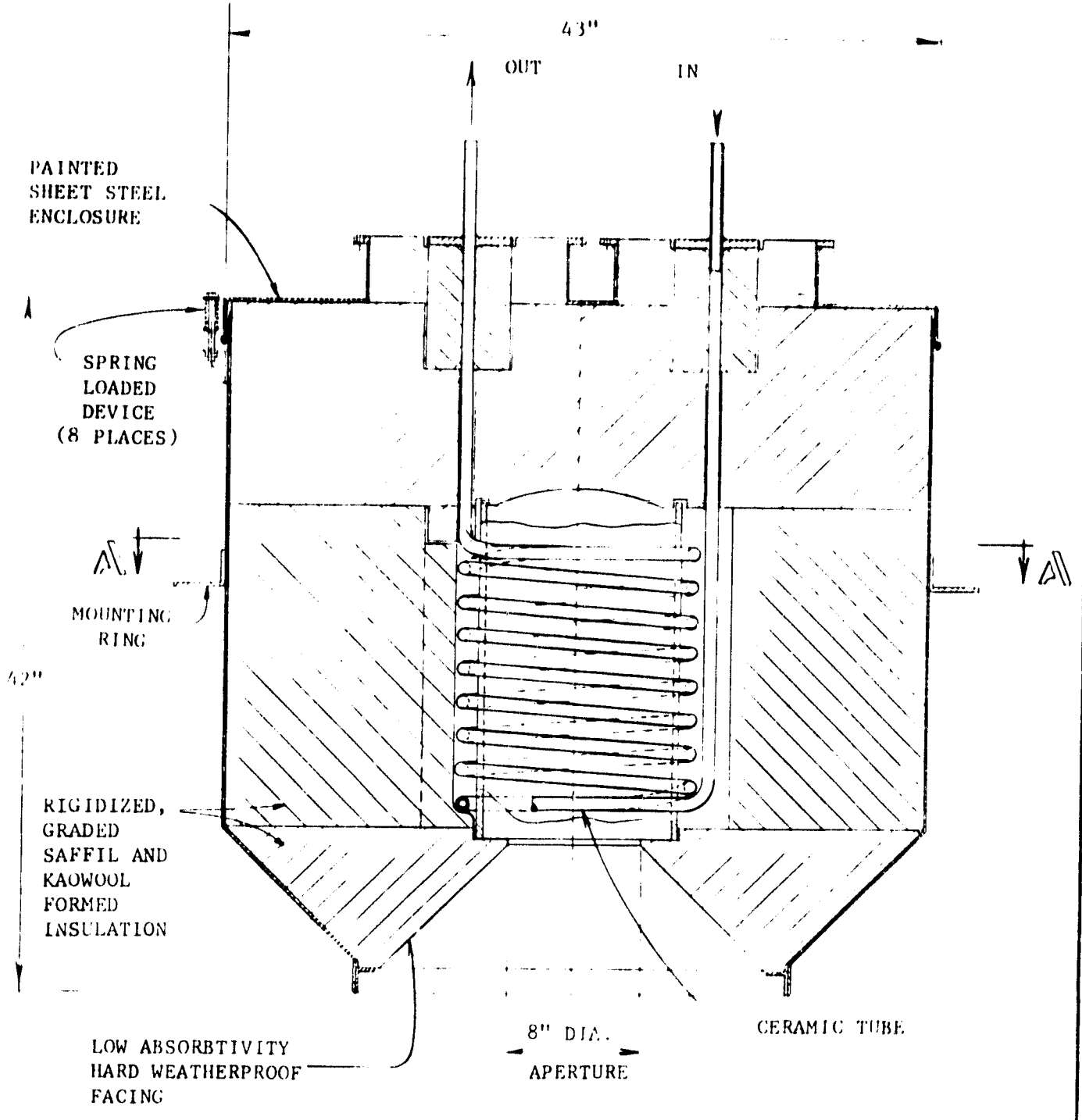

Figure 3-1. Helical Coiled Tube Concept

the working fluid at above atmospheric pressure, and is the only component which must be leaktight. It is surrounded by an insulation package of rigidized fibers, whose density and stiffness vary to provide both structural integrity and low heat loss. The entire unit is encased in a sheet metal can which provides support for the unit and a convenient means of attaching the receiver to the concentrator. The facing of the solar flux entrance cone is coated with a low absorptive surface which is weather proofed. The two seals (or joints) at the top of the receiver serve to terminate the helix and to decouple the receiver heat exchanger from the exterral heat transfer components.

2. Matrix Heat Transfer Concept (Concept No. 2)

Figure 3-2 shows the arrangement of the matrix heat transfer concept. Solar radiation from the concentrator enters the cavity through a fused silica dome and impinges on a cylindrical honeycomb heat transfer matrix. This matrix is made of high temperature ceramic and has many passages parallel to the axis of the receiver. It is similar in concept to the rotary regenerators developed for use in automotive gas turbines, although the material and hole size will likely have to be different.

Gas enters the receiver through a sealed joint, cools the fused silica dome and passes upwards through the matrix. The gas then leaves the receiver through another sealed joint. In order to minimize high stresses on ceramic parts, the entire receiver is pressurized, including the insulation package. Thus the only pressure seals are at the perimeter of the fused silica dome and at the sealed joints. The outer metal shell, at near-ambient temperature, is the primary pressure barrier. The insulation package is made of similar materials to the first concept. Thermal energy storage is provided by the matrix itself as well as the insulation package.

Figure 3-3 shows another version of this concept. In it, the gas flow enters through the center of the matrix by means of a ceramic tube. Orifices in the tube permit control of the flow over the fused silica dome and through the matrix. All attachments are at the top of the receiver where a relatively complex set of seals and joints separates the inlet and outlet flows.

3. Tube and Header Concept (Concept No. 3)

Figure 3-4 shows a concept using a ceramic tube and header heat exchanger. As with Concept No. 1, the solar flux impinges on a ceramic thermal inertia sleeve. Between this sleeve and the hot surface of the insulation package are located a number of small diameter ceramic hairpin tubes. Each is connected to two toroidal headers with a spigot type joint. Gas flows into one of the toroidal headers and is split between the hairpin tubes. After being heated the gas is collected in the outlet header and leaves through a tube and joint arrangement. Except for a different heat exchanger configuration, this concept is quite similar to Concept No. 1.

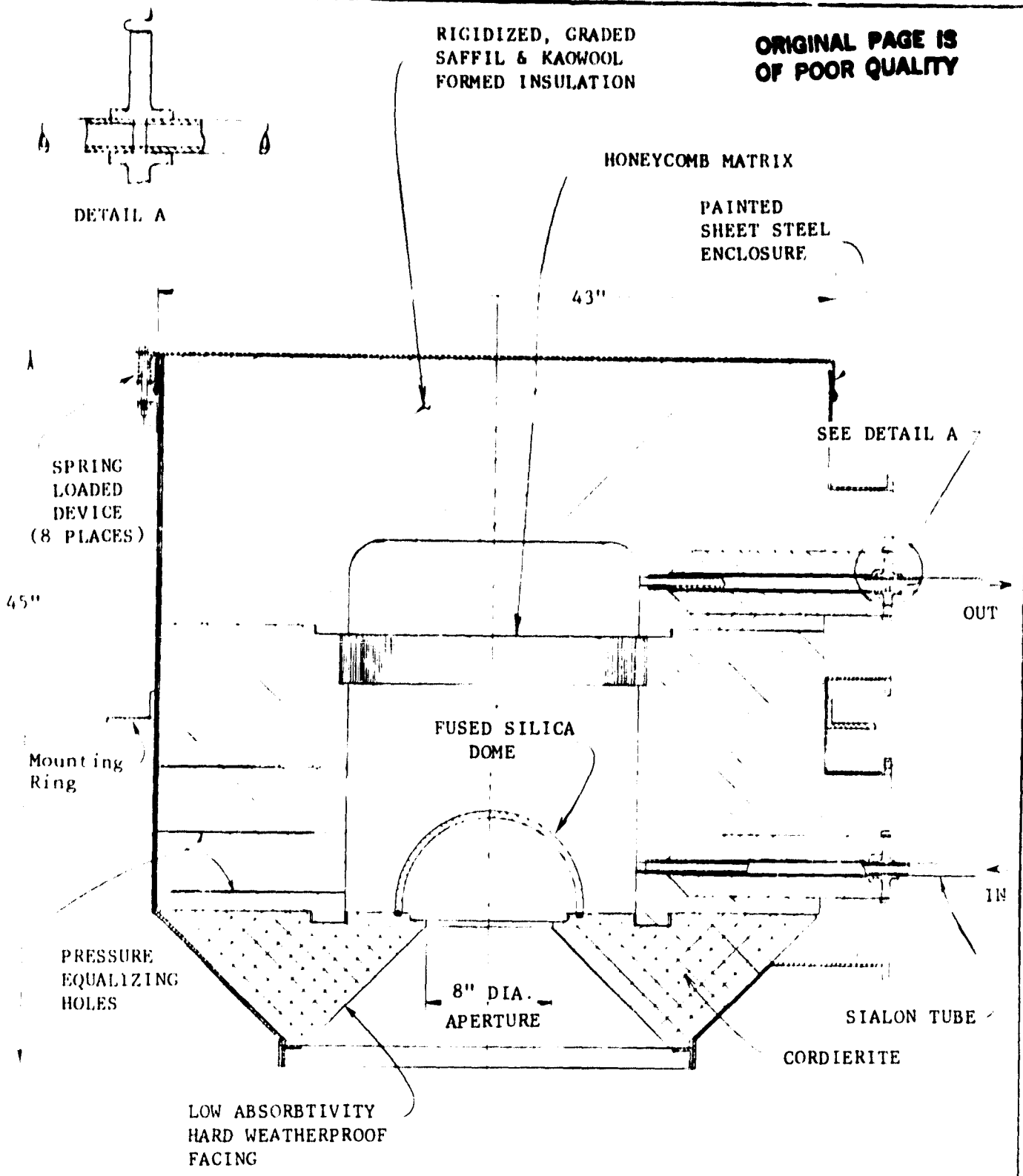

Figure 3-2. Matrix Heat Transfer Concept

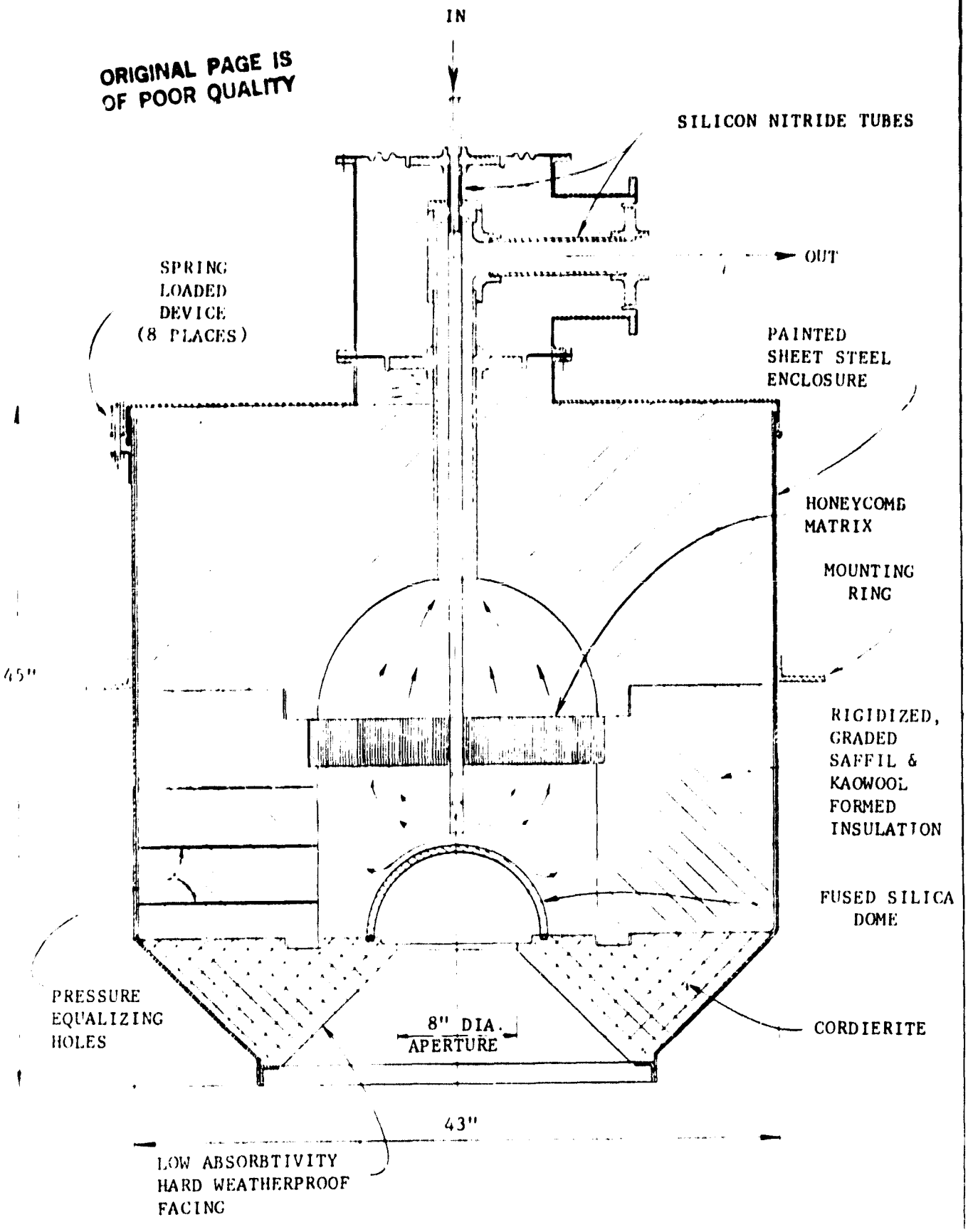

Figure 3-3. Alternate Matrix Concept

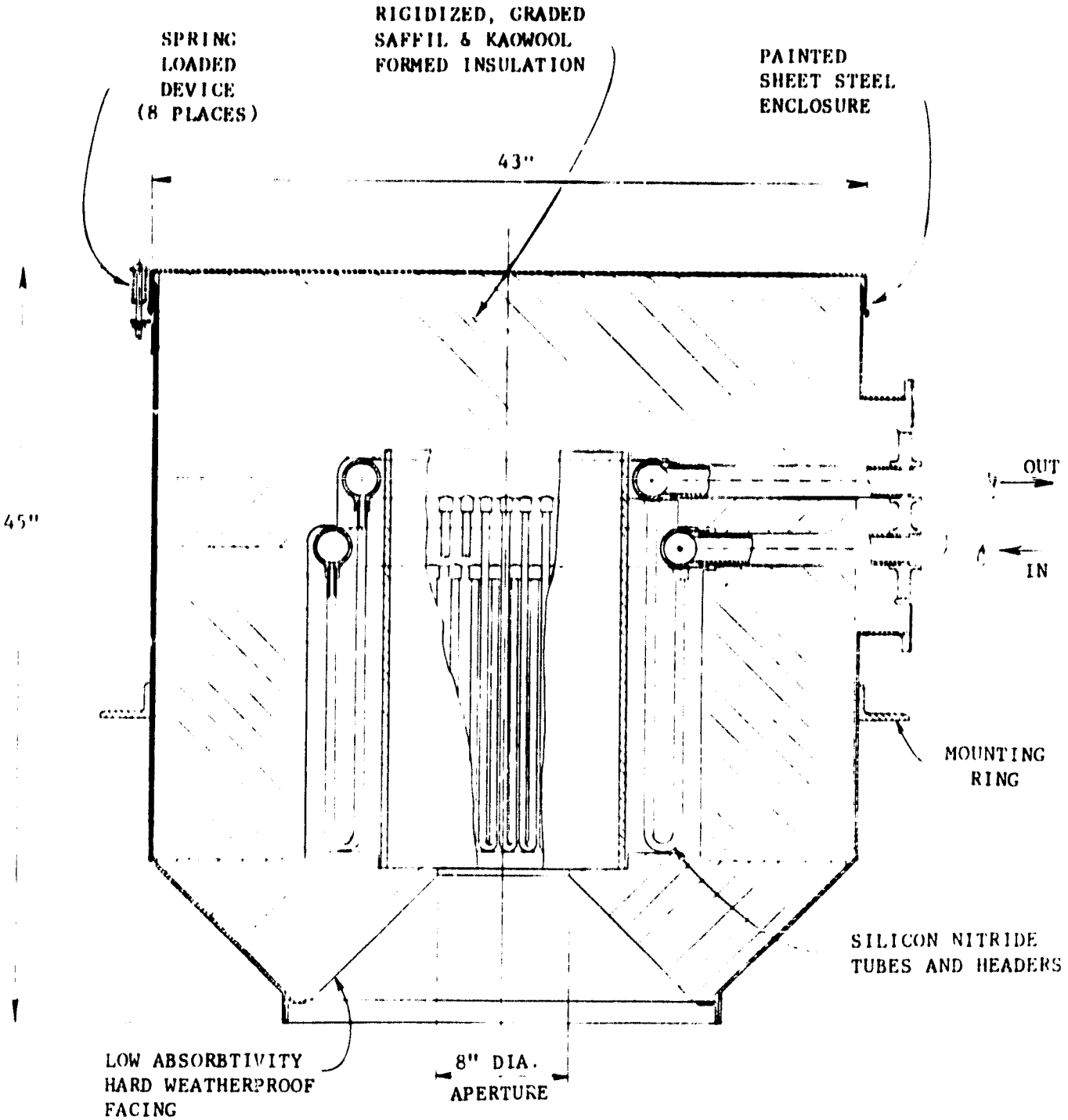

Figure 3-4. Tube and Header Concept

C. MATERIALS SELECTION

During this portion of this project, a preliminary selection of appropriate material for each component for each concept was made. The best material was identified along with other potential choices. Properties for each were collected from the literature and reviewed for reliability.

Based on this preliminary data, the operating limits, compatibility with working fluids, and thermal shock capabilities were assessed. In many cases, it was possible to identify potential commercial producers of the materials and shapes required. A rough start at determining the mass production cost was made.

Materials for the following components were studied in some detail:

- Ceramic tubing
- Thermal inertia sleeve
- Insulation
- Ceramic structural supports
- Transparent dome or window
- Honeycomb matrix

Other components, primarily low temperature structural parts, were selected using conventional engineering judgement.

1. Ceramic Tubing

Ceramic tubing is the key pressure containing component in both the helical coiled tube concept and the tube and header concept. Sizes required range from 8 mm (0.3 in.) to 90 mm (3.5 in.) diameter in lengths from 0.7 m (2 ft.) to 13.5 m (45 ft.). Required wall thicknesses, primarily determined by fabrication limits rather than stress, range between 5 and 10 percent of the diameter.

Desired properties include:

- Usable strength to above 1650°C (3000°F)
- Stable in air, nitrogen, and helium
- Good thermal shock resistance
- Good thermal conductivity
- Potential adaptability to mass production
- Low cost and non-strategic constituents

The two possible materials identified were sintered silicon carbide and sintered silicon nitride. Appendix A contains an overview of the possible fabrication procedures and material options available.

Both materials are under development for numerous applications requiring reasonable strength thermal shock resistance, and stability at high temperatures. Table 3-1 compares the properties of several different types of these two ceramics. It was determined that either material would be acceptable and could lead to low cost in mass production.

Table 3-1. Comparison of Silicon Nitride and Silicon Carbide

Property	Units	Material	
		Silicon Nitride	Silicon Carbide
Density	kg/m^3 (lb/ft^3)	3000 (187)	3200 (200)
Modulus of Elasticity @ 20°C	GPa (ksi)	234 (34000)	392 (57000)
Poisson's Ratio	-	0.29	0.16
Linear Coefficient of Thermal Expansion	$^oC^{-1}$ ($^oF^{-1}$)	$3x10^{-6}$ ($1.7x10^{-6}$)	$r \times 10^{-6}$ ($3.3x10^{-6}$)
Thermal Conductivity			
@ 20°C	W/m-°K	13 (7.3)	110-70 (70-40)
@ 1650°C	(Btu/hr-ft-°F)	6 (3.5)	20-30 (11-17)
Flexure Strength @ 20°C (Approximate)	MPa (ksi)	390 (57)	490 (70)
Allowable Engineering Stress @ 1500°C (For parametric analysis)	MPa (ksi)	76 (11)	--

Based on silicon nitride's lower thermal expansion and lower modulus, it was selected as the prime choice. Figure 3-5 shows an extruded helical coil of half-inch diameter silicon nitride tube before firing.

The joints between the hairpin tubes and the inlet and outlet toroidal headers required for Concept 3 were investigated. Although no single method of fabricating these joints was selected, several methods were identified, including the use of a viscous glass in a configuration similar to a brazed or soldered metal joint.

2. Thermal Inertia Sleeve

Both Concepts 1 and 3 require a ceramic sleeve to act as a thermal inertia element and as a protection for the heat exchanger from the direct solar insolation. This component has an inside diameter of 175 to 500 mm (7 to 20 in.), a height of 500 to 1000 mm (20 to 40 in.), with a wall thickness of 6 to 20 mm (1/4 to 3/4 in.). Since this component does not have to withstand pressure stress or be gas leak tight, its major requirement is to withstand the thermal shock of rapid solar heating. Desirable properties include:

- Stability in air to above 1650°C (3000°F)
- Thermal shock resistance
- High thermal conductivity
- High emissivity
- Potential for thermal energy storage

A number of materials were investigated as possible candidates. Both silicon carbide, usable in air to 1750°C (3200°F), and silicon nitride are potentially useful. Many refractory oxides, such as mullite, alumina, magnesia, spinel, zirconia, beryllia, and uranium oxide can be used above 1750°C (3200°F), but have potential problems such as low thermal conductivity, toxicity, and/or poor resistance to thermal cycling. Table 3-2 shows selected properties for these materials.

Since acceptable grades of silicon carbide appear available, such as Crystar® from the Norton Company, this material was selected for the conceptual design phase. A major advantage is excellent thermal conductivity, which leads to better receiver performance. However, some of the other materials, especially mullite, may be ultimately preferred from a cost standpoint.

3. Insulation

All concepts require a relatively high quality and effective insulation package to keep heat losses low. In addition, the availability of rigid, self-supporting insulation forms led to design concepts in which the insulation itself would become part of the structure.

The size of the insulation package sections range up to 2 m (6.6 ft.) in diameter and up to 1 m (3.3 ft.) in height. Requirements include:

Figure 3-5. Extruded and Coiled 1/2" O.D. Silicon Nitride Tubing Before Firing to Remove the Binder and to Sinter the Ceramic Particles

Table 3-2. Selected Properties of Potential Inertia Sleeve Materials

Material	Property							
	Melting Point		Density (Theoretical)		Thermal Conductivity @ 1100°C		Maximum Service Temperature	
	°C	°F	kg/m^3	lb/ft^3	W/m-°K	BTU/hr-ft-°F	°C	°F
Silicon Carbide	1980	3600	3200	200	20	11	1760	3200
Mullite ($3Al_2O_2$-SiO_2)	1850	3370	-	-	4.7	2.7	1760	3200
Alumina	2040	3700	4000	250	5.2	3	1540	2800
Magnesia	2840	5150	3600	225	6.9	4	-	-
Spinel (MgO-Al_2O_3)	2130	3870	3600	225	5.2	3	-	-
Zirconia	2760	5000	5700	356	2.6	1.5	-	-
Beryllia	2570	4650	3000	187	17	10	-	-
Uranium Dioxide	2870	5200	10900	680	2.6	1.5	-	-

- Stability in air, helium, and nitrogen above 1650°C (3000°F)
- Relatively low thermal conductivity
- Rigidness and strength to support itself and other light components
- Fabricability into reasonably complex shape
- Potential for low cost in mass production

Several materials made of alumina, silica, and zirconia appeared satisfactory. Rigidized fiber products supplied by Babcock and Wilcox out of Saffil® and Kaowool® can be used up to 1650°C (3000°F) and are available in reasonably complex forms with varying material composition and density. Other companies, such as Zircon Products also make this type of insulation. In areas where temperatures are lower, below 1260°C (2300°F), many less expensive materials such as Fiberfrax® or Min-K-2000® are commercially available.

For the parametric analysis, the insulation was assumed to be made out of formed parts using graded density Saffil® and Kaowool® rigid insulation.

4. Rigid Ceramic Structural Elements

As an alternate design for Concepts 1 and 3, and for the structural aperture cone and support element in Concept 2, rigid ceramic parts are required. These are ring shaped pieces up to 1 m (40 in.) in diameter and up to 300 mm (12 in.) thick. These parts should have the following properties.

- Low thermal expansion
- Thermal shock resistance
- Moderate-to-high flexural strength
- Moderate cost

Possible candidates are:

- Cordierite
- Beta spodumene
- Zircon
- Glass-ceramics (Cercor® for example)
- Mullite

Based on these requirements, Cordierite was selected for use below 1370°C (2500°F) and Mullite for use above this temperature.

5. Transparent Dome or Window

Concept 2 requires a dome or window which must function as part of the pressure containing system. The required diameter is 76 mm (3 in.) to 200 mm (8 in.) with a thickness of about 6 mm (1/4 in.). Desired properties include:

- High transmittance for radiant energy
- Moderate strength
- High thermal shock resistance
- Compatible with air to above 1650°C (3000°F)

After an extensive search, only two materials were identified. Fused silica has all of the required properties except that it devitrifies in air above 1090°C (2000°F). Yttralox®, transparent, sintered yttria, is useable to about 1760°C (3200°F), and has been developed for various applications, but its transmittance is rather low, and would seriously degrade the receiver performance. In addition, its cost is expected to be rather high.

Fused silica is the clear choice where its temperature limit allows its use. No good material has been identified for extended use above 1090°C (2000°F).

6. Honeycomb Matrix

The heat transfer surface for Concept 2 is a cylindrical honeycomb matrix about 200 mm (8 in.) to 600 mm (24 in.) in diameter and 25 mm (1 in.) to 100 mm (4 in.) thick. It has many small channels through it parallel to the axis. These holes are rectangular, triangular, or hexagonal depending on the method of manufacture and have equivalent hole diameters between 0.5 mm (0.02 in.) and 6.4 mm (1/4 in.).

Desired properties are:

- High thermal shock resistance
- Compatibility with air, helium or nitrogen to above 1650°C (3000°F)
- Fabricability to the desired shape

Several materials have been developed and fabricated for automotive gas turbine rotary regenerators. Some of these and their temperature limits are:

- Corning 9460 Aluminosilicate (AS): to 1000°C (1832°F)
- Magnesium Aluminosilicate (MAS): to 1000°C (1832°F)
- GE-7808 (Zr MAS): to 1250°C (2282°F)

Additional candidate materials, some of which have been used for automotive catalytic converters are:

- Alumina (Alsimag 614, for example): to 1540°C (2800°F)
- Cercor®: to 1010°C (1850°F)
- Silicon carbide: to 1760°C (3200°F)
- Silicon nitride or Sialon: to 1760°C (3200°F)
- Mullite: to 1760°C (3200°F)

For the high gas temperature desired, it appears that one of the higher temperature materials such as silicon carbide, silicon nitride, or mullite will be required, and these were selected for the parametric analysis.

D. PERFORMANCE ANALYSIS

1. Scope and Basis for Analysis

Performance analysis, specifically defined as overall receiver efficiency while meeting pressure drop requirements, was performed on the three concepts described above. The helical coiled tube concept was analyzed in the most detail, while sufficient analysis was performed on the other two concepts to allow their evaluation to be compared.

As used for all of the analysis performed, "peak thermal power" is defined by a subset of specifications pertinent to the ADS-1 concentrator. These are:

- 1 kW/m^2 insolation
- 86% efficient concentrator
- 0.9% blocked area at concentrator center

The "peak thermal power" to the receiver is defined as the total reflected energy which could be collected by a concentrator of a particular size with the above specifications. The receiver efficiency is defined as that percent of the "peak thermal power" which is transferred to the working fluid. The heat losses thus accounted for in the receiver efficiency include:

- Intercept factor losses
- Insulation losses
- Reradiation losses
- Convective losses

2. Helical Coiled Tube Concept Analysis

a. Analysis Methods. A computer code was written to perform the iterative calculations necessary to determine the receiver efficiency. In addition, the size, weight, and a rough cost parameter were calculated.

This computer code performed an essentially one-dimensional heat transfer calculation which included:

- Radiant and convective losses from the cavity
- Conduction through the thermal inertia sleeve
- Radiation interchange to the helix from the sleeve
- Conduction and convection through the tube to the gas

The calculation performed a double iteration to balance tube diameter and length against desired pressure drop and required heat transfer area, and then mass flow versus available energy to the gas. For each calculation, the pressure level, inlet and outlet temperatures, pressure drop, and incident energy were fixed, as were certain geometric ratios such as coil spacing to tube diameter and sleeve diameter to aperture size.

Some of the calculation techniques were nonstandard and are described below. These include the heat transfer coefficient and friction factor for the gas within the coiled tube, the calculation of reradiation losses, and the convective heat transfer coefficient for the interior of the receiver cavity.

The heat transfer coefficient and friction factor correlations were taken from Rohsenow and Hartnett's Handbook of Heat Transfer, Section 7. These correlations were checked extensively against others, and after an error in the printed equation for the pressure drop was corrected, good comparisons with others tended to validate their use.

Reradiation was calculated by calculating radiation view factors and interchange factors between the aperture and three surfaces of the cylindrical cavity with the aperture in it. By using emissivities for each surface it is possible to make quite an accurate calculation even in a parametric analysis.

The convection heat transfer from the receiver cavity was calculated by means of relationships derived from experimental work done on an experimental receiver which was designed and tested as part of the Shenandoah solar project*. The correlation developed takes into account the proportions of the receiver cavity, the size of the aperture, the angle of inclination of the concentrator-receiver, and the wind speed and directions.

b. Parametric Evaluation Overview. It was found that the efficiency of the receiver was determined by the interaction of the radiant heat losses from the cavity and the convective heat transfer between the inside surface of the tube and the working fluid. For high efficiency the temperature drop between the gas and the sleeve must be as low as possible. This requires relatively large surface areas within the cavity to avoid a high ΔT across the sleeve. It also required a large heat transfer surface on the coiled tube. It became possible to trade off size and thus cost against efficiency.

For all this analysis, only single tubes were considered. This causes the low pressure drop requirement to become significant, especially for low pressure levels and high mass flows. In order to keep the heat transfer coefficient reasonably high, it is desirable to operate in the turbulent flow regime, and all cases met this requirement.

The analysis was performed by varying one parameter at a time rather than running a full matrix of all possible combinations of parameters. The parameters investigated included:

- The major study variables
  - Exit gas temperature
  - Inlet-outlet temperature difference
  - Pressure level
  - Power level
  - Working fluid

*Koenig, A.A. and Marvin, M., "Convective Heat Loss Sensitivity in Open Cavity Solar Receivers", General Electric Co. To be Published.

- Tube spacing and coil proportion
- Concentrator quality
- Aperture size
- Heat exchanger effectiveness
- Off design performance

Except as otherwise noted, all parametric analysis was performed using a 1 milliradian slope error concentrator.

c. Performance Results With Air or Nitrogen. Figure 3-6 shows the efficiency of receiver using air as the working fluid. These calculations were all made for the same coil height to sleeve diameter ratio, about 2. This value appears to give a good balance between efficiency and weight, and also gives a well proportional helix for ease of manufacture. The efficiency varies with this height to diameter ratio so that within the range of 1.5 to 3.0 the efficiency changes by about 2 points. This should be considered when interpreting Figure 3-6. Thus only the variation in exit gas temperature is really significant. For the other three major variables, the effect on efficiency is quite small.

One result of this analysis was the determination of the effect of coil spacing and proportion. For a given set of thermal condition , that is inlet and exit temperatures, power level and pressure level, t e total tube length and diameter are nearly constant. By changing the spacing between coils and the coil diameter (and hence number of turns), the proportions of the receiver cavity can be varied over a wide range. Shown in Table 3-3 are typical results from one set of calculations. Similar results were obtained for changing the spacing between coils. For air, a minimum weight and high efficiency was obtained with a ratio of tube spacing to tube diameter of about 1.3. For comparison purposes, coil height to sleeve diameter ratio of approximately 2 was used. As will be seen later, this type of variation is more significant for helium cases than for air.

Nitrogen showed little parametric difference than air from any viewpoint. The silicon nitride material is not affected by either, so there is little performance difference.

d. Performance Results With Helium. Helium has a much better heat transfer coefficient than air, and a higher heat capacity. Therefore the tube length and diameter required for a given power level, temperature condition, and pressure level are lower than for air. This means that receiver coils can be smaller for helium. The smaller coils can fit around a smaller cavity and a smaller inertia sleeve. This causes the sleeve temperature to be higher and the reradiation losses greater By opening up the helium coil, it is possible to achieve the same efficiency as for air, but the weight increases to about the same level as for air. Table 3-4 shows a comparison of an air case with two helium cases, one which has the same coil spacing and one which has nearly the same overall size. Note that the smaller, lighter (and potentially cheaper) helium unit is 4 points lower in efficiency than either the air receiver or the larger helium unit. The conclusion reached is that helium receiver can be much smaller and lighter than air receivers, but only at an efficiency penalty.

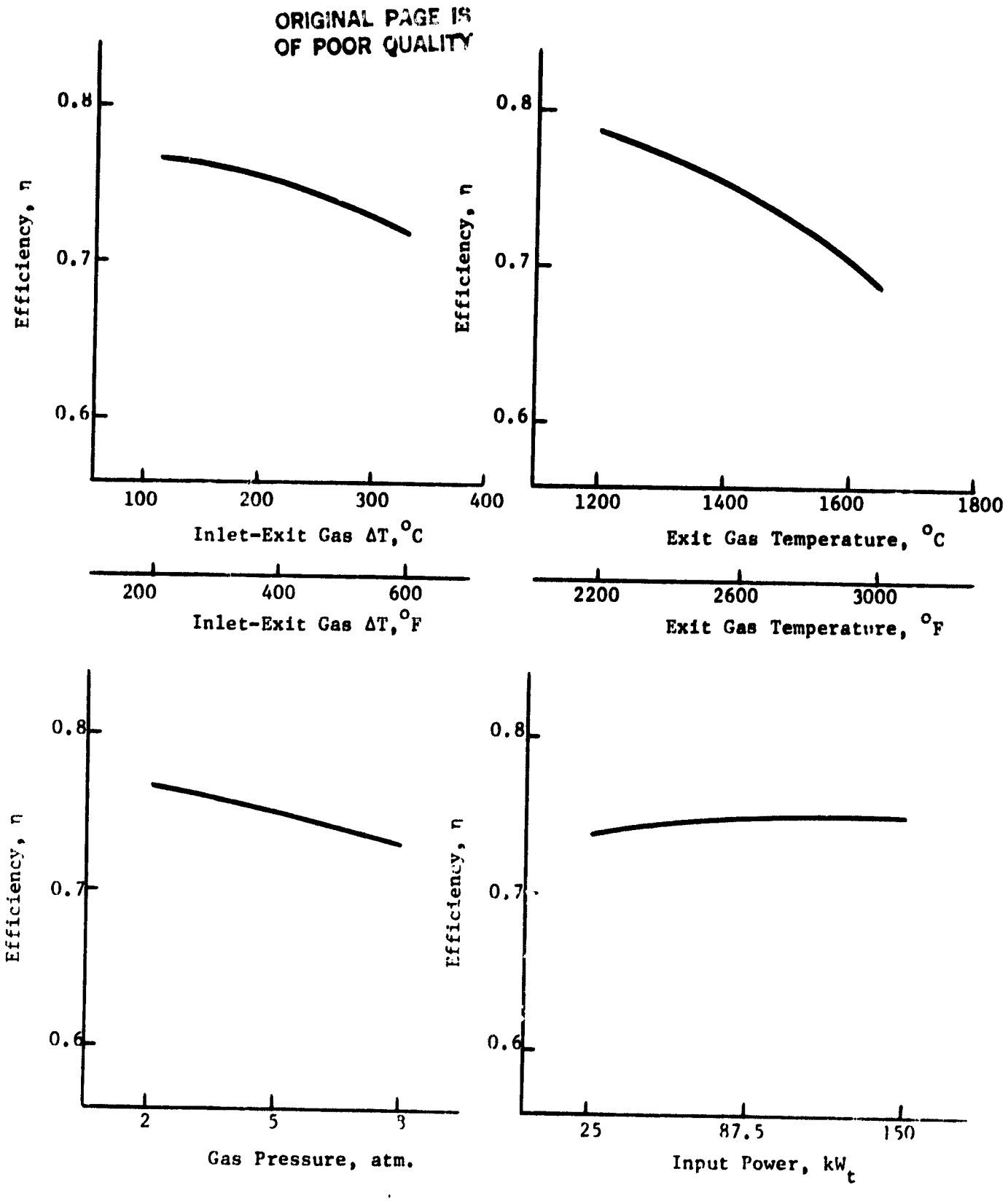

Figure 3-6. Performance of Coiled Tube Concept With Air

Table 3-3. Effect of Cavity Proportion Change on Performance

Parameter	Units	Case		
		1	2	3
Total Input Power	kW_t	87.5		
Pressure Level	Atmosphere	5		
Exit Gas Temperature	°C (°F)	1427 (2600)		
Inlet-Exit Temp. Difference	°C (°F)	333 (600)		
Working Fluid	-	Air		
Ratio of Sleeve Diameter to Aperture Diameter	-	1.3	1.7	2.1
Ratio of Coil Height to Sleeve Diameter	-	2.79	1.87	1.52
Efficiency	%	70.6	72.3	73.8
Tube Length	m (ft)	6.5 (21.2)	6.7 (22.0)	7.8 (25.5)
Tube I.D.	mm (in)	44 (1.74)	45 (1.76)	45 (1.77)
Weight	kg (lbm)	102 (224)	114 (251)	140 (308)

Table 3-4. Use of Helium As a Working Fluid

Parameter	Units	Gas		
		Air	Helium	
Coil Spacing to Tube Diameter	-	1.3	1.3	2.54
Power Level	kW_t	87.5		
Pressure Level	Atmos.	5		
Exit Gas Temperature	°C (°F)	1427 (2600)		
Inlet Exit Temp. Difference	°C (°F)	222 (400)		
Coil Height to Sleeve Diameter	-	2.16	1.71	1.93
Efficiency	%	74.7	70.7	74.5
Overall Height	mm (in)	1.39 (55)	0.91 (36)	1.44 (57)
Overall Diameter	mm (in)	1.26 (50)	0.78 (31)	1.26 (50)
Weight	kg (lb)	259 (572)	85 (187)	260 (574)
Tube Length	m (ft)	9.4 (31)	5.2 (17.1)	5.5 (18.2)
Tube Diameter	mm (in)	55 (2.18)	43 (1.71)	44 (1.74)
Heat Transfer Coefficient	$BTU/hr\text{-}ft^2\text{-}°F$	82.0	159.6	156.4
Heat Transfer Coefficient	$W/m^2\text{-}°K$	142	276	271
Sleeve Temperature	°C (°F)	1610 (2930)	1766 (3210)	1621 (2949)

e. Effect of Collector Accuracy. Except for the calculations discussed in this paragraph, all of the parametric calculations were made using a concentrator with a nominal accuracy represented by a 1 milliradian (mrad) slope error. For a 92.5% intercept factor, 87.5 kW nominal peak power and the assumed concentrator data, this requires a 130 mm (5.12 in.) diameter aperture. Changing to a lower accuracy concentrator of 2 mrad slope error, the aperture becomes 194 mm (7.62 in.). This change in aperture size increases the losses from the receiver significantly, and decreases the efficiency by 10 to 12 points, or from about 75% to 65-63%.

f. Effect of Changing Aperture Size. The effect of changing the aperture size, which therefore changes the intercept factor, was investigated. Increasing the aperture will capture more energy but also increase losses from reradiation and convective losses. The results of several calculations showed little effect on efficiency over a relatively wide range of aperture sizes. Additional work was performed as part of the conceptual design and reported in Section IV-B-1.

g. Effect of Heat Exchanger Effectiveness. Early work showed that the effectiveness of the coiled tube as a heat exchanger was a significant variable. The effectiveness was defined as:

$$\varepsilon = \frac{\left(T_{\text{gas out}} - T_{\text{gas in}}\right)}{\left(T_{\text{tube}} - T_{\text{gas in}}\right)}$$

and was used to fix the tube wall inner temperature. Low effectiveness implies a higher wall temperature for the same gas temperatures, and hence a higher sleeve temperature and lower receiver efficiency. A low effectiveness also causes a smaller coil. After correction of a computational error, it was found that high effectivenesses of 0.9-0.95 could be used without significant weight penalty and thus this parameter is no longer very significant.

h. Off-Design Performance. A small amount of off-design analysis was performed during Task 1. The condition investigated was one for a fixed concentrator-receiver operating at constant temperature conditions while the input energy decreases due to early morning or late afternoon operations. Since the receiver losses are primarily proportional to temperature level, the efficiency drops off significantly below about 60% of input power. Figure 3-7 shows the results of this calculation.

3. Matrix Concept Analysis

The efficiency of the matrix concept is determined primarily by the face temperature of the heat transfer matrix. The matrix can be a very effective heat exchanger, and the predominant losses are reflection and absorbtions in the fused silica window and reradiation losses from the face of the matrix. Pressure drop through the matrix can be made very low, and the major flow problem is achieving a uniform flow distribution through the matrix. In addition, performance is relatively insensitive to pressure level.

Parametric analysis showed that the efficiency of the matrix concept was at least as high as the coiled tube concept. This work orig-

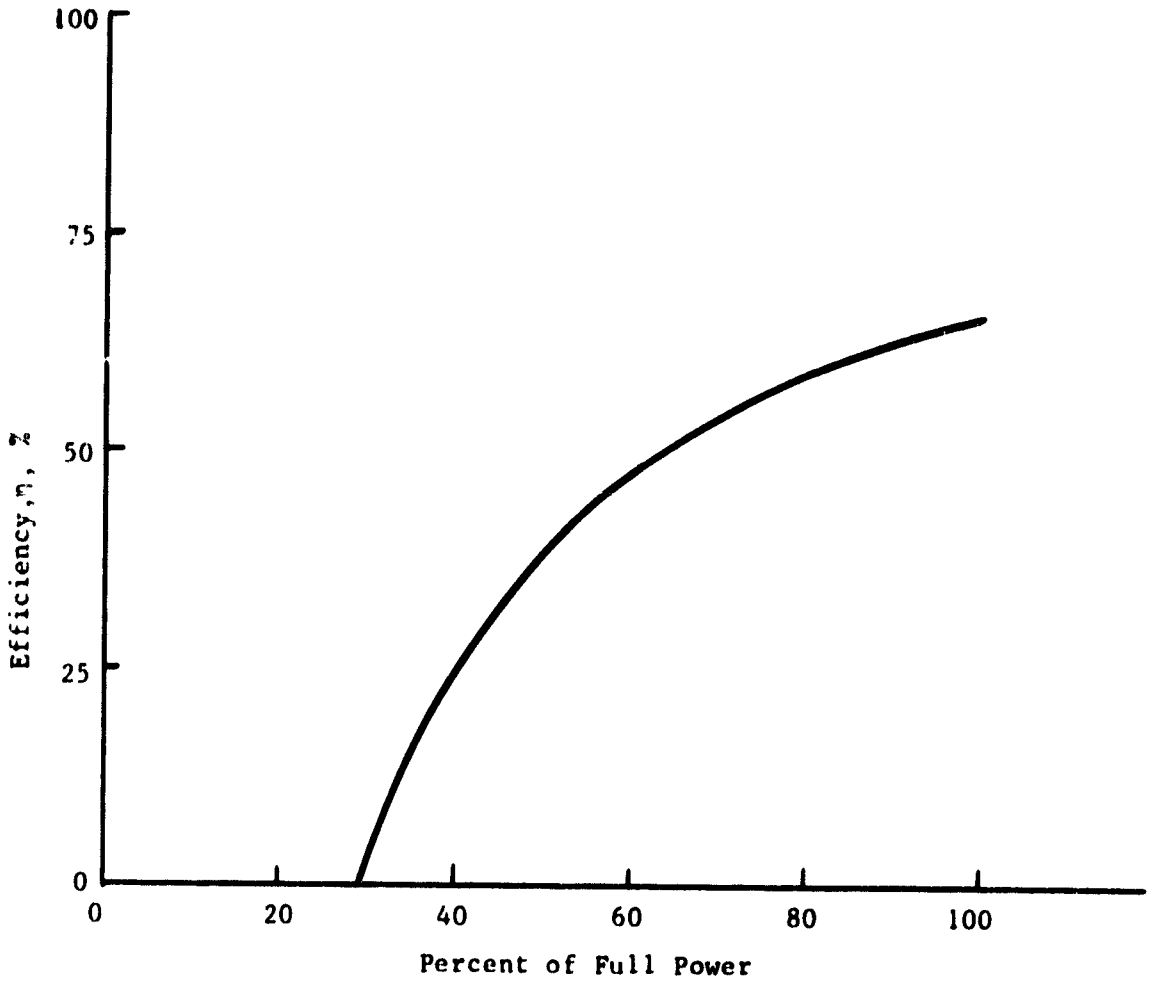

Figure 3-7. Off-Design Performance

inally showed that very high matrix surface temperatures and gradients would exist, and would cause potential materials problems. Subsequent evaluation showed that surface temperatures were much lower, well within the capability of silicon carbide or silicon nitride. The temperature gradients were also lower, but still may require additional attention during conceptual design.

Because of the fused silica temperature limit, only parametric cases with inlet temperature less than 1090°C (2000°F) were considered. It would require a separate cooling circuit and additional complexity to go above this temperature.

4. Tube and Header Concept

Analysis of the tube and header concept showed that essentially the same performance as Concept 1 could be obtained. Although the heat exchanger had a different configuration, its effectiveness and pressure drop requirements were similar to the helical coiled tube concept.

5. Summary

Surprisingly, all concepts were able to achieve essentially equivalent efficiency, for the same external conditions. The differences between concepts are determined by their fabricability, weight, and potential for low cost in mass production.

E. WEIGHT, SIZE, AND COST ANALYSIS

1. Helical Coiled Tube Concept

Figure 3-8 shows the weight of the receiver, using air, as a function of the major study variables. It is apparent that low pressure levels, and low gas temperature rises tend to require very large receivers. This is caused by the pressure drop limitation imposed. The increased weight of receivers with high exit gas temperatures is caused primarily by the added insulation needed. The effect of power level on weight is nearly linear.

Figure 3-9 shows the approximate overall diameter of the receiver as a function of the major study variables. For units having approximately the same coil properties, the height is about 250 mm (10 in.) greater than the diameter.

Figure 3-10 shows a very approximate cost parameter plotted versus the major variables. The shape of these curves follows the weight curves closely.

2. Matrix Concept

Table 3-5 shows the size and weight for a representative matrix configuration. It is appreciably lighter and somewhat more expensive than a similar coiled tube concept would be, primarily due to the cost of the matrix and window arrangement. Its cost would be expected to decrease with mass production to be slightly less expensive.

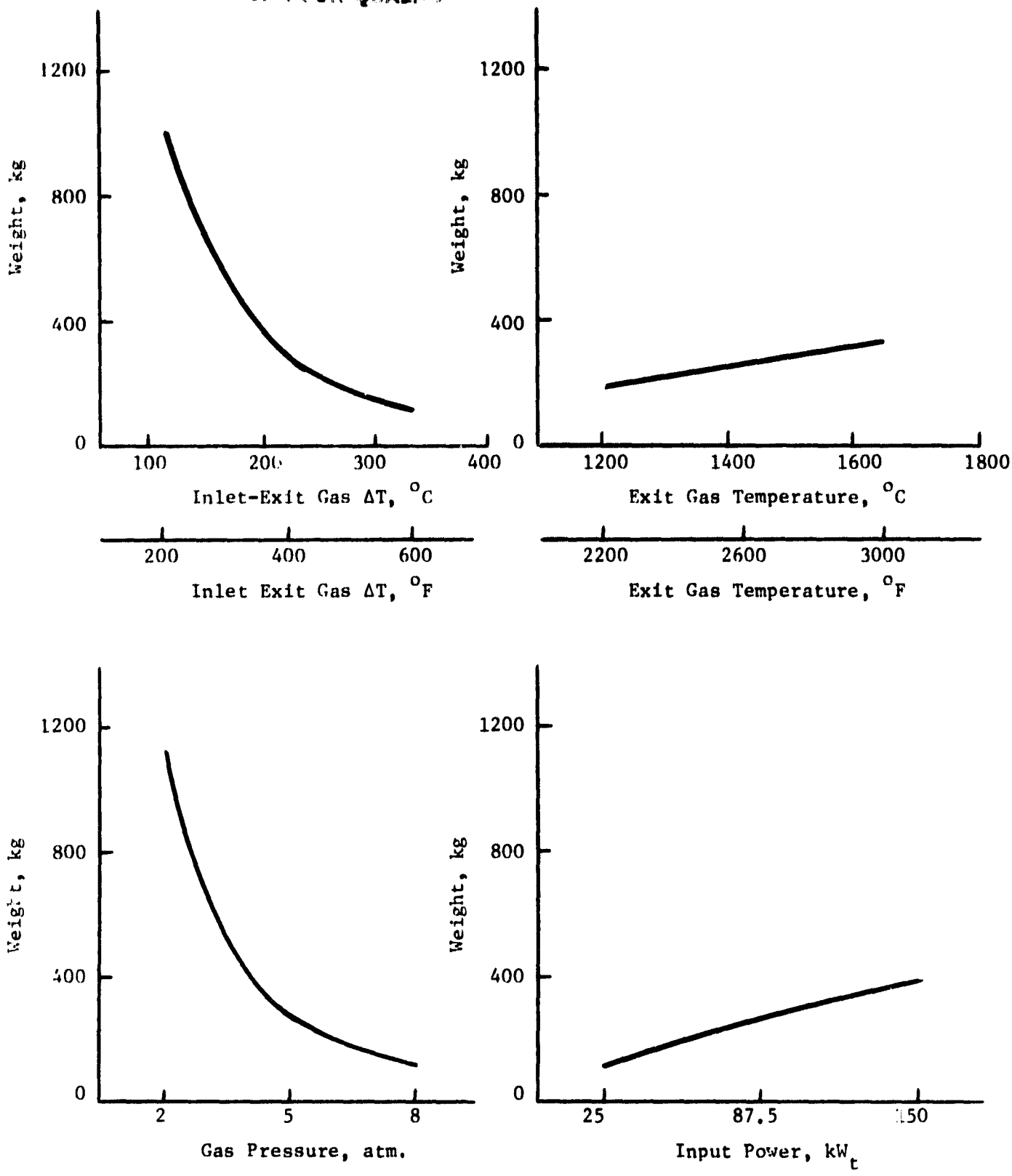

Figure 3-8. Parametric Weight Variation for the Coiled Tube Concept With Air

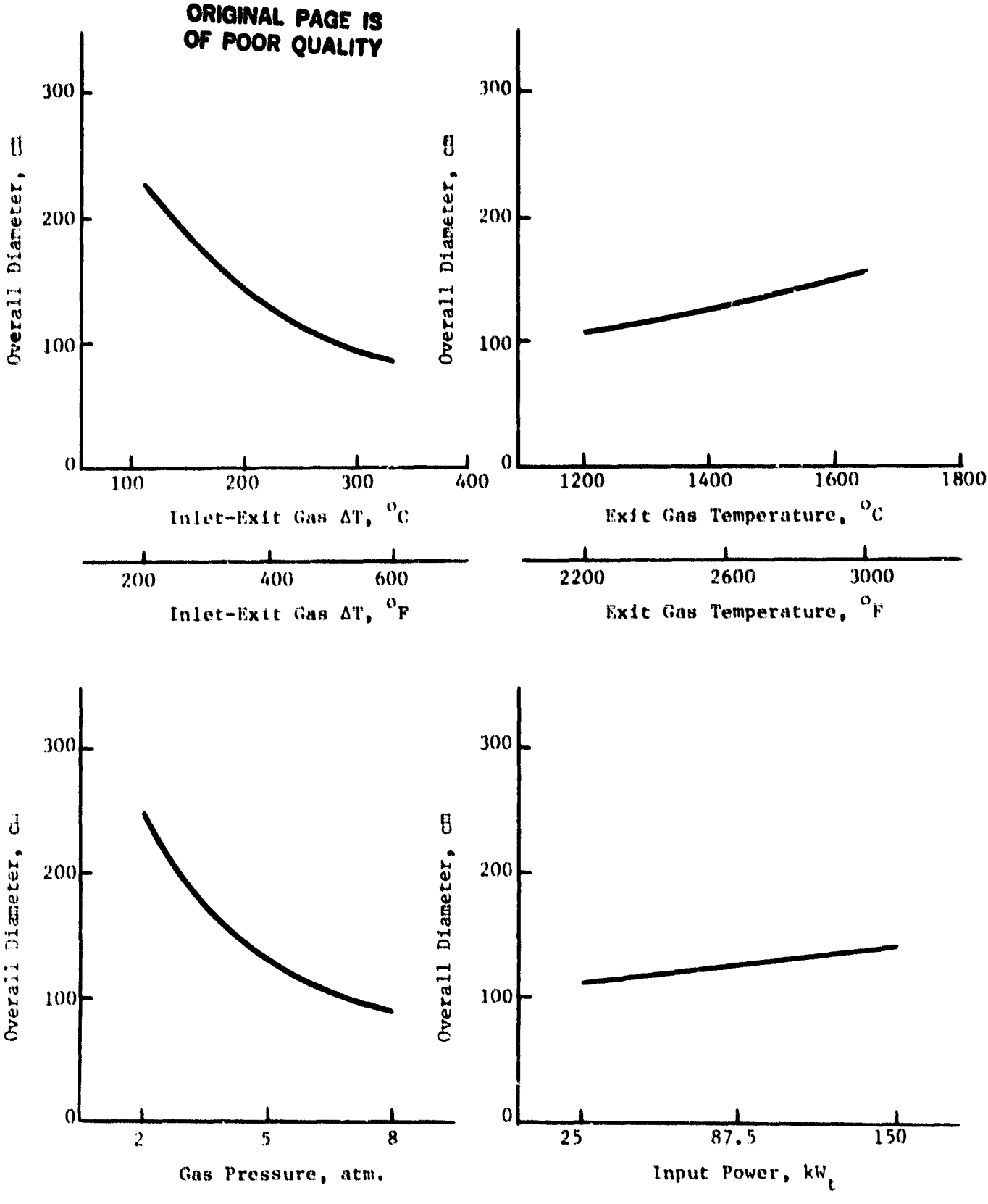

Figure 3-9. Overall Diameter of Coiled Tube Concept With Air

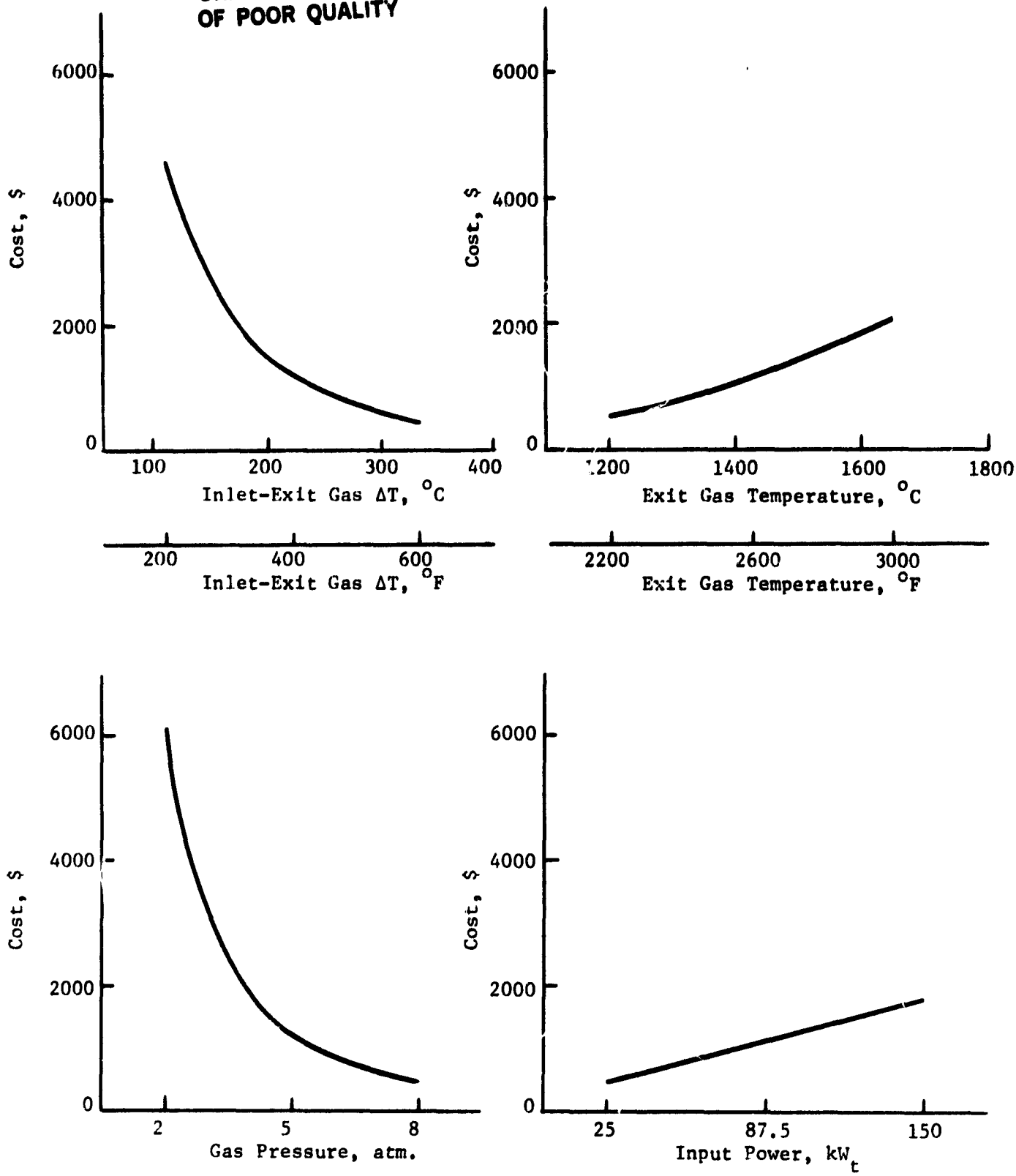

Figure 3-10. Approximate Parametric Cost for Coiled Tube Concept With Air

Table 3-5. Matrix (Honeycomb) Concept

Weight and Cost

Concept	Matrix	Coiled Tube
Working Fluid	Helium	
Power Level	87.5 kW	
Exit Gas Temperature	1200°C (2200°F)	
Inlet Gas Temperature	980°C (1800°F)	
Pressure Level	5 atmospheres	
Overall Height, mm (in)	851 (33.5)	902 (35.5)
Overall Diameter, mm (in)	582 (22.9)	678 (26.7)
Weight, kg (lb)	48 (105)	66 (246)
Cost, $	300	173

3. Tube and Header Concept

The tube and header concept has nearly the same weight and size as the helical coiled tube concept. It should cost slightly more due to the more elaborate heat exchanger design.

F. ADAPTABILITY TO FUELS PRODUCTION AND CHEMICAL REACTIONS

A small effort was made to see if these concepts would be adaptable to fuels production or chemical reactions. It is apparent that the ultimate goal must be to use the high temperature solar energy where it is generated, in the receiver, and not attempt to transport sensible heat through ducts. This would avoid losses in transmission as well as the expense of high-temperature insulated ducts. It is also desirable to couple a recuperator to the receiver so that essentially all of the thermal energy goes to the process reaction and is not wasted.

The key area investigated in this task was the possible location of catalysts in each concept.

In the two concepts using extruded tubing, it was determined that extended surfaces on the inside of the tube, for example as shown in the sketch below, could be made almost as easily as the plain tube could be. The catalyst could be chemically deposited on these surfaces in a highly automated fashion.

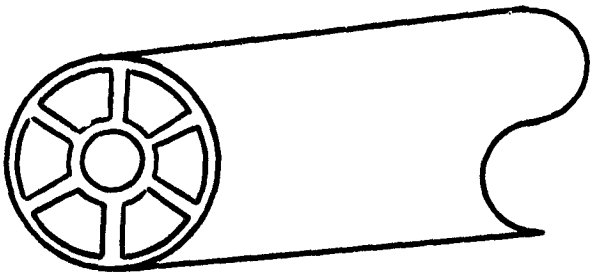

Sketch of Extruded Extended Surface Tube

For the matrix concept, the catalyst can be placed exactly like that on an automobile catalytic converter.

G. THERMAL ENERGY STORAGE EVALUATION

An assessment of the capability of these concepts for up to three minutes of thermal energy storage was made. Considering the temperature level and the short time required, the use of latent heat storage in liquid metals such as iron, silicon, and titanium, all of which melt in the correct temperature range, was discarded. Problems of materials compatibility, and differential thermal expansion were the primary reasons.

Scoping calculations showed that the sensible heat storage in the thermal inertia sleeve will provide about 45 seconds of storage with a temperature drop of about 110°C (200°F) for concepts 1 and 3. The tube or heat exchanger adds a little more. By placing a second sleeve in back of the coil or heat exchanger, even more storage time could be provided.

H. CONCEPT EVALUATION

Table 3-6 shows a summary of the evaluation of the three concepts studied.

The helical coiled tube concept is clearly an excellent design. It has a large number of advantages, especially the wide range of application and adaptability to the higher temperatures required for this study. Except for the coiled tube, all other components are presently available commercially. The materials for the coiled tube are developed and only the large size and shape require fabrication development.

For the lower end of the required temperature range, the matrix concept is a good choice for further development. It shows excellent efficiency and potential low weight and cost.

The tube and header concept shows no significant advantages over the helical coiled tube design, and has several potential development problems, especially the many joints needed. Its cost should be higher than the others also.

Table 3-6. Concept Evaluation

Concept	Advantages	Disadvantages
Helical Coiled Tube	- Wide Range of Applicability - Good Efficiency - Reasonable Weight (and Cost) - Adaptable to Chemical Reactions - Available or Developable Materials	- Heavy and Costly With Low Pressures and Low ΔT
Matrix Concepts	- Best Efficiency - Low Weight - Available or Developable Materials - Adaptable to Chemical Reactions	- Limited Temperature Range - Thermal Stress in Matrix May be a Problem - Pressure Seals Will Need Development
Tube and Header	- Reasonable Efficiency - Weight and Cost Comparable to Coiled Tube Concept	- Complex Structure With Many Joints - Required Development of Joints

SECTION IV

CONCEPTUAL DESIGN

At the conclusion of the parametric analysis, the helical coiled tube design was selected for further conceptual design. A design point representative of an advanced Brayton cycle application was specified. Table 4-1 shows these specifications. Using these specifications, a design configuration was selected as the basis for the remainder of the work.

Table 4-1. Design Point for Conceptual Design

Working Fluid	Air
Inlet Temperature	954°C (1750°F)
Outlet Temperature	1371°C (2500°F)
Temperature Difference	417°C (750°F)
Mass Flow	0.11 kg/sec (0.25 lbm/sec)
Inlet Pressure	310 kPa (45 psia)
Pressure Drop	0.04 ΔP/P Maximum
Concentrator Slope Error	2 mrad

A. CONCEPTUAL DESIGN CONFIGURATION

The conceptual design selected for detailed analysis is shown in Figure 4-1. A parts list indicating the type of material and estimated weight of each part is indicated in Table 4-2.

The design consists of a coiled silicon nitride (sintered) tube through which the process fluid to be heated will pass. Inserted inside the coil is a silicon carbide sleeve which provides some thermal inertia to the heat receiver and acts as a buffer between the concentrated rays of the sun and the ceramic heat exchanger (i.e., coiled tube). This sleeve also forms the cylindrical cavity of the solar heat receiver. The coiled ceramic tube is surrounded with rigidized "graded" insulation. The inner portions of the insulation are capable of withstanding tempertures up to 1650°C (3000°F). The outer portions of the insulation are made from a less expensive material capable of withstanding much lower temperatures. The difference in material composition as a function of depth into the insulation results in the use of the term "graded".

Ceramic to metal joints are employed to attach the coil to the metallic support structure of the heat receiver. These joints fit the

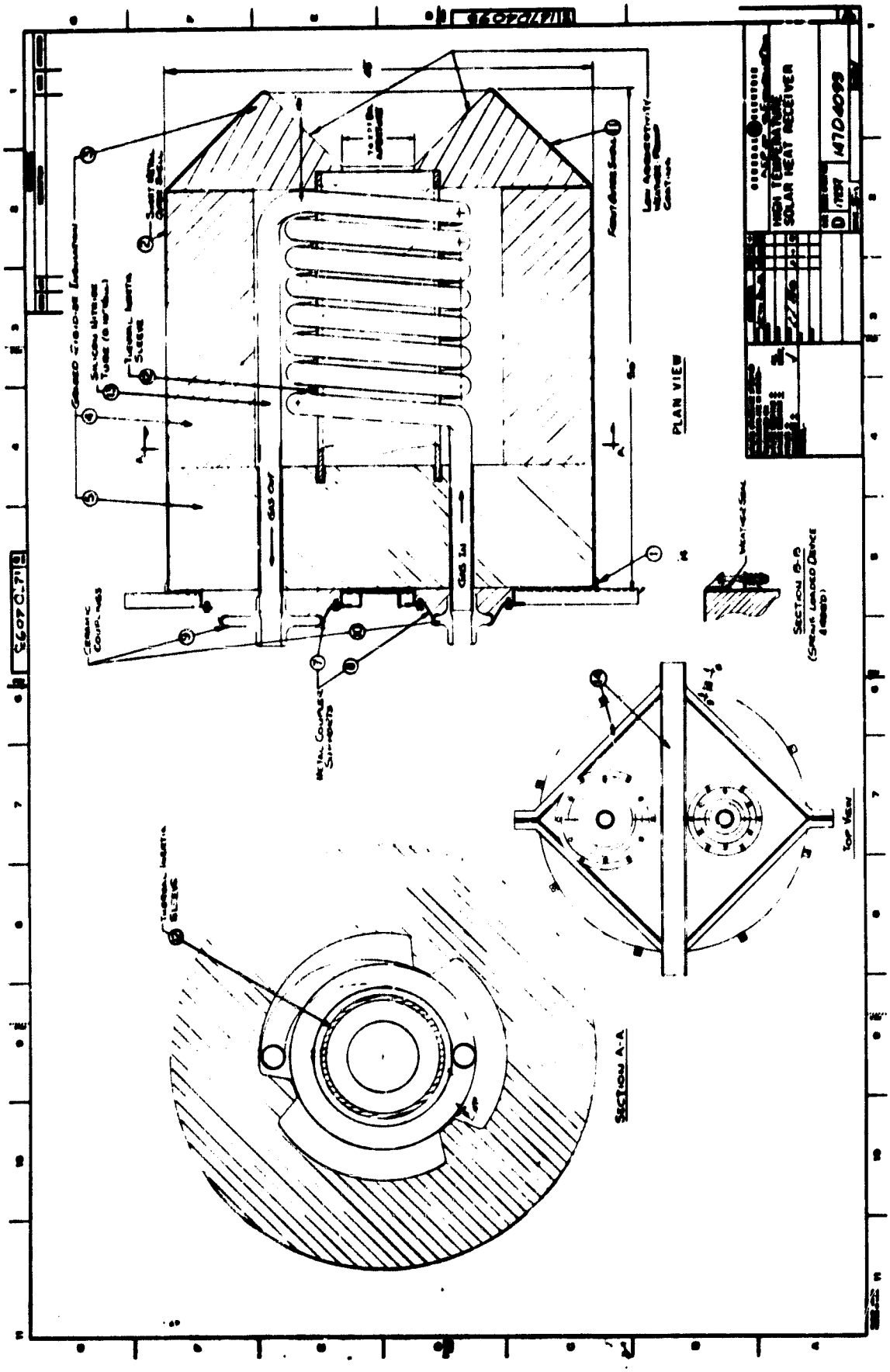

Figure 4-1. Layout Mechanical Design

Table 4-2. Parts List

Part No.	Description	No. Req'd.	Material	Configuration	Size	Weight kg	Weight lbs
1	Top Cover	1	Sheet Steel 20 Ga (Painted)	Round Reinforced Sheet	109.2 cm (43 in.) dia.	7.0	15.5
2	Outer Shell	1	Sheet Metal 20 Ga (Painted)	Formed Cylinder	109.2 cm (43 in.) dia. 127 cm (50 in.) high	26.5	58.4
3	Insulation, Aperture End	1	Saffil/Kaowool 10 lb/ft^3	Graded and Rigidized Form	109.2 cm (43 in.) dia. ~25 cm (~10 in.) high	18.5	40.8
4	Insulation, Side Wall	1	"	"	109.2 cm (43 in.) dia. 74 cm (29 in.) high	70.6	155.6
5	Insulation, Top	1	"	"	109.2 cm (43 in.) dia. 30.5 cm (12 in.) high	42.0	92.7
6	Insulation, Loose	-	Fiberfrax	Blanket	128 kg/m^3 (8 lb/ft^3)	Nil	Nil
7	Metal Seals	1	Inconel or Other Super Alloy	Formed Sheet 16 Ga	----	1.4	3.0
8	Metal Seals	1	"	"	----	1.1	2.5
9	Ceramic Seal Coupler	1	Sintered Silicon Nitride	----	~17.8 cm (~7 in.) dia.	1.6	3.5
10	Ceramic Seal Coupler	1	"	----	~13 cm (~5 in.) dia.	1.1	2.5
11	Front Casing	1	Sheet Metal Painted 20 Ga	Cone	109.2 cm (43 in.) base	7.1	15.6
12	Thermal Inertia Sleeve	1	Recrystallized Silicon Carbide	Cylinder	78.7 cm (31 in.) long 1.3 cm (0.5 in.) thick 29 cm (11.4 in.) ID	28.1	62.0
13	Silicon Nitride Tubing	1	Sintered Silicon Nitride	Coiled Tube ~7.5 Turns	5.97 cm (2 352 in.) OD 0.254 cm (0.1 in.) Wall ~11.3 m (~37 ft.) Long	~15.4	~34.0
14	Support Structure	1	Commercial Structural Steel	10.2 cm (4 in.) Channels 3.8 cm x 3.8 cm Angle	----	13.6	30.0
					Total Weight	234.0	516.0

coil at the inlet and outlet connections and support the coil within the confines of the insulation in a cantilevered manner. Connections to the inlet and outlet of the ceramic coil would be made in a variety of ways. The concept indicated in Figure 4-1 indicates a ceramic coupling. Further discussion of attachment methods is covered farther on in the text.

The preferred graded insulation is encased in a cylindrical sheetmetal container. The rear cover of the container supports the ceramic coil and is reinforced with structural steel shapes which, in turn, are used to mount the entire heat receiver at the concentrator focal mount ring. The cylindrical section of the sheet metal container is attached to the rear cover with spring-loaded bolts. These fasteners will allow for some relative movement between the sheet metal container and the insulation which may exist due to thermal expansion. Insulation exposed to the weather (i.e., the area surrounding the aperture), would be treated with a low absorptivity weatherproof coating. The entire low carbon steel container would be painted to provide protection from oxidation and sunlight.

Figure 4-2 provides an approximate definition of the heat receiver envelope indicating the total weight and center of gravity.

B. RECEIVER PERFORMANCE

1. Preliminary Design Evaluation

a. Design Point Size and Preliminary Performance Analysis. Based on the design point selected, the parametric analysis computer code was used to select an optimum configuration for use in the conceptual design task. Table 4-3 shows the details for this calculation. This meets the requirement shown in Table 4-1 and has an efficiency of 63% with a little over 3% $\Delta P/P$. The helical coil is 7.5 turns of 60 mm (2.35 in.) silicon nitride tube for a total length of 9.8 m (32 ft.). The thermal inertia sleeve runs at 1540°C (2800°F), well below the limit for silicon carbide. All other parameters appeared to fully meet the requirements.

Two items received extra attention during this phase of the analysis. These were an evaluation of the convective heat transfer within the cavity and the selection of an optimum aperture size.

b. Aperture Diameter Analysis. There is a trade-off possible between the reradiation and convective losses from the receiver cavity and the amount of the total incident flux which enters the receiver. A large aperture captures nearly all the incident flux but permits high losses. A small aperture has low losses but does not permit much flux to enter. Figure 4-3 shows the results of an analysis of efficiency versus aperture diameter (and thus intercept factor). It shows a fairly flat optimum between 170 mm (6.7 in.) and 210 mm (8.3 in.) aperture diameter. The selected aperture size of 187 mm (7.36 in.) is near the peak efficiency and is thus an acceptable choice for the conceptual design.

c. Convective Heat Transfer Within the Cavity. An analysis was made of the effect of convective heat transfer within the cavity. An

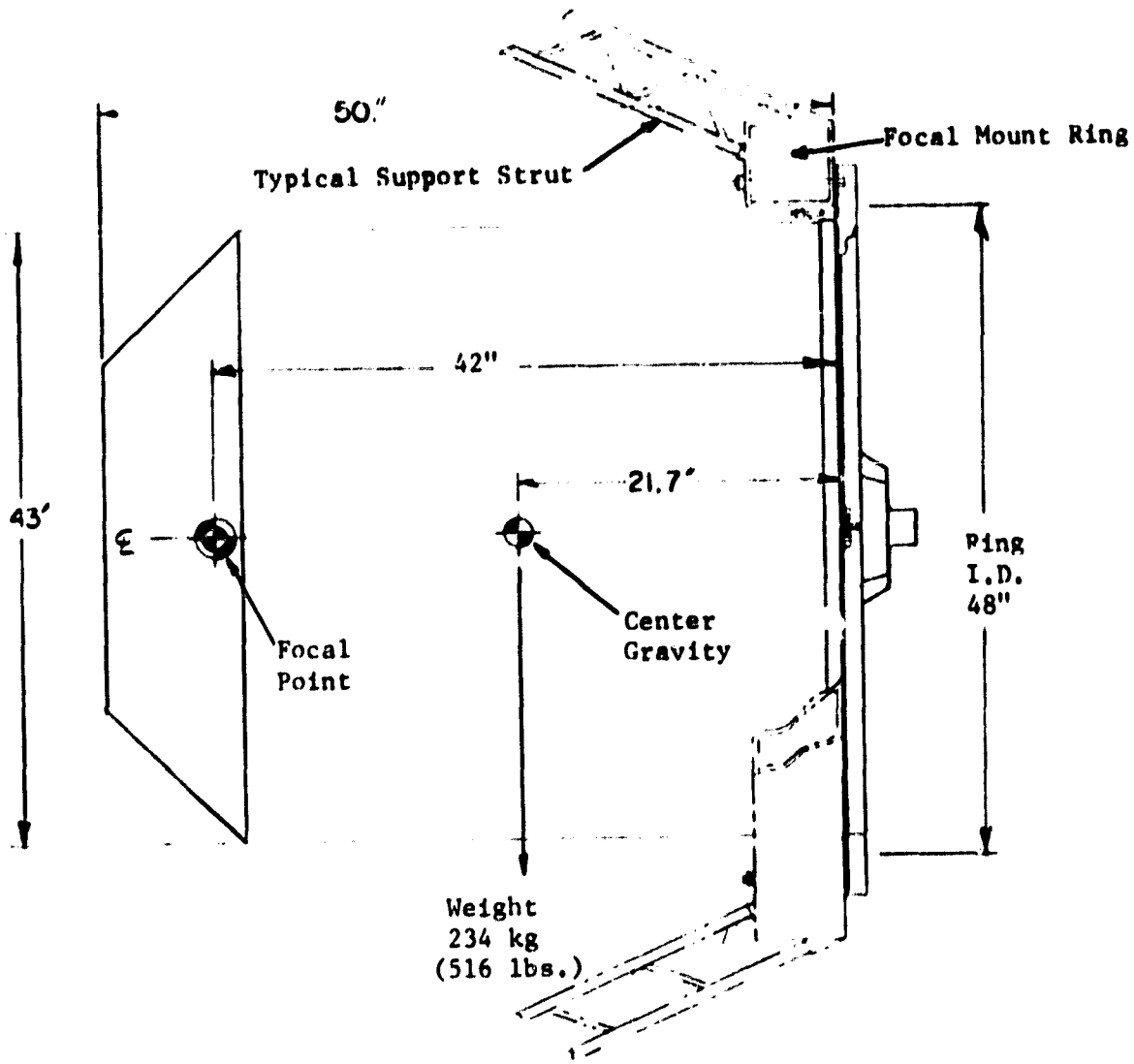

Figure 4-2. High Temperature Solar Receiver Envelope

Table 4-3. Conceptual Design Configuration and Preliminary Analysis

Parameter	Results	
	Metric	Customary
Assumed Concentrator Diameter	11.72 m	38.45 ft.
Nominal Peak Solar Flux to Receiver	91.8 kW	314000 Btu/hr
Intercept Factor Power	0.90	-
Power Entering Receiver Cavity	82.6 kW	282200 Btu/hr
Aperture Diameter	187 mm	7.36 in.
Coiled Tube Outside Diameter	60 mm	2.35 in.
Coiled Tube Wall Thickness	2.5 mm	0.10 in.
Number of Coil Turns	7.5	-
Coil Diameter (Center-to-Center)	425 mm	16.3 in.
Coil Height	575 mm	23 in.
Coiled Tube Length	9.8 m	32 ft.
Ratio of Tube Spacing to Tube Diameter	1.31	-
Receiver Overall Height	1.33 mm	52 in.
Receiver Overall Diameter	1.17 mm	46 in.
Thermal Inertia Sleeve Inner Diameter	290 mm	11.4 in.
Thermal Inertia Sleeve Inner Temperature	1540°C	2800°F
Coiled Tube Outer Wall Temperature	1412°C	2573°F
Heat Losses:		
Through Insulation	4.2 kW	14400 Btu/hr
Cavity Convection	3.6 kW	12500 Btu/hr
Reradiation	16.7 kW	56900 Btu/hr
Net Power to Gas	58.1 kW	198400 Btu/hr
Mass Flow	0.114 kg/s	0.251 lb/sec
Efficiency	0.633	-
Pressure Drop	3.1% ΔP/P	-
Approximate Weight	220 kg	490 lb

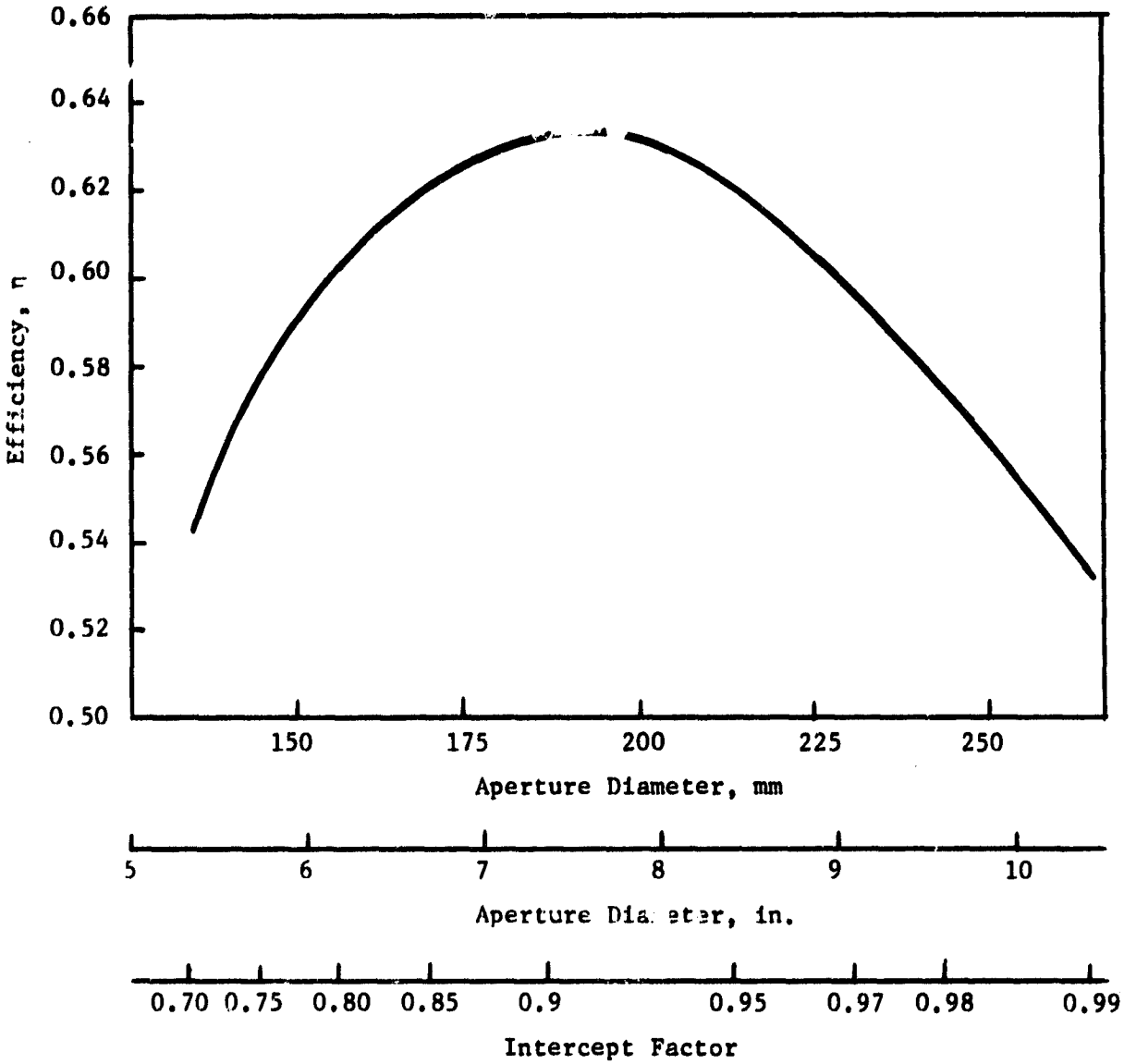

Figure 4-3. Efficiency As a Function of Aperture Diameter

analysis* from work done as part of the Solar Total Energy-Large Scale Experiment at Shenandoah, GA was used to determine the combined effect of wind and natural convection on the heat transfer coefficient to use in this present analysis. The correlation was based on experimental work performed on a test prototype receiver under controlled conditions.

This correlation depends on three variables. The first is the elevation of the receiver measured by the angle ϕ. Zero degrees represents the horizontal position and 90 degrees represents vertical with the cavity facing downwards. The second is the angle of the cavity axis with respect to the wind, with zero degrees represents the wind coming straight into the receiver. The third is the wind velocity in miles per hour. Figure 4-4 shows the effect of these three variables on the heat transfer coefficient. Note that the concentrator will shield, or at least interfere with the wind for wind angles less than about 45°, and that operation at elevations less than 10-15° are not likely due to low solar insolation. A value of the heat transfer coefficient of 3.1 $W/m^2\ ^oC$ (0.53 $Btu/hr\text{-}ft^2\text{-}^oF$) was used to account for various probable conditions.

2. Detailed Analysis

The receiver design was analyzed in more detail using a finite-element heat transfer program that performs a steady-state heat balance calculation. A nodal diagram was constructed as shown in Figure 4-5, showing its geometric and boundary condition details used by the program to calculate the receiver temperature distribution profile, heat losses and tube-air exit temperature. Some of the features of the program include:

- Heat generation due to insolation as a function of flux profile. Figure 4-6 shows a representative flux mapping of the dimensionless intensity ratio at various positions in the receiver for a collector specification as shown. This data was used to provide the flux profile shown in Figure 4-7 giving the receiver axial distribution and the insulation top-cap (z = 30 in.) distribution. The incident radiation in BTU/hr is given as:

$$Q_{inc} = 0.982 \times (\text{area, in}^2) \times (J/\rho I)$$

- Convection heat transfer by natural convection and natural circulation within the receiver cavity.

- Conduction, accounting for thermal conductivity variations with temperature.

- Sleeve radiation losses through the aperture using Script-FA matrix techniques.

- Sleeve-tube-insulation radiation heat transfer.

- Fluid flow and heat-pickup analysis, with air flow temperatures calculated incrementally along the length of the tube.

*Koenig, A.A. and Marvin, M., "Convective Heat Loss Sensitivity in Open Cavity Solar Receivers", General Electric Co. To be Published.

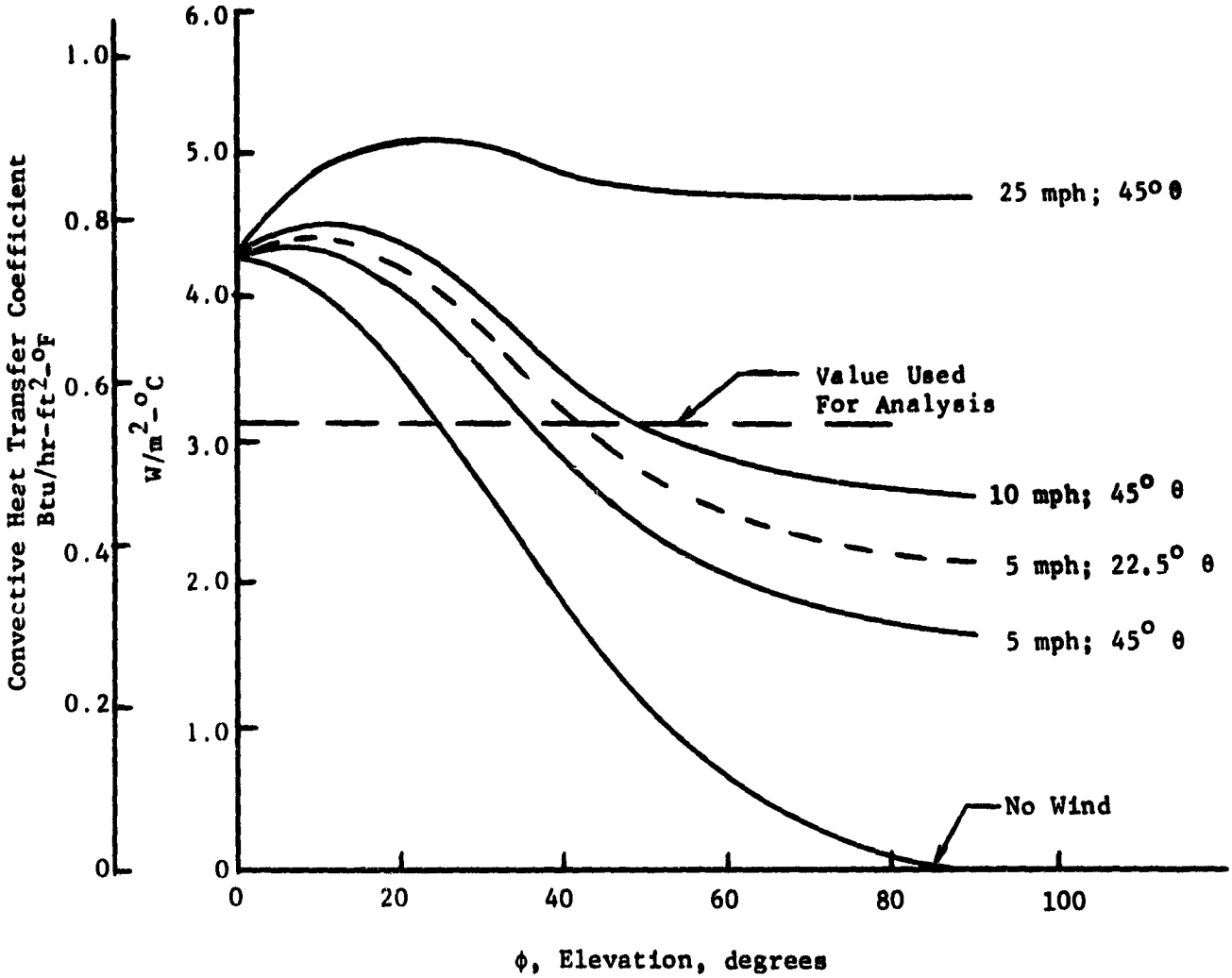

Figure 4-4. Combined Effect of Wind and Natural Convection Within Cavity

ORIGINAL PAGE IS
OF POOR QUALITY

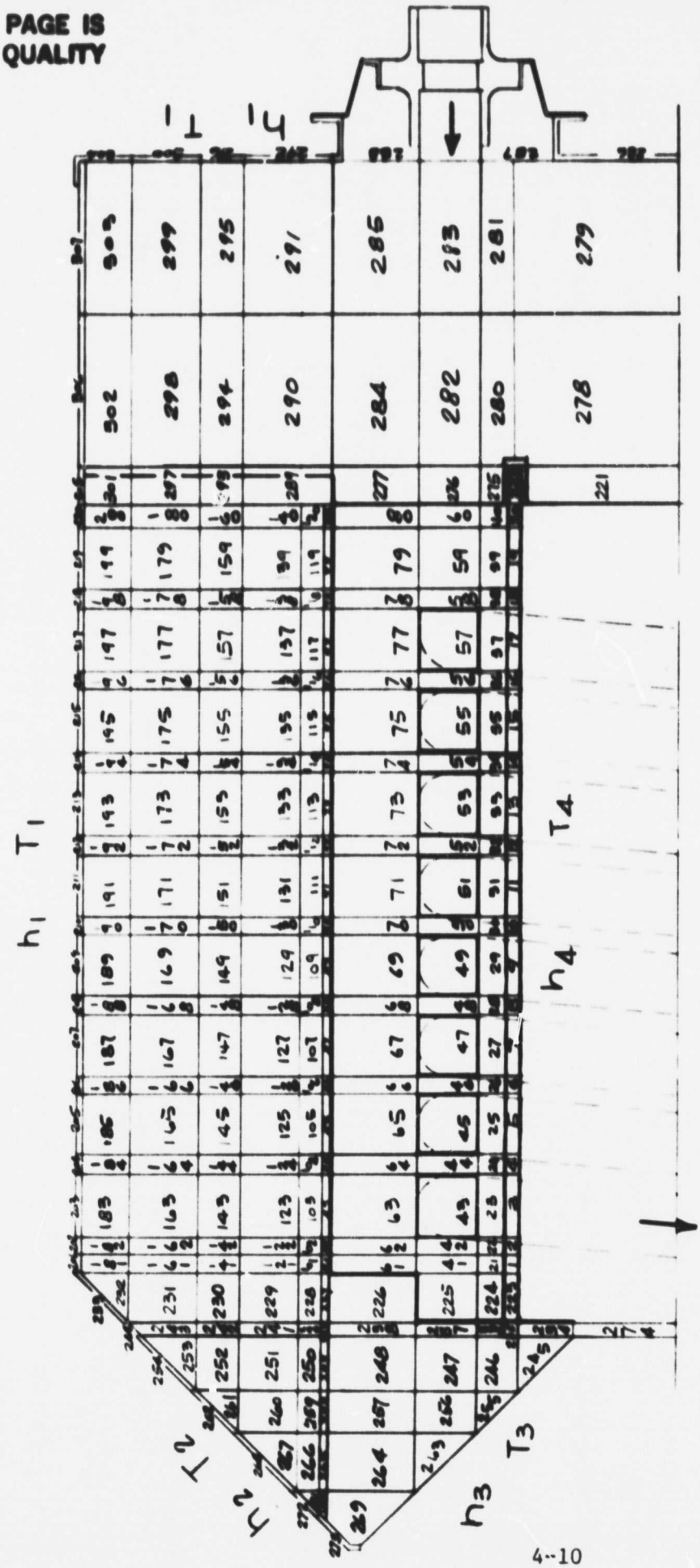

Figure 4-5. Receiver Nodal Diagram for Steady State and Transient Heat Transfer Analysis

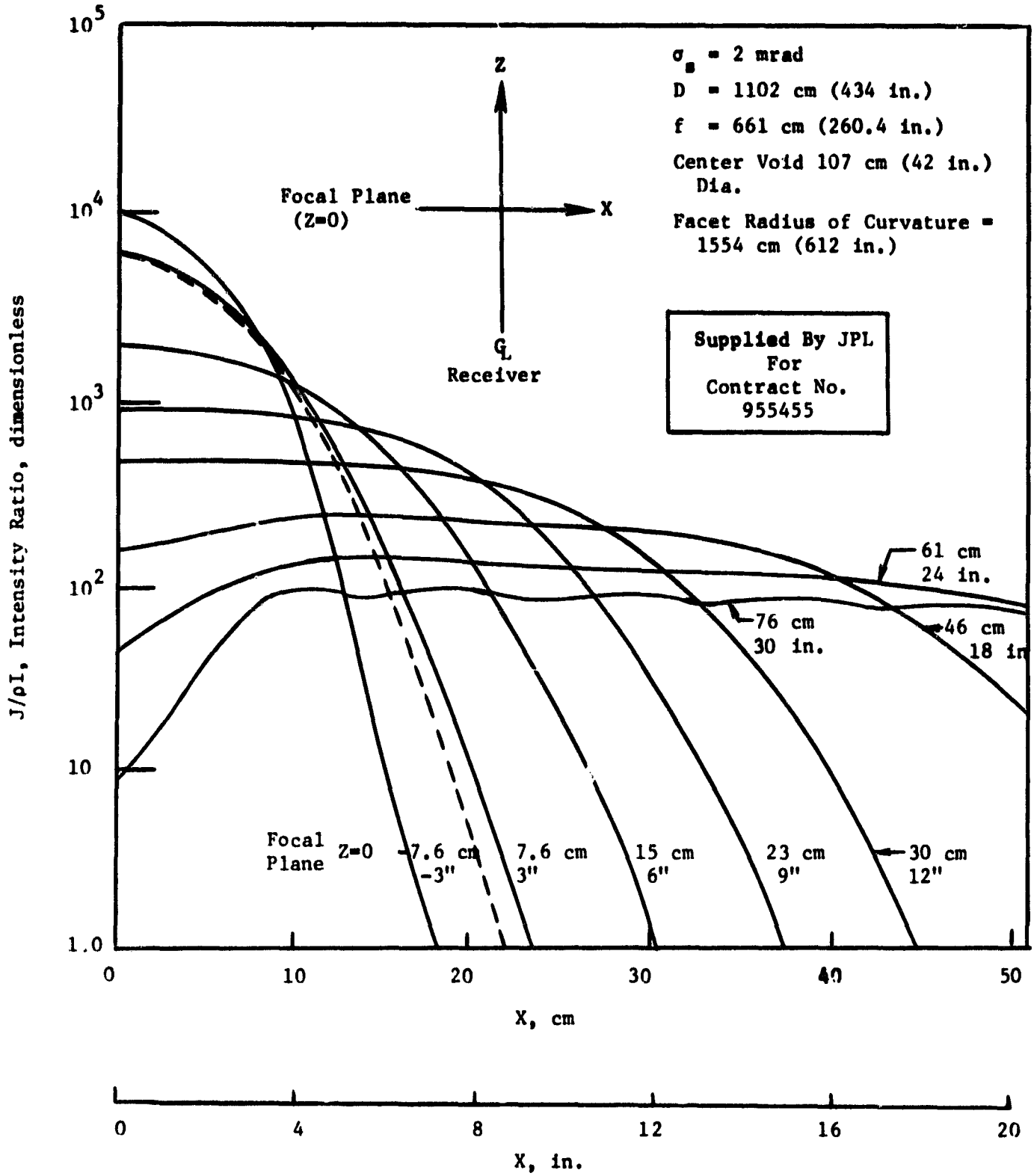

Figure 4-6. Representative Flux Mapping of Receiver

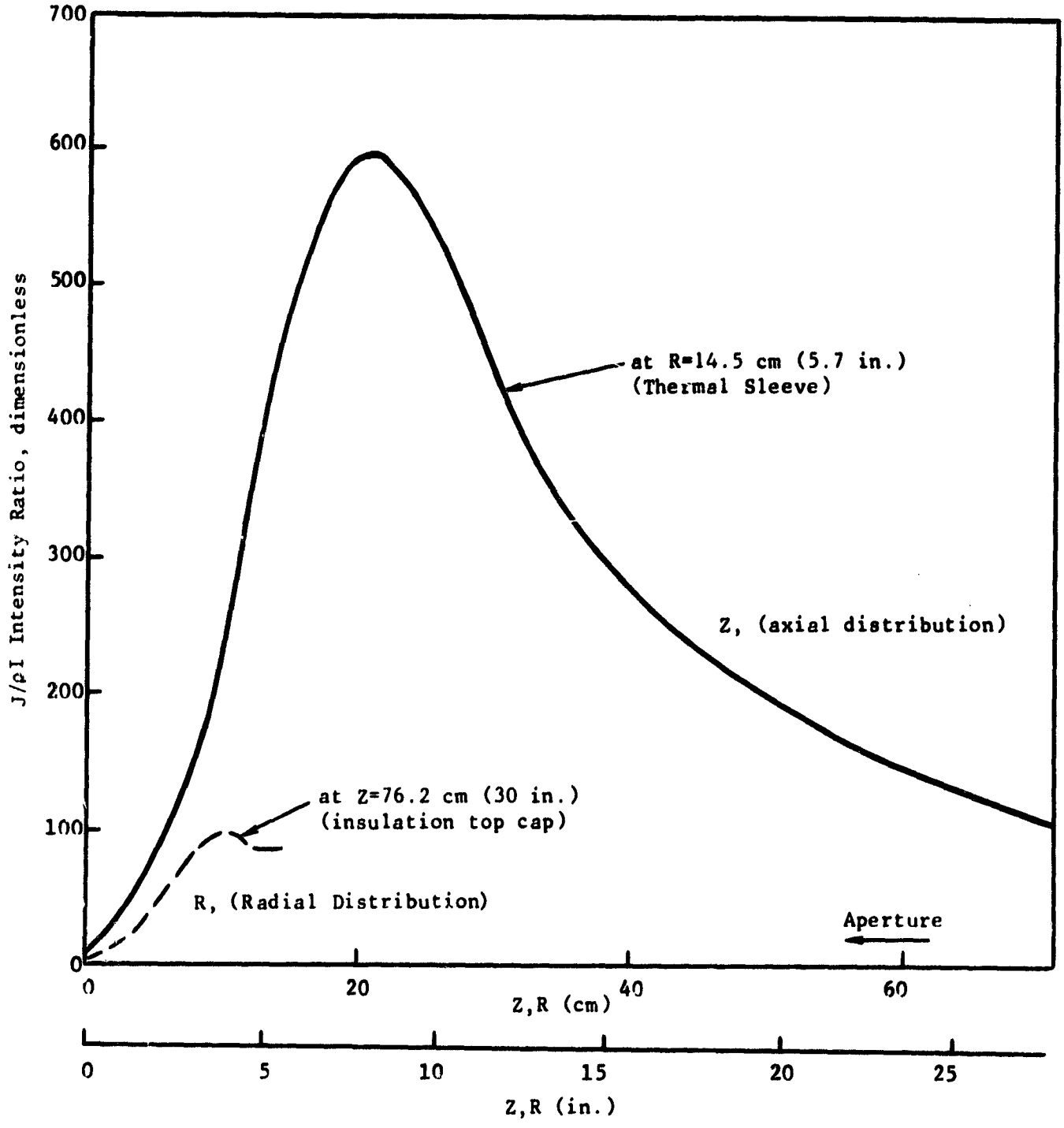

Figure 4.7 Receiver Solar Flux Profile

a. Steady State Temperature Distribution. For a solar influx of 91.8 kW and a 0.9 interception efficiency, with 0.11 kg/sec (0.244 lbs/sec) of air entering at 954°C (1750°F), the steady state temperature profile of the receiver is as shown in Figure 4-8. Average tube, sleeve and insulation temperatures are plotted axially, and air temperatures inside the tube are also shown. Figure 4-9 shows a typical receiver radial temperature distribution.

On the average, a 167°C (300°F) drop is seen between the thermal inertia sleeve and the tube, whereas tube and insulation temperatures follow closely due to low insulation losses. Air exit temperature is 1378°C (2513°F), comparing well with preliminary design expectations.

The highest insulation temperatures were seen inside the thermal sleeve (top cap of insulation) at 1474°C (2685°F), well within insulation capabilities.

b. Heat Losses. The receiver heat-balance is shown in Table 4-4 which details losses through the insulation, reradiation through the aperture and cavity convection, in addition to gas heat pickup. The results are compared to the preliminary analysis using the design program.

Higher reradiation losses than in the preliminary design analysis are seen as expected due to nonuniform sleeve temperatures, whereas insulation losses were lower when insulation detail was considered. An overall efficiency of 62.2% is calculated, including the 90% incidence factor of the aperture (intercept efficiency).

A cavity convection coefficient of 3.12 W/m^{2}-°C (0.55 Btu/hr-ft^{2}-°F) was used, calculated as an average for operating conditions (wind at 8-16 km/hr (5-10 mph), and 25°-55° elevation). Convection losses through natural circulation in the cavity are significant, with an air flow of approximately 0.0018 kg/sec (0.004 lbs/sec) (∿ 1.7% of design flow) pumped through the cavity and exiting at close to sleeve temperatures (1538°C (∿ 2800°F)).

c. Pressure Drop Calculation. Table 4-4 also shows the pressure drop calculation results for the receiver, using air-temperature detailed results from the steady-state analysis (Figure 4-8). A 3.3% pressure loss is experienced in the coiled tube section for an air inlet pressure of 3 atmospheres. If inlet and outlet tube sections are included the pressure loss for the unit becomes 3.8% $\Delta P/P$ (1.67 psi).

d. Effect of Thermal Inertia Sleeve. The high reradiation losses through the aperture, along with the high 169°C (∿ 300°F) temperature differential between the sleeve and the tube indicate that higher receiver efficiencies may be obtained by removing the thermal inertia sleeve and radiating directly onto the tube. Lower cavity temperatures will reduce aperture losses appreciably due to the fourth-power-law radiation loss.

The design program was modified to simulate the no-sleeve case. For the 91.8 kW concentrator input and 0.9 interception efficiency, re-

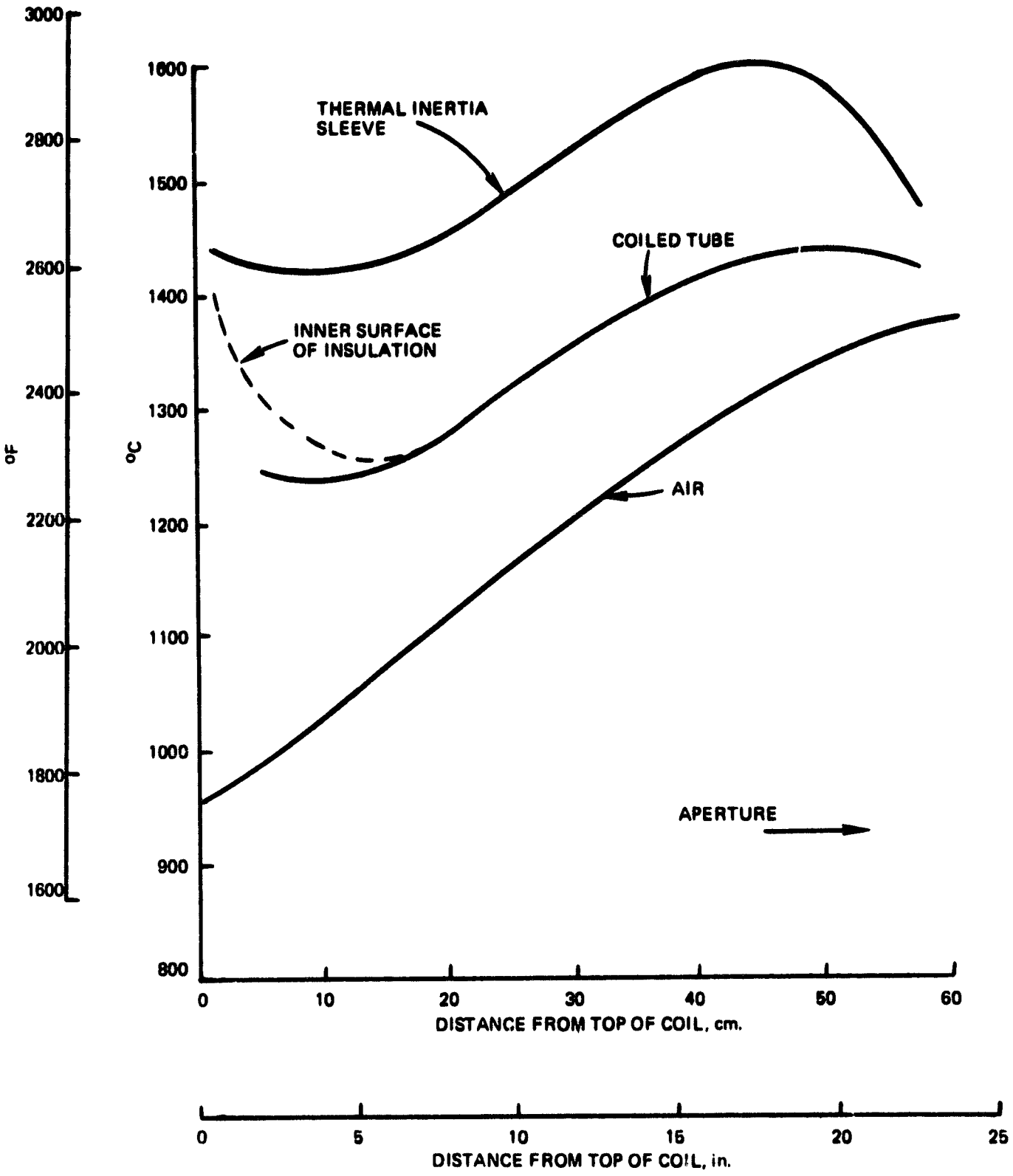

Figure 4-8. Design Point Steady State Axial Temperature Distribution

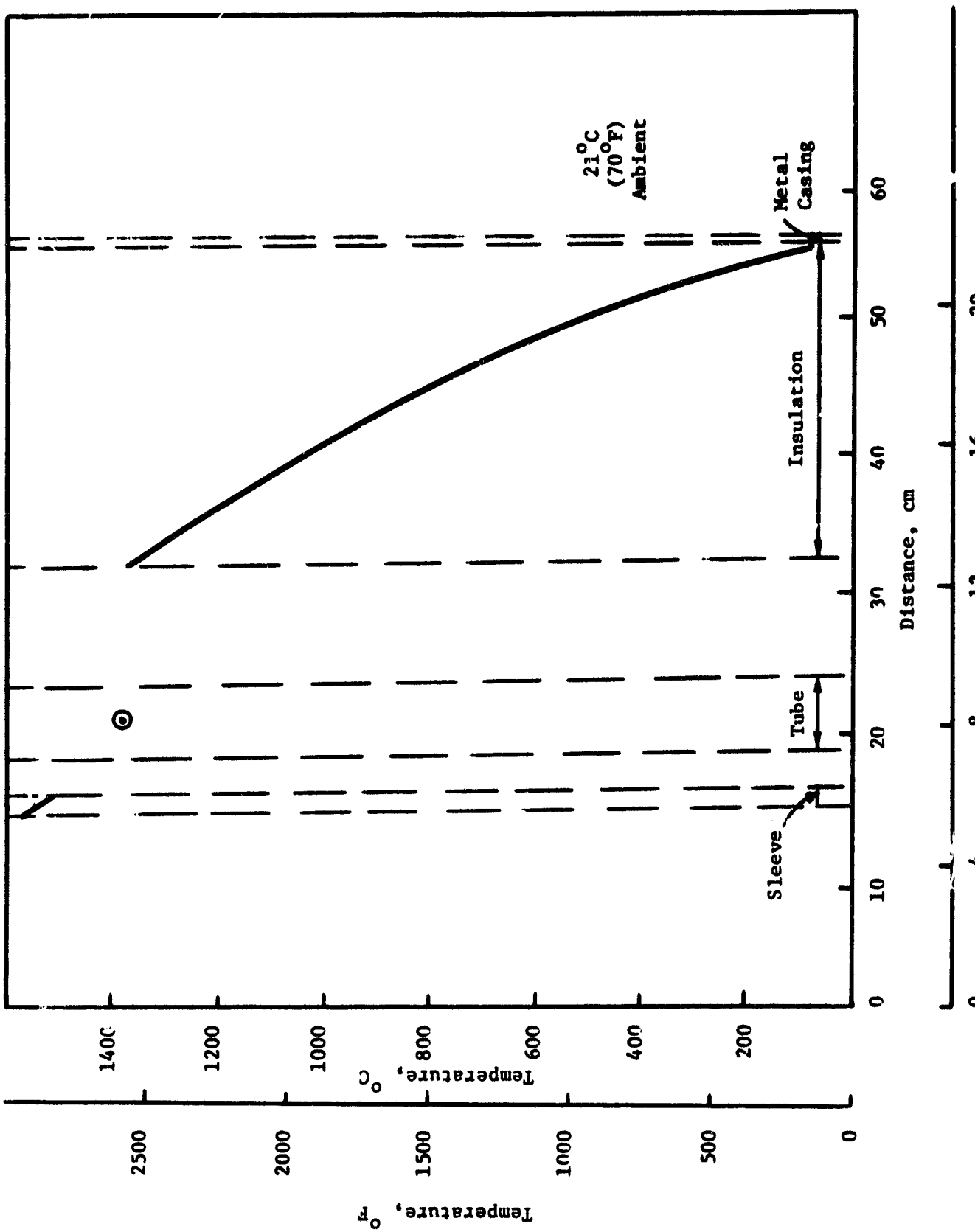

Figure 4-9. Receiver Radial Temperature Distribution (25 cm From Aperture)

Table 4-4. Heat Loss and Efficiency Comparison

Parameter	Units	Parametric Analysis Computer Code Results	Detailed Steady State Heat Transfer Analysis
Power Reflected from Concentrator	kW	91.8	
Power Entering Aperture @ 90% Incidence Factor	kW	82.6	
Losses: Through Insulation	kW	4.2	2.6
Cavity Convection	kW	3.6	3.5
Reradiation	kW	16.7	19.4
Total Losses	kW	24.5	25.5
Net Power to Gas	kW	58.1	57.1
Efficiency	%	63.2	62.2
Pressure Drop, Coil Alone	% ΔP/P	3.1%	3.3%
Pressure Drop, Entire Unit	% ΔP/P	-	3.8%

ceiver over-all efficiency went up to 68.8%, up by 8.7% from the sleeve case. The efficiency gain is due to lower aperture losses in addition to lower cavity convection losses for the wider cavity at lower temperatures.

The increase in efficiency is certainly desirable, but the need for the sleeve is also based on other critical considerations. The sleeve improves transient response capabilities by shielding the tube against thermal shock during abrupt insolation jumps. The large sleeve mass also improves receiver thermal energy storage capacity in case of passing cloud cover. It becomes critical in providing system response-time in case of loss-of-flow transients. Receiver transient response is analyzed in a subsequent section (V-C.).

3. Off-Design Performance Analysis

a. Introduction. The performance at the design point for the high temperature solar receiver is presented in Section III-D. It is of interest to investigate how the efficiency, pressure drop, etc. change with the values of mass flow rate, fluid pressure, and temperature. For the off-design performance analysis the range of values investigated are as follows:

Mass Flow Rate	0.09-0.14 kg/sec (0.2-0.3 lbm/sec)
Inlet Fluid Pressure	2-8 atmospheres
Inlet Temperature	$\pm$ 83°C ($\pm$ 150°F)
Outlet Temperature	$\pm$ 83°C ($\pm$ 150°F)

The analysis was performed by systematically changing only one variable at a time while other parameters were held constant at the design point.

b. Influence of Mass Flow Rate. The change in mass flow rate through the receiver (0.09-0.14 kg/sec) is associated with change in input power level to the receiver which varies from 80 kW to 115 kW thermal. As the mass flow rate increases, the tube inside film coefficient increases giving a higher heat transfer rate. Thus the receiver efficiency and the output power increases as the flow rate increases, as can be seen in Figures 4-10 and 4-11. The pressure drop across the coil which is dependent on the fluid velocity head increases as mass flow rate increases. From the receiver efficiency standpoint, it is advantageous to operate the receiver at high mass flow rates and input power levels. The resulting high value of $\Delta P/P$ can be reduced by operating the receiver at higher pressures (see Section IV-B-3-c).

c. Influence of Inlet Fluid Pressure. The inlet fluid pressure was varied from 2 to 8 atmospheres while the input power level and the fluid temperatures were held constant at the design values. For constant mass flow, and as a first approximation, the conventional relationship for pressure drop is directly proportional to the specific volume of the fluid. For a perfect gas, the pressure drop is therefore inversely proportional to the pressure level, and the fractional pressure drop is given by the following relationship.

$$\frac{\Delta P}{P} \propto \frac{1}{p^2}$$

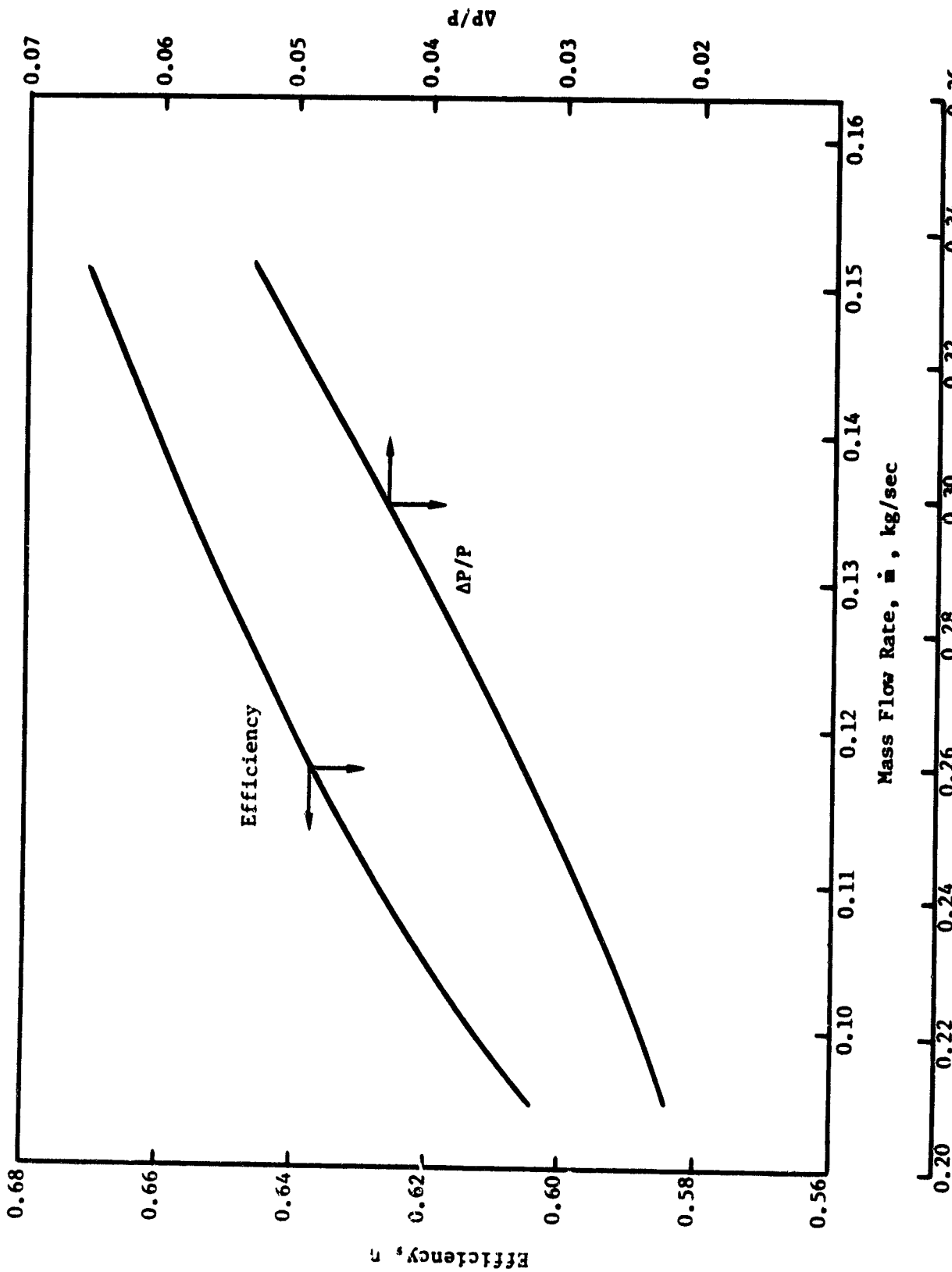

Figure 4-10. Off-Design Performance as a Function of Mass Flow Rate

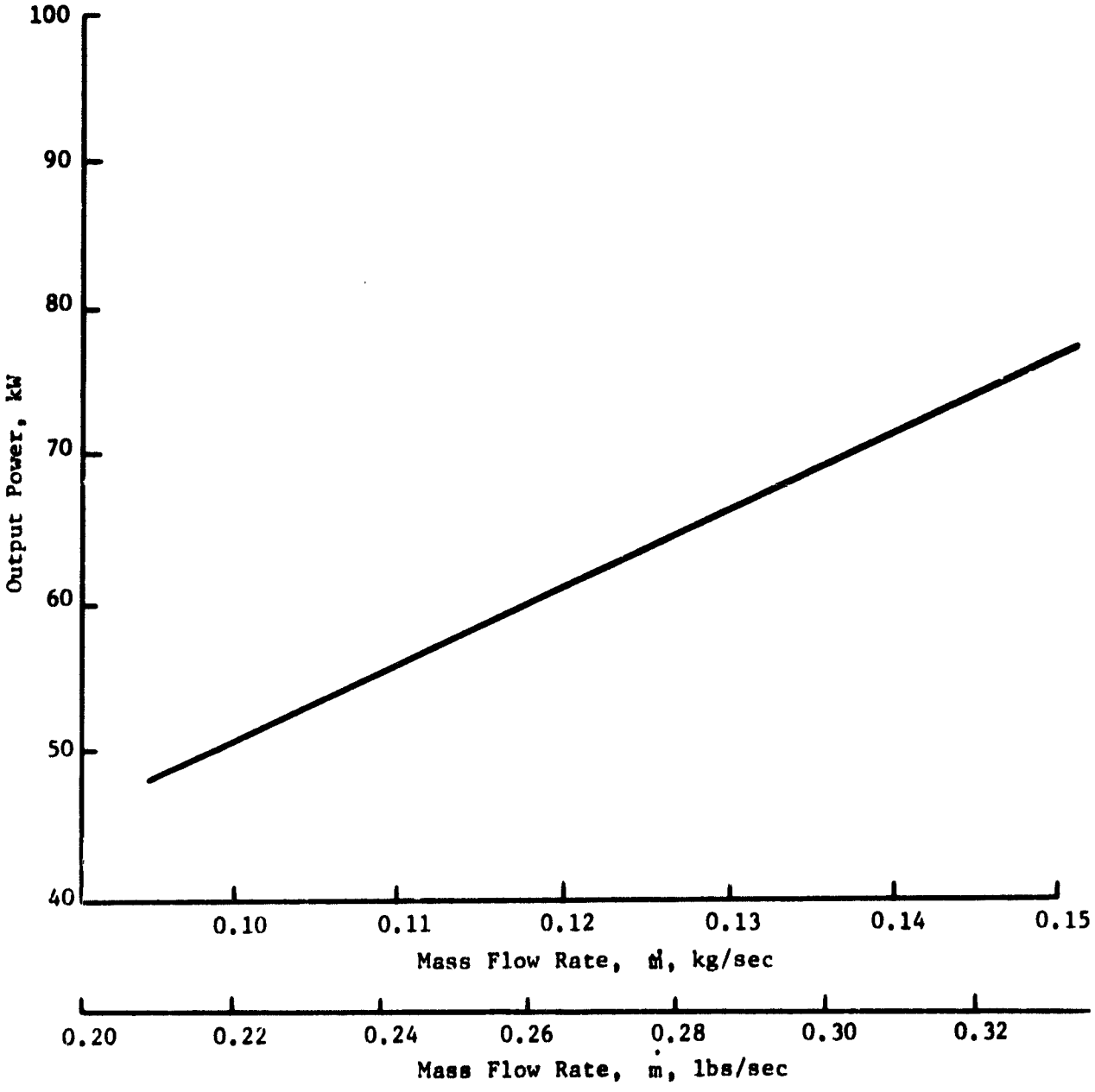

Figure 4-11. Output Power as a Function of Mass Flow Rate

Thus, in Figure 4-12, the computed variation of $\Delta P/P$ is plotted as a function of inlet fluid pressure. $(\Delta P/P)$ decreases rapidly at small values of P and becomes asymptotic at higher pressures. Thus, in order to reduce $(\Delta P/P)$ and consequently the operating cost, the fluid pressure should be maintained as high as possible without inducing excessive mechanical stress in the tube. The receiver efficiency and mass flow rate are not affected by the pressure level.

d. Influence of Exit Fluid Temperature With a Constant ΔT Across The Coil ($417^{o}C$). The exit gas temperature was changed from $1232^{o}C$ to $1454^{o}C$ keeping the fluid ΔT across the coil at $417^{o}C$ ($750^{o}F$) and the power level at 91.9 kW thermal. As the exit gas temperature is increased there is a proportional increase in the sleeve inside temperature which increases the losses due to radiation and convection. Thus at constant input power level, the heat loss increases as the exit gas temperature increases and consequently the useful heat transfer rate to the gas is reduced. Thus the efficiency decreases with increase in gas temperatureas shown in Figure 4-13. Furthermore, since ΔT is held constant, with the decreased power output ($mC_p\Delta T$) the mass flow rate and hence the pressure drop decrease with increase in gas temperature as also shown in Figure 4-13.

e. Influence of Fluid Temperature Rise Across the Coil. At a constant input power level, the variation of efficiency, mass flow rate and pressure drop as a function of temperature rise across the coil (ΔT) are shown in Figures 4-14, 4-15 and 4-16. In this study the exit gas temperature is an independent parameter.

At a constant exit gas temperature, the sleeve inner temperature and the receiver heat loss increase slightly as ΔT increases. Thus the drop in efficiency is very small since the input power is constant, the output power follows the same trend as efficiency. The mass flow rate and consequently the pressure drop decrease as ΔT increases (Figure 4-15 and 4-16).

As the exit gas temperature is increased, there is a proportional increase in sleeve inner temperature which increases the receiver heat loss. The ΔT has no significant influence on the efficiency.

C. MATERIALS SELECTION AND EVALUATION

1. Introduction

The key components of the receiver are made out of engineering ceramics. Consideration of the brittle behavior and shock resistance are the prime material property parameters to be addressed.

Brittle behavior is best controlled by careful processing to limit and minimize structural defects which in turn control the usable strength of the material and then designing the component to be stressed

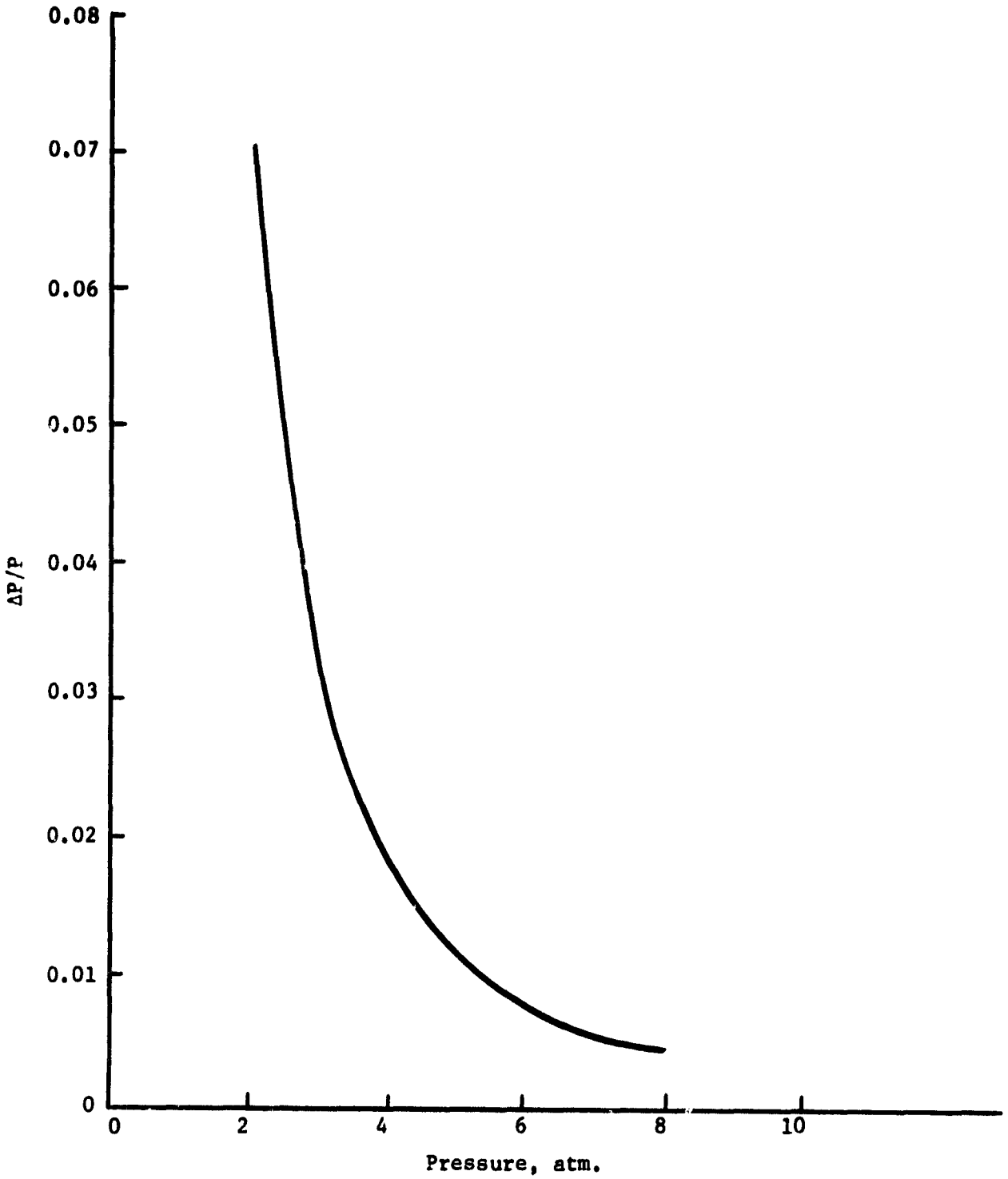

Figure 4-12. Pressure Drop Variation With System Pressure Level

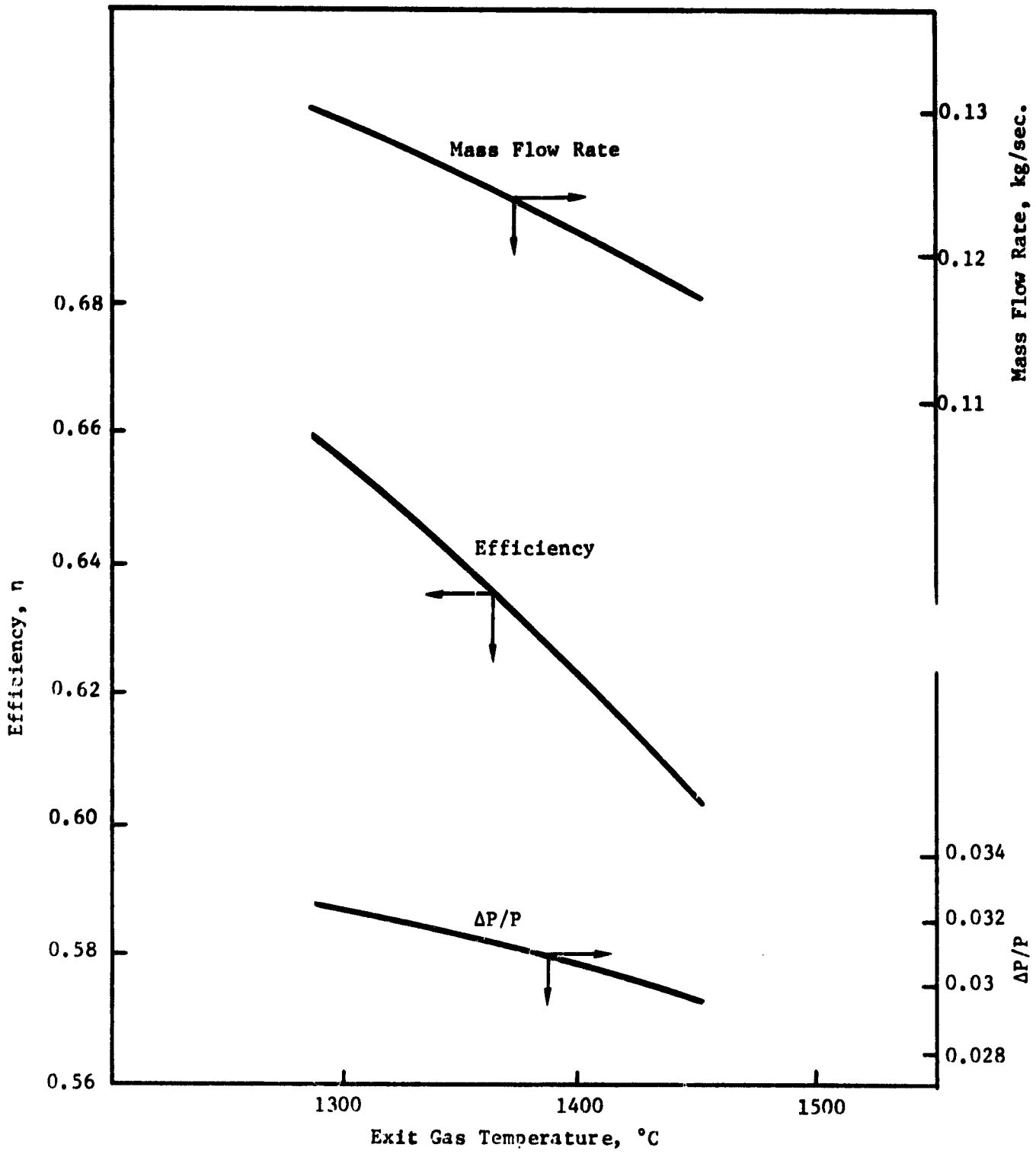

Figure 4-13. Effect of Exit Gas Temperature With a Constant Inlet-Exit Temperature Rise

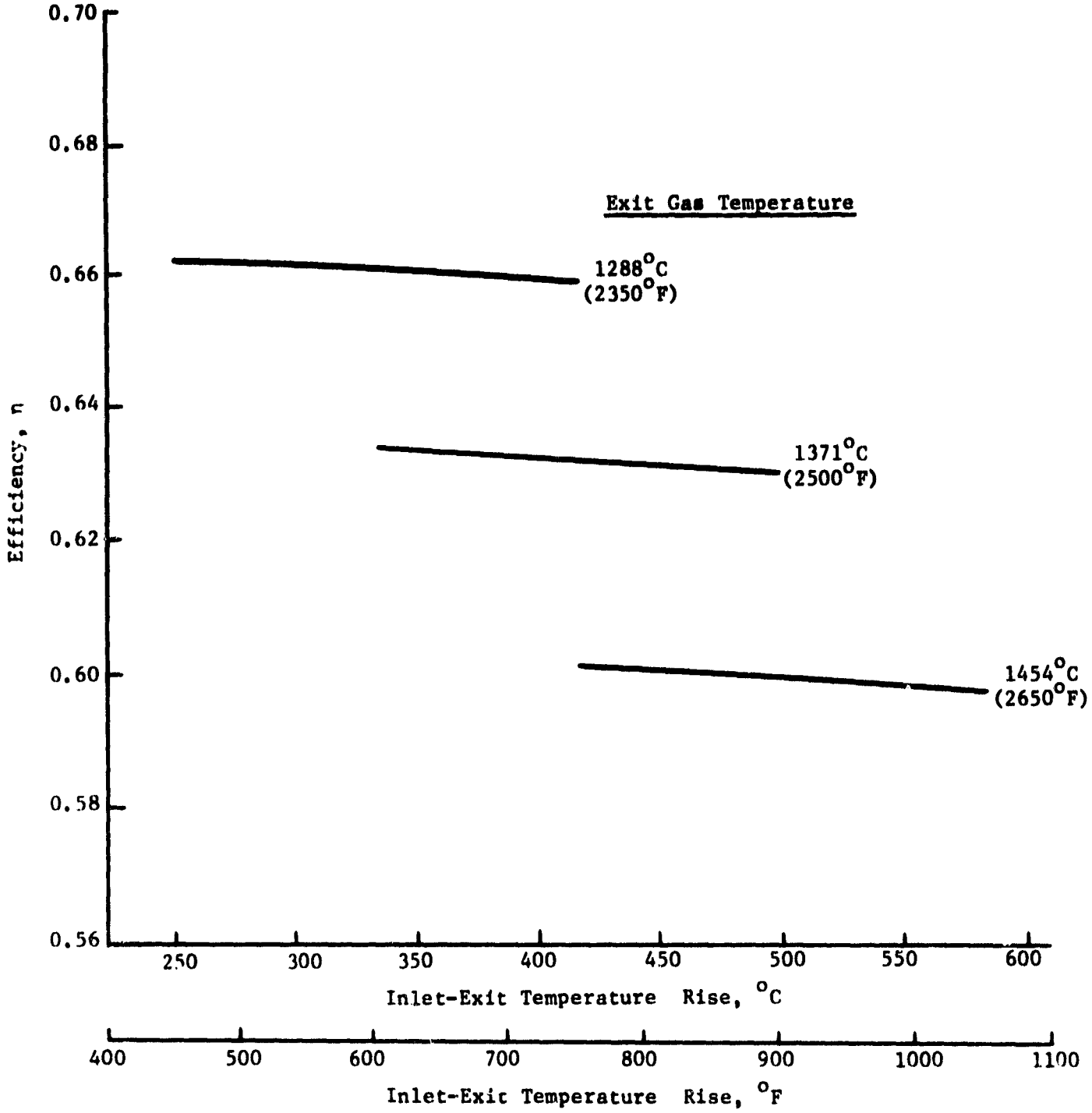

Figure 4-14. Performance as a Function of Temperature Rise.

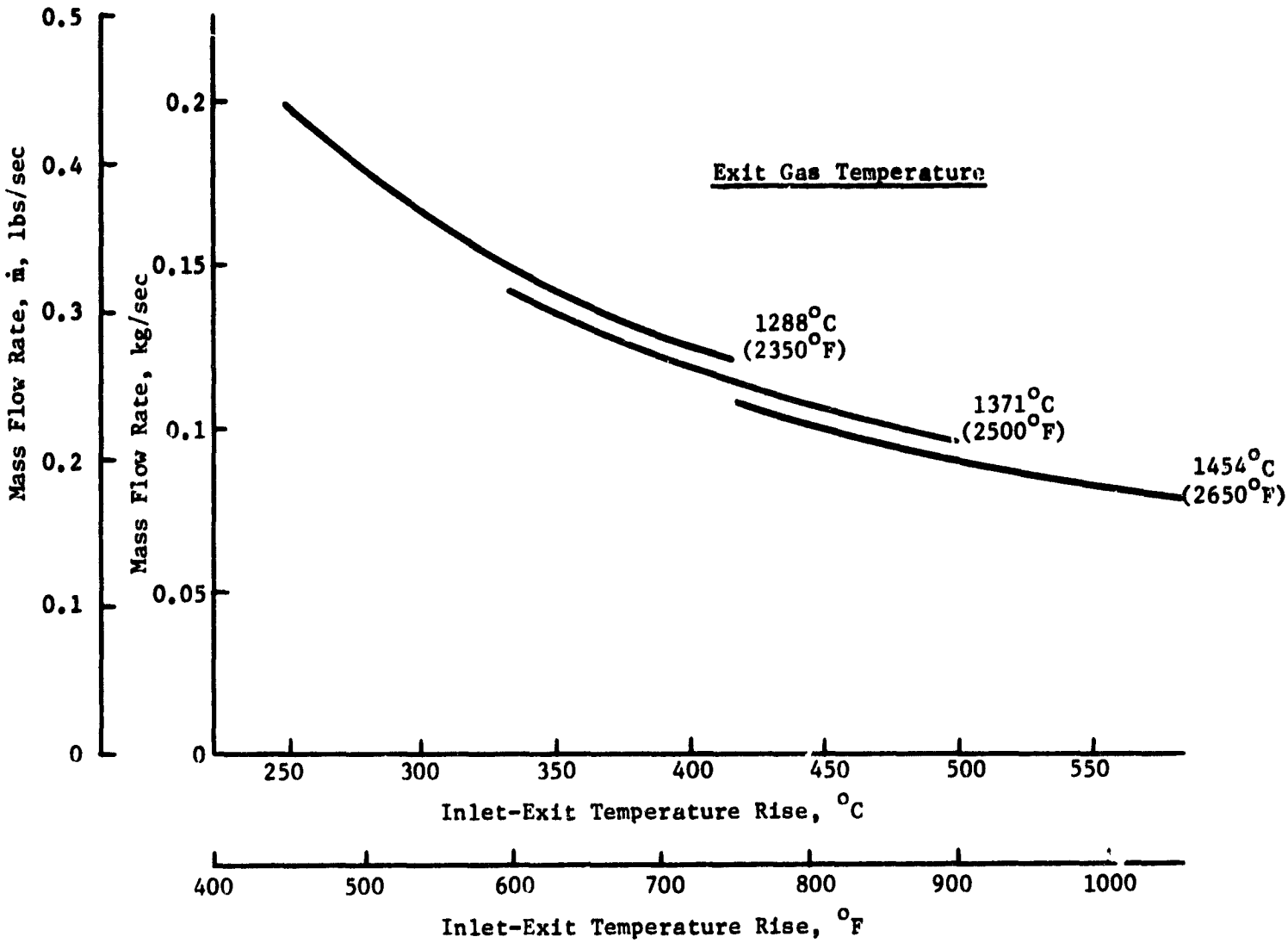

Figure 4-15. Effect of Temperature Variation on Mass Flow Rate

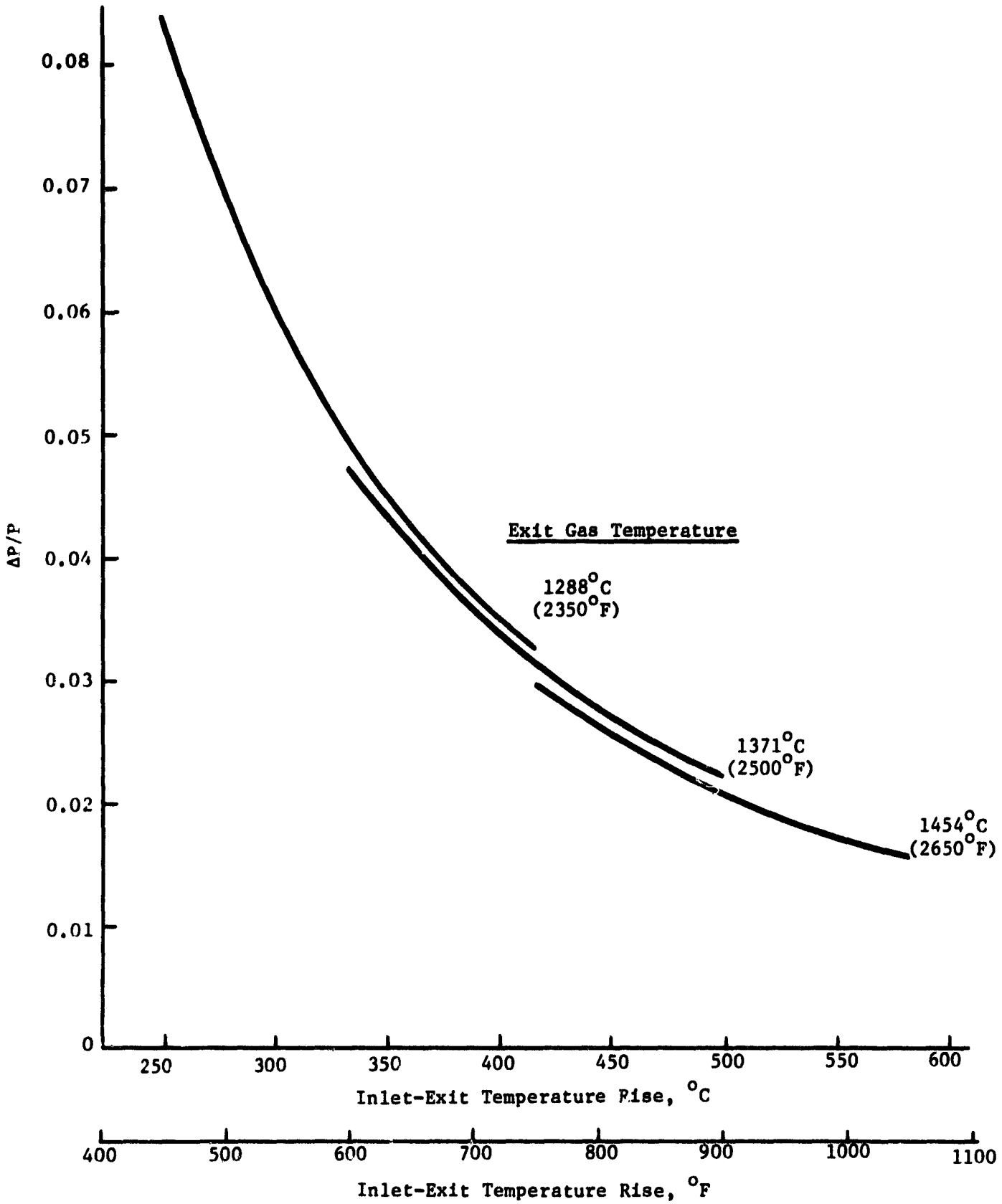

Figure 4-16. Effect of Temperature Variations on Pressure Drop

at strength levels considerably below measured values. Statistical studies of such brittle materials have been made using Weibull statistical data that can predict strength behavior to the 99.99% confidence level. This approach is being actively used to utilize structural ceramic components in heat engines such as gas turbines, Stirling engines, diesel engines, both regenerative and recuperative heat exchangers, etc.

Thermal shock resistance is described theoretically by considering strength, (σ), thermal conductivity, (k) and Youngs modulus (Y) such that a thermal shock parameter:

$$T_s \propto \frac{\sigma k}{Y}$$

is as large as possible.

These further limitations of strength and thermal shock resistance narrow the choices of materials of construction of the components including the heat exchanger helical coil, thermal sleeve, and pressure seals to silicon nitride, silicon carbide and mullite ($3Al_2O_3 \cdot 2SiO_2$) which are the materials choices settled upon for heat engine applications as well.

Finally, the insulating system was considered combining the parameters of melting point, thermal conductivity, structural weight, strength, and cost.

2. Component Parts

a. Helical Coil and Pressure Sleeves. The choice of materials for these components as mentioned earlier are the silicon nitrides or carbides and possibly mullite. With the exception of mullite, there is also a question of which particular composition to choose from a rather vast range even within these two generic groups of materials. When one considers properties, fabricability, and expected performance however, there appears to be some distinctive reasons for selecting the silicon nitride rich sialons. Briefly, while the silicon carbides are sinterable and show high conductivity and strength, the higher thermal expansion (6.2 vs. 3 to 3.3 x 10^{-6}/°C for silicon nitride) and the lower modulus (60 x 10^6 vs. 35 x 10^6 psi for silicon nitride), the fracture behavior, and the degradation mechanism(s) in reducing atmospheres appear to be causes for concern mitigating against their choice in this application. Further, it is the high silicon nitride sialons which are formable and sinterable by essentially conventional ceramic techniques which add to their status as the material of choice for these applications.

The third material considered for this applicaiton, mullite, also does not compare favorably with sialon when thermal expansion (5.3 x 10^{-6}/°C) and thermal conductivity are compared although it is an easily fabricated, conventional, and inexpensive oxide ceramic material.

Typical intrinsic properties of GE128 sialon recently developed at the General Electric Space Science Laboratories and considered the prime material of choice for these applications are shown in Figures 4-17, 4-18 and Table 4-5. Figure 4-19 shows how a Weibull analysis shifts strength parameters down to about 50% of their measured value to reach a 99.99% confidence level of performance.

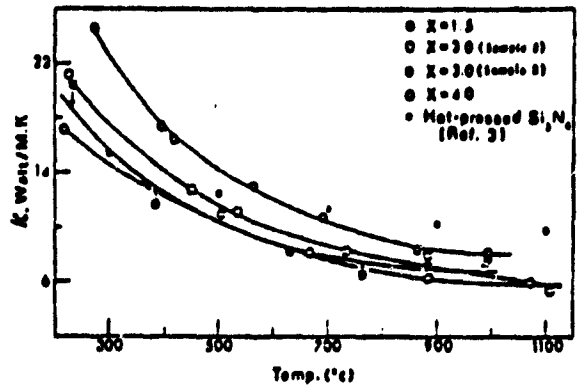

Figure 4-17. Thermal Conductivity of Hot Pressed Silicon Nitride and Selected $Si_{6-x}Al_xO_xN_{8-x}$ where x=1.5, 3 and 4 after Rao, Kokhtev and Lockman, "Electrical and Thermal Conductivities of Sialon Ceramics," Dept. of Materials Science and Eng., Univ. of Florida, Gainsville, Fla. 32611

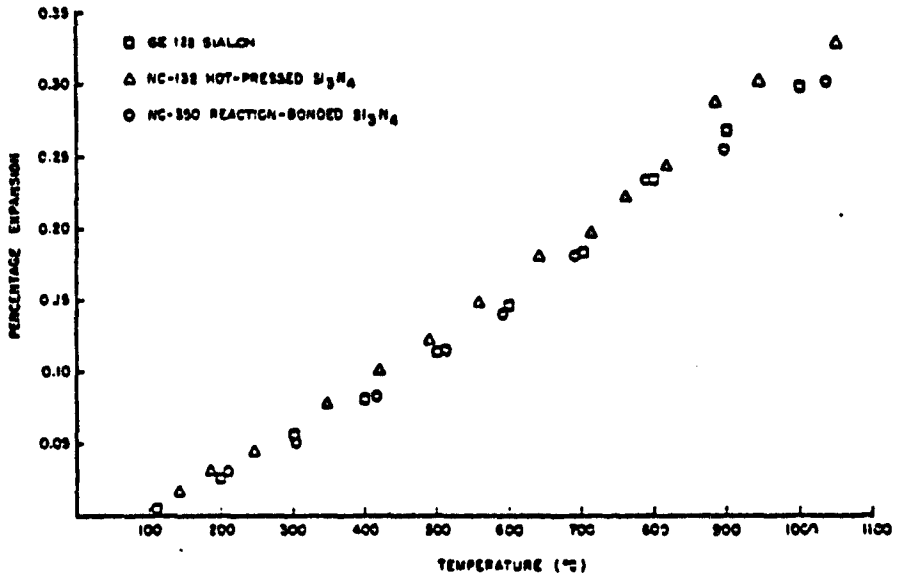

Figure 4-18. Thermal Expansion of GE-128 Sialon, Hot Pressed and Reaction Bonded Silicon Nitride

Table 4-5. Physical Properties of Some GE-SSL Sinterable Si_3N_4 Compositions

Designation	Composition in percent by weight before processing			Modulus of Rupture(a)				Density	Young's Modulus	
	Si_3N_4	Al_2O_3	AlN	Room T		1370°C		gm/cc		
				MPa	psi	MPa	psi		GPa	psi
GE-102	40	60	15	414	60,000	165	24,000	3.07	218	31.6x10^6
GE-128	66	24	10.0	345	50,000	190	27,500	3.10	251	36.4x10^6
GE-129(b)	88.7	8.0	3.3	345	50,000	Not tested		3.10	258	37.4x10^6
GE-130(b)	94.5	4	1.5	345	50,000	Not tested		2.96	Not tested	

(a) Best values

(b) Determined by P. Land, AFML, to be published

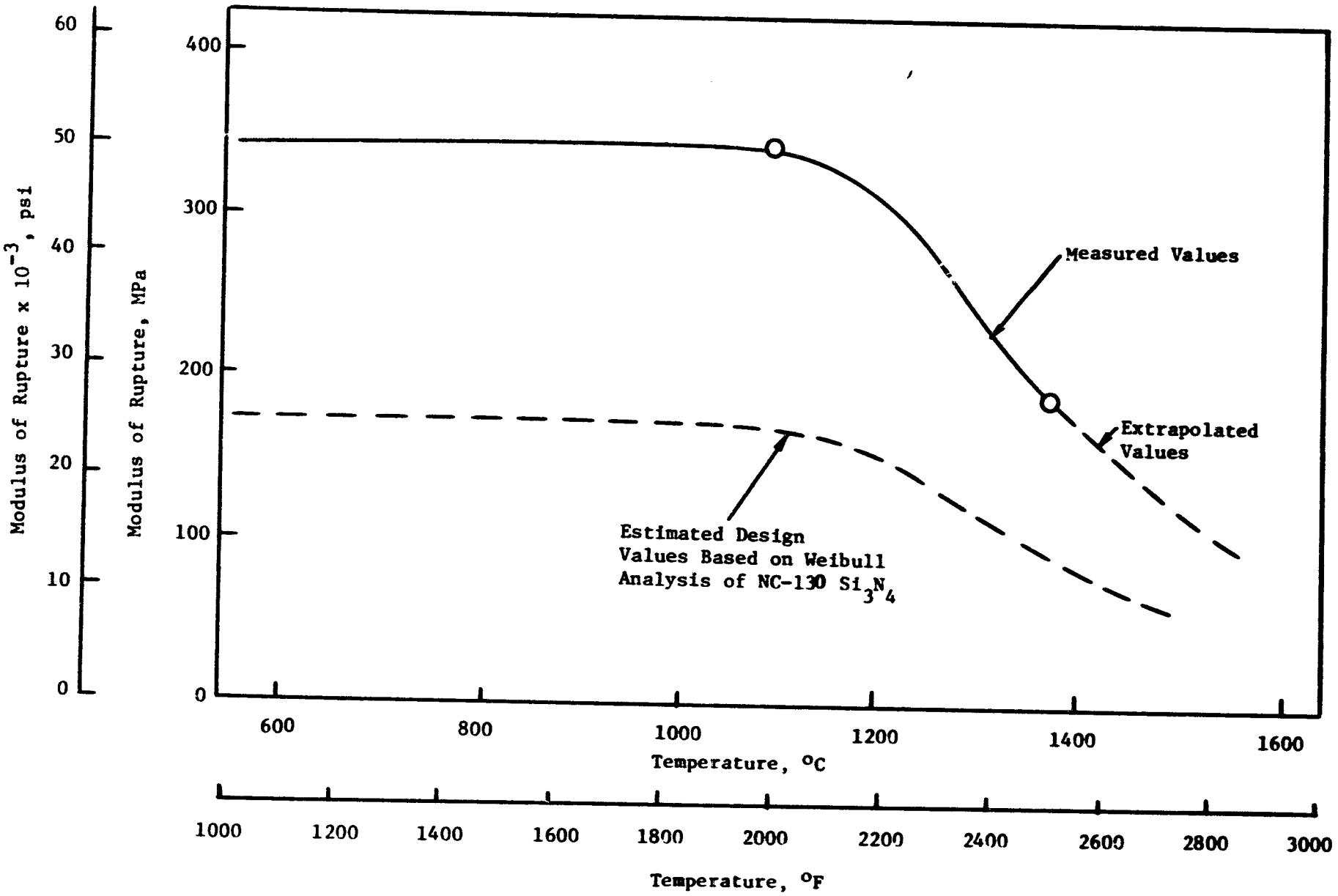

Figure 4-19. Rupture Strength of GE 128 Sintered Silicon-Nitride

b. Thermal Inertia Sleeve. The thermal inertia sleeve is the first refractory component to receive the solar energy flux. It must be refractory, have high emissivity, good thermal shock resistance, high thermal conductivity, and moderate cost. From previous discussions, silicon nitride or a sialon would be a good choice for this component also, except that such a massive part is presently beyond the state-of-the-art. It is recommended then that the thermal inertia sleeve be a purchased part fabricated from Norton Company Crystar® silicon carbide. Typical material properties of this material are shown in Table 4-6.

c. Thermal Insulation. Numerous kinds (compositions) and shapes of materials are available commercially for use as thermal insulation. Examples are mica in flake form, asbestos, glass, oxide and mixed oxide fibers, and glass and mixed oxide hollow spheres. For this program, we have selected two generic fibrous insulations. One type, useful to 1260°C (2300°F), consists of roughly equal (52 w/o: 48 w/o) parts of alumina (Al_2O_3) and silica (SiO_2) and is commonly made from a high purity kaolin clay. The other type consists of 95% Al_2O_3 and 5% SiO_2 and is useful to 1650°C (3000°F). The former material is variously marketed as Kaowool®, Barikaid®, and Fiberfrax® depending on the manufacturer. The high alumina fiber is made by only one firm under the tradename Saffil®, and is available through Babcock and Wilcox in the U.S.

Fibrous thermal insulation depends on small, enclosed pockets of air or gas which retard heat flow. Each pocket must be small enough to slow convective heat flow and the heat flow path must be long and circuitous to minimize conduction. In addition the fibers should be opaque to reduce radiative heat flow.

The availability of fibrous insulation as loose fibers, felt, semi-rigid or rigid board presents the engineer with a design versatility that many materials cannot match. For example, heat losses can be controlled not only by the inherent thermal conductivity of a material, but in the case of fibrous materials, also by the density to which the fibers are packed.

Fibrous insulation forms the conical large opening in the solar receiver. This surface is thus not naturally highly reflective and may require a highly reflecting (or at least low absorbtivity) surface coating to reduce heating and to perhaps reflect some energy in this area. Coatings and glazes are readily available for this application. A dense alumina wash, followed by a highly reflecting refractory glass coating would be fired on the conical surface to form a thin dense reflecting skin.

Fibrous insulation will form the mechanical and structural member which may have to support the helical coil in position within the solar receiver through welded protrusions. These fibrous protrusions may not have adequate compressive strength to carry the expected loads (although in the present design they can). If necessary, means are available to reinforce these pressure areas. An alumina wash would be ap-

Table 4-6. Typical Material Properties of Norton Company Crystar® Silicon Carbide*

Chemical Constituents	Recrystallized silicon carbide (99% pure)
Maximum Use Temperature (in oxidizing atmostphere)	3200°F 1760°C
Bulk Density (typical)	162 lbs/ft^3 2.6 g/cc
Apparent Porosity (typical)	18%
Thermal Conductivity	
1000°F	180 BTU/hr/sq ft/in./F°
1500°F	165 BTU/hr/sq ft/in./F°
2300°F	145 BTU/hr/sq ft/in./F°
2900°F	135 BTU/hr/sq ft/in./F°
Specific Heat	.15 @ room temperature .35 @ 3000°F
Electrical Resistivity	
at room temperature	100 ohm-cm
at 600°C (1110°F)	0.3 ohm-cm
Modulus of Elasticity	30 x 10^6 psi
Crushing Strength	100,000 psi
Modulus of Rupture	
at room temperature	14,000-18,000 psi
at 1500°C (2730°F)	18,000-22,000 psi
Linear Thermal Expansion	4.8 x 10^{-6} per °C (30-1500) 2.7 x 10^{-6} per °F (70-2600)

*From Norton Data

plied to these protrusions and fired to form a strong thin layer of dense alumina. This reinforcement would serve to spread the anticipated compressive loads over a large area so that adequate mechanical support would be available.

D. MECHANICAL DESIGN

For purposes of discussion, the heat receiver conceptual design as shown in Figure 4-1 is broken down into five (5) major components. These components are as follows:

- The Ceramic Coil (heat exchanger)
- The Thermal Inertia Sleeve
- The Pre-formed Insulation
- The Outer Casing and Support
- The Ceramic Joints

1. Ceramic Coil

The ceramic coil is fabricated from sintered silicon nitride. The coil geometry, along with some dimensional data, is shown in Figure 4-20. The coil was computer-modeled and stress-analyzed at operating pressure and temperature. With the inlet and outlet ends of the coil fixed in space, stresses were computed with the coil in various attitudes. Since the stresses were relatively low (see Engineering Analysis Section IV-E), it was decided that mounting the coil from the inlet and outlet connection couplings and allowing freedom for the coil to expand thermally in all directions would be desirable. The ceramic couplings would be joined to the coil prior to assembly of the coil into the heat receiver. The metallic-to-ceramic external type of seal would be brazed to the ceramic coupling after the couplings are joined to the end of the coil.

The ceramic tubing wall thickness was selected as being adequate for extrusion. The spacing between coil turns will allow insertion of a mold for coil support during the "green" state of fabrication. Long sweeping radii at the junction of inlet and outlet sections with the coil are indicated to facilitate ease of fabrication.

2. Thermal Inertia Sleeve

The thermal inertia sleeve is of cylindrical shape and fabricated from silicon carbide (SiC). The sleeve acts as a thermal buffer between the sun's rays and the coiled ceramic heat exchanger and also provides some mass for thermal energy storage. The sleeve is piloted at each end into the graded thermal insulation which surrounds the heat exchanger. Clearance for axial and radial thermal expansion of the sleeve with respect to the rigidized insulation is provided. Stress analysis indicates a reasonable steady state thermal stress for the selected 12.7 mm (0.5 in.) thick sleeve. Thermal stresses due to transient type startup conditions are, of course, higher than steady state values; however, they are within established stress limitations for SiC. A reduction in sleeve thickness to reduce possible transient thermal stresses would be

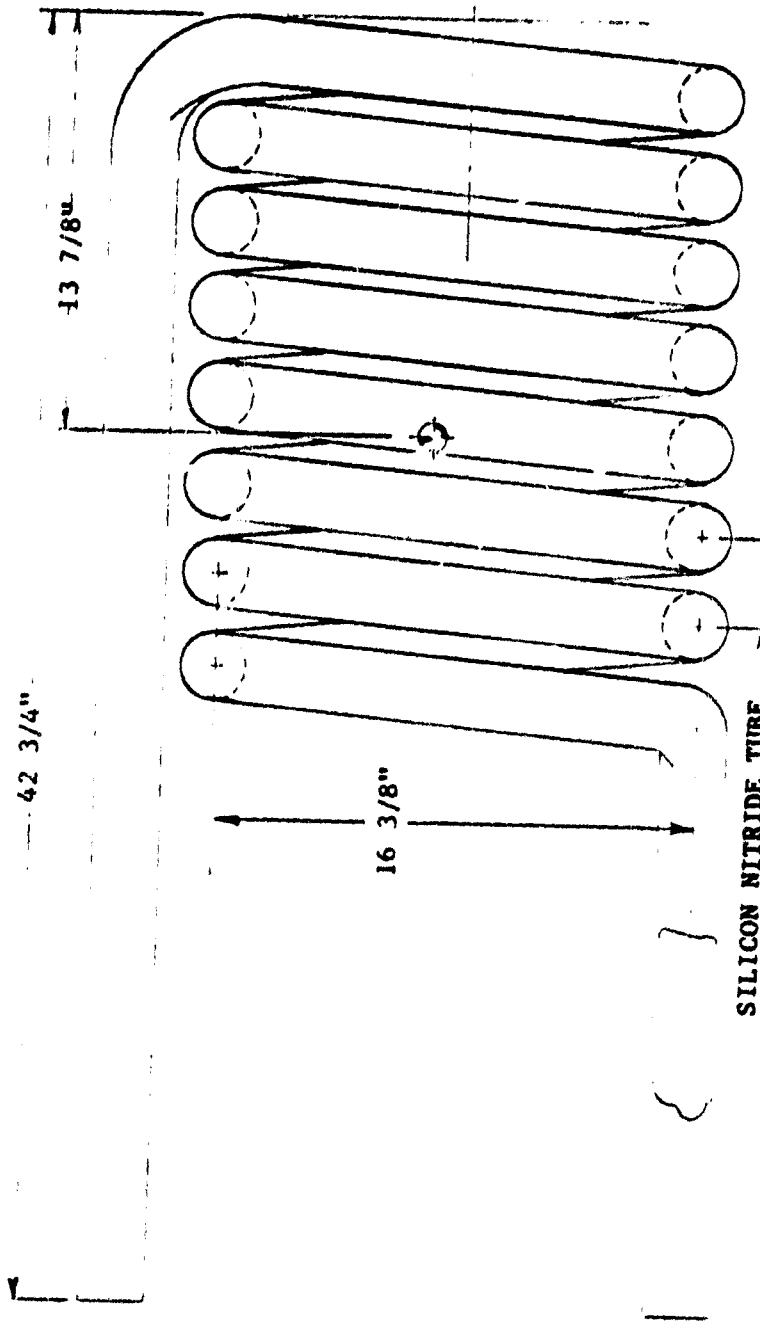

Figure 4-20. Silicon Nitride Coil/High Temperature Receiver

dependent upon fabrication requirements and limitations. This matter would be investigated further in future designs.

3. Pre-formed Insulation

The thermal insulation consists of three (3) pre-formed graded (i.e., various materials) sections; namely, the front conical section, midcylindrical section and rear disc section. The front and rear sections contain pre-formed pilots to accept the thermal inertia sleeve and provide its support. The rear section is split through the centerline of the coil inlet and outlet tubes to facilitate assembly of the heat receiver. The mid, hollow cylindrical sections contain three internal teeth running in a longitudinal direction. The height of these teeth is such that no contact between them and their ceramic coil exists at ambient temperatures (i.e., clearance exists). When the coil reaches normal operating temperature the clearance is reduced to zero and the insulation can act as a partial support for the coil. A cold clearance of 1.8 mm (0.070 in.) is required and is indicated on the conceptual drawing. Axial cold clearance between the ceramic coil and the front conical insulation section is 4.6 mm (0.180 in.) as indicated in the conceptual design.

Since it will not be possible to control the ceramic coil dimensions to tolerances which would permit actual support of the coil by the insulation at operating temperature, the insulation configuration, as described above, will serve mainly to limit deflections produced by shock loads or other imposed rapid accelerations.

The front conical section of insulation forms the receiver aperture and supports the total weight of the thermal inertia sleeve. A weatherproof coating would be applied to the surface in the aperture area as indicated on the drawing. This coating would prevent the entrance of water, etc., into the porous insulation structure.

4. Outer Casing and Support

As indicated in the parts list, the outer casing consists of a top cover and outer shell. The casing would be fabricated from mild steel sheet metal. The top cover is reinforced with structure steel shapes and incorporates supports utilized to attach the solar receiver to the concentrator focal mount ring. The top cover is attached to the cylindrical shell via spring-loaded fasteners so that thermal expansion of the rigidized insulation, with respect to the casing, may be compensated for. The top cover employs an elastomer-type weathertight seal between itself and the shell. The configuration as outlined above allows dismantlement of the solar receiver from the operating end for coil inspection, etc., without disturbing the coil or its connections to the inlet and outlet tubes. Temperature sensing devices, etc., which might be attached to the ceramic coil and lead out through the top cover would also be left in place during inspection.

Without the knowledge of what other pieces of process equipment or machinery might be located at the focal point, it is difficult to determine how the solar receiver should best be supported. The mounting design must be integrated with the overall focal mounted system.

5. Ceramic Joints

Ceramic joints consist basically of two types (i.e., a ceramic-to-ceramic and ceramic-to-metal). Both of these types of joints could be employed in the high temperature receiver design. The conceptual design indicated in Figure 4-1 utilizes ceramic-to-ceramic joints to attach couplings to the inlet and outlet tubes of the coiled heat exchanger. The inlet gas coupling could be made with a glass-type joint due to the relatively low temperature (954°C). The outlet gas coupling would be attached to the tube with a ceramic phase bonded type joint capable of operation at 1371°C (2500°F). The ceramic couplings serve two purposes. The first is to provide a means to attach to the inlet and outlet connections and the second is to support the heat exchanger coil in the axial directions. The conceptual design indicates one possible method for transferring the coil load through the ceramic coupling to the rear support structure. In this design the rear insulation disc is used to support the coil laterally and thus remove bending moment loads from the ceramic coupling. The coupling, therefore, when attached to the support structure sees only axial loads. Attachment of the ceramic coupling via metallic parts must be at a diameter where the temperature in the ceramic has been decreased to a value where superalloy metallics are usable. To determine this a finite element computer model of a typical ceramic coupling was prepared and the temperature profile for the two couplings (i.e., inlet and outlet) determined. From this data approximate diameters, at which metal and ceramic interfaces could be established, were determined. See Figure 4-21 and Figure 4-22.

Alternate methods of attaching the ceramic coupling to the rear support structure utilizing a brazed ceramic-to-metal joint are indicated in Figure 4-23 and Figure 4-24. In both cases bending moment loads are taken by the rear insulation disc. In a brazed ceramic-to-metal joint, the metallic material selected should have a coefficient of thermal expansion at operating temperature as close to the ceramic material as possible. Although materials such as Kovar are utilized in many ceramic-to-metal seals, operation at temperatures in the 700-870°C (1300-1600°F) range for such joints has not been proven. The alternate concepts as indicated would require developmental testing, etc., before they could be employed in any solar receiver design.

Without the knowledge of what process equipment or machinery might be mounted at the focal point and coupled to the solar receiver, it is difficult to determine what type of connections to the ceramic coil are necessary. Figures 4-25, 4-26 and 4-27 indicate some conceptual designs for consideration.

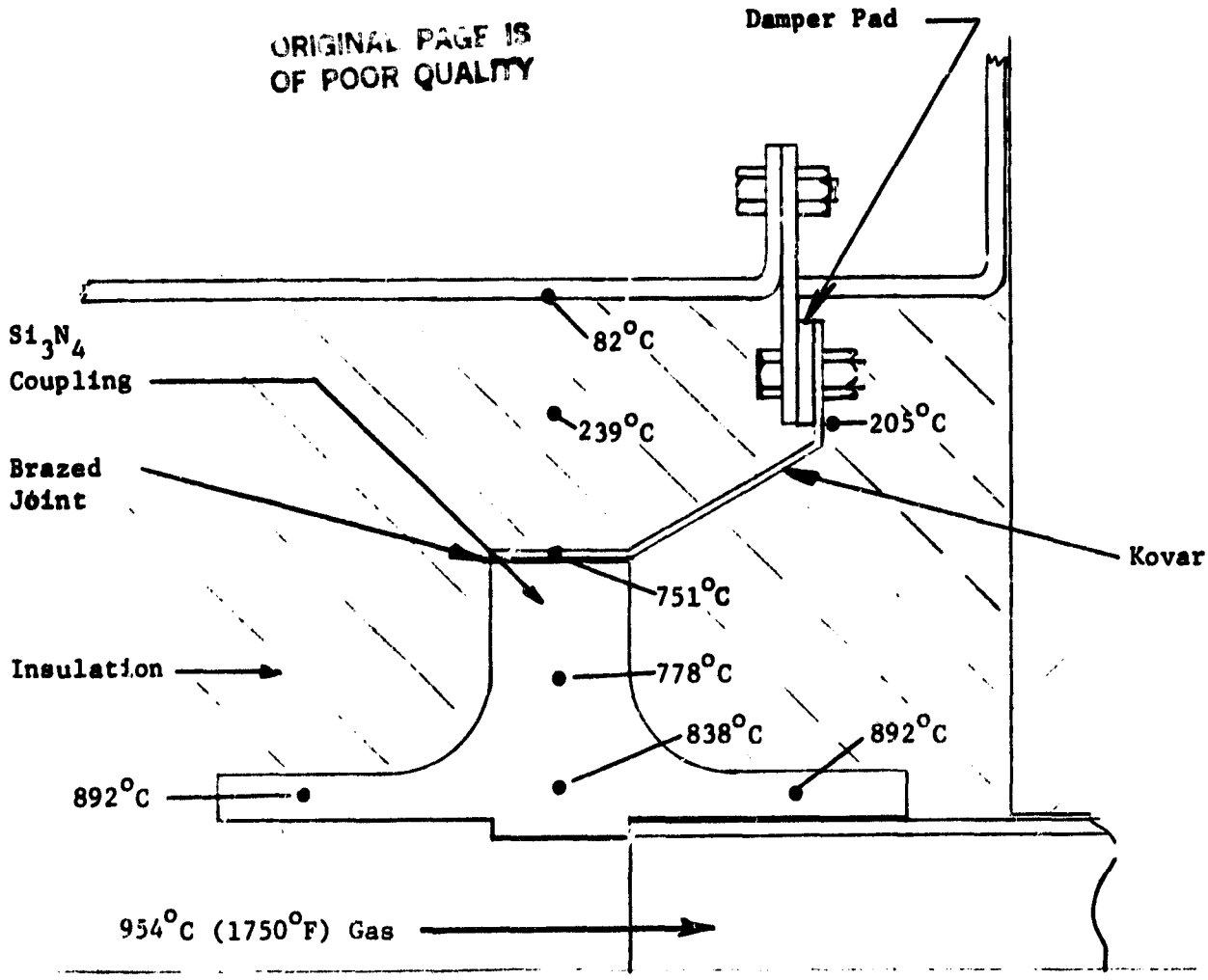

Figure 4-21. Typical Ceramic Coupling Temperature Profile 954°C (1750°F) Gas

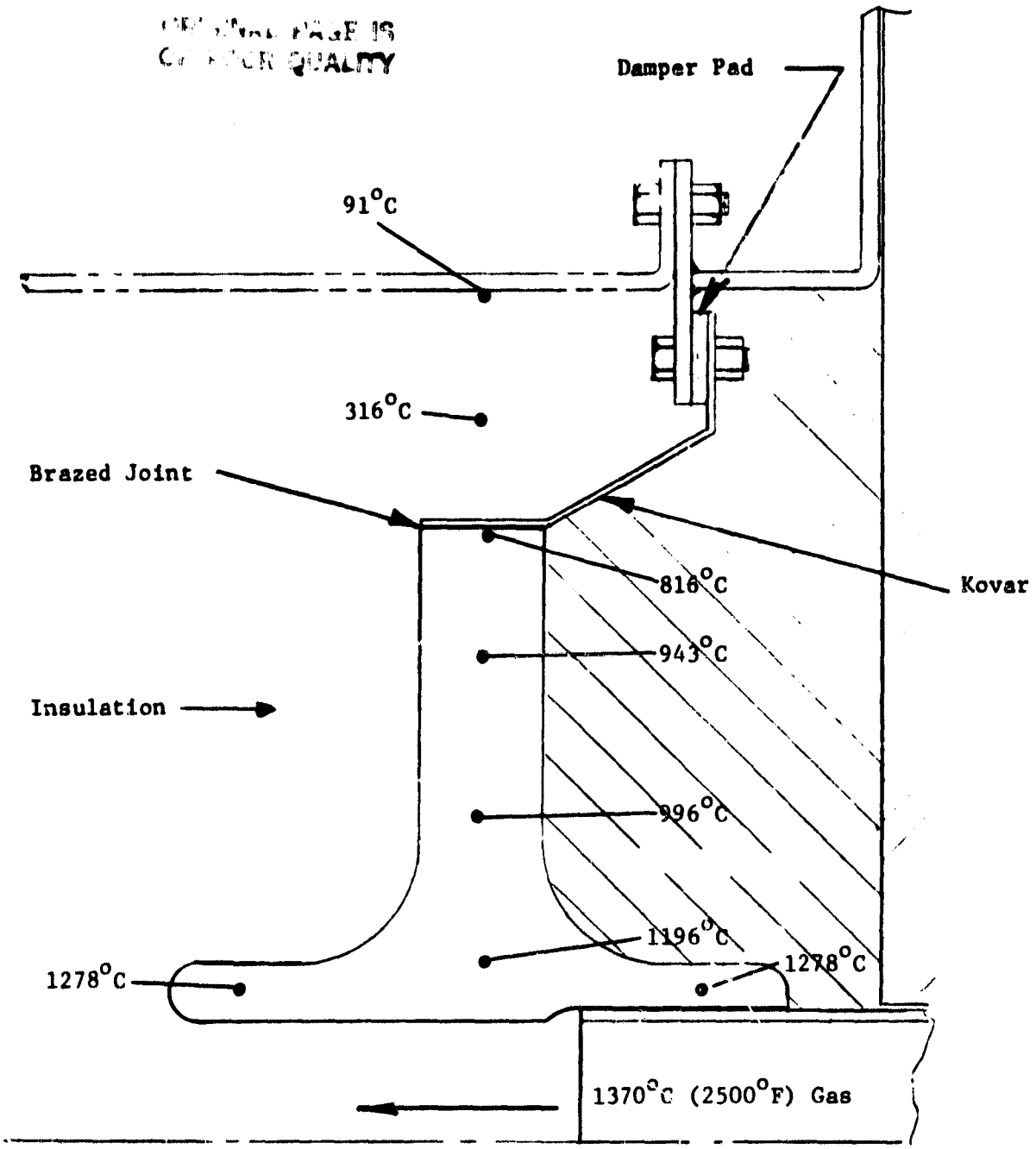

Figure 4-22. Typical Ceramic Coupling Temperature Profile 1370°C (2500°F) Gas

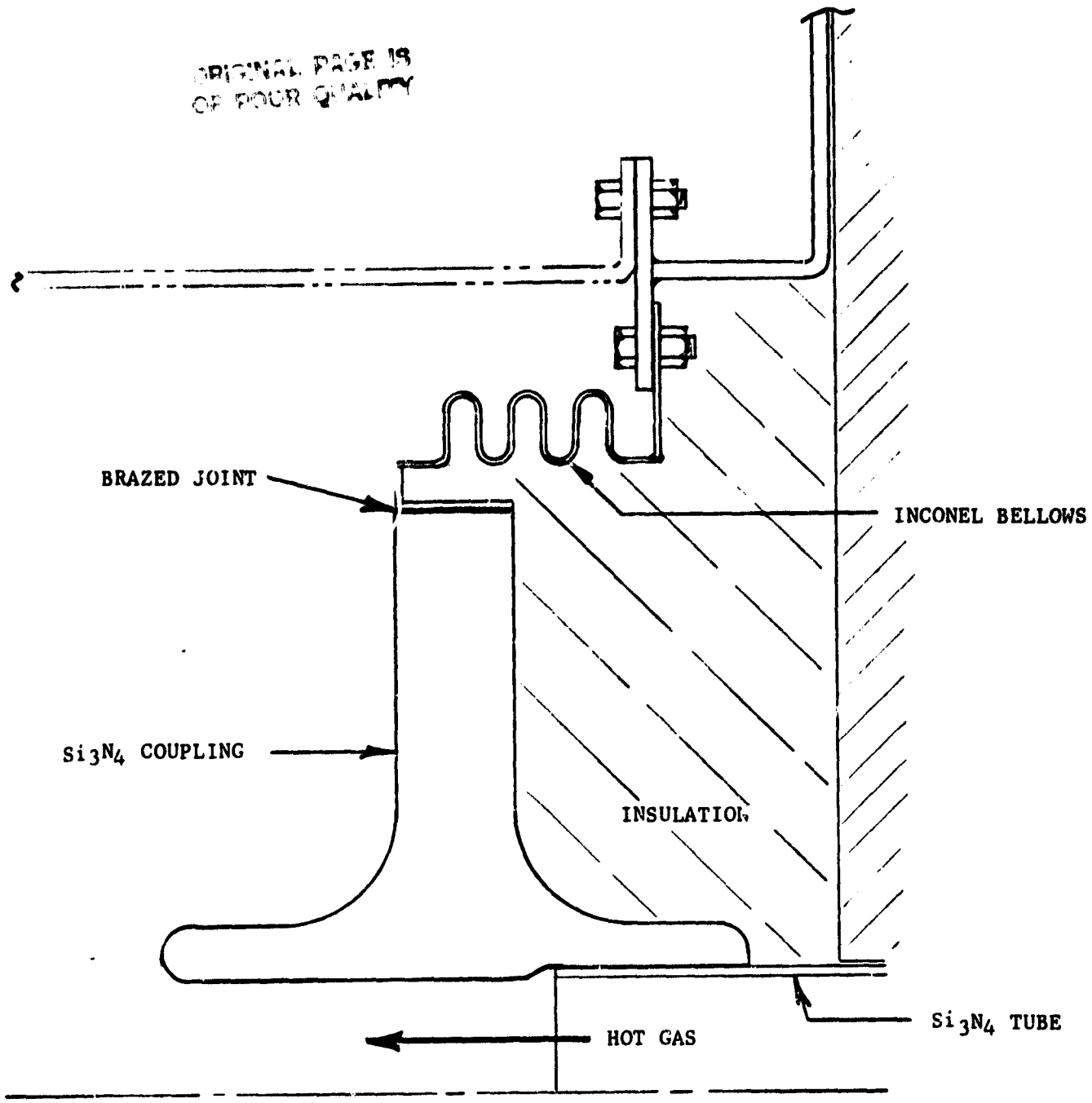

Figure 4-23. Alternate Ceramic Coupling Connection to Structure

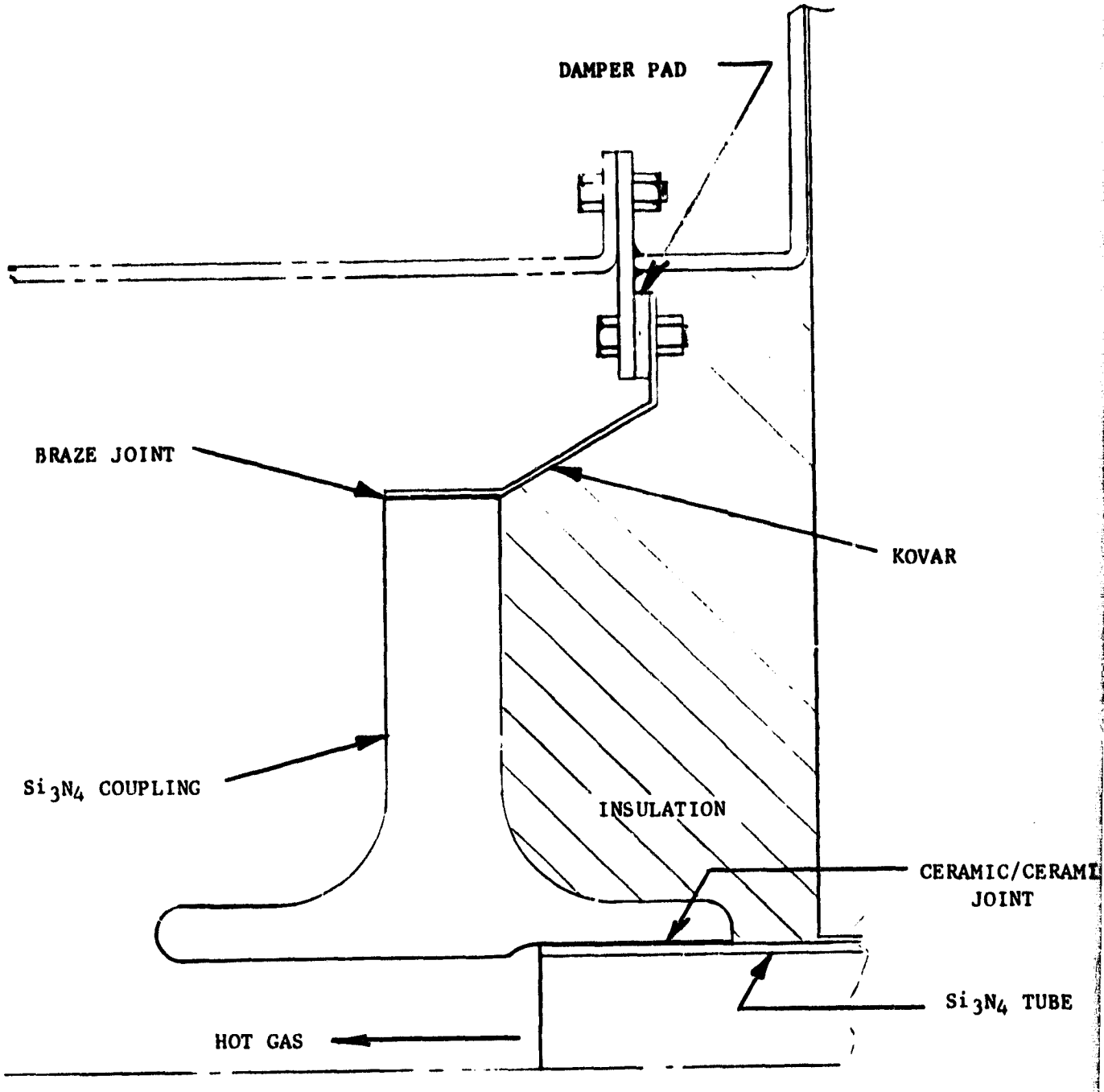

Figure 4-24. Alternate Ceramic Coupling Connection to Structure

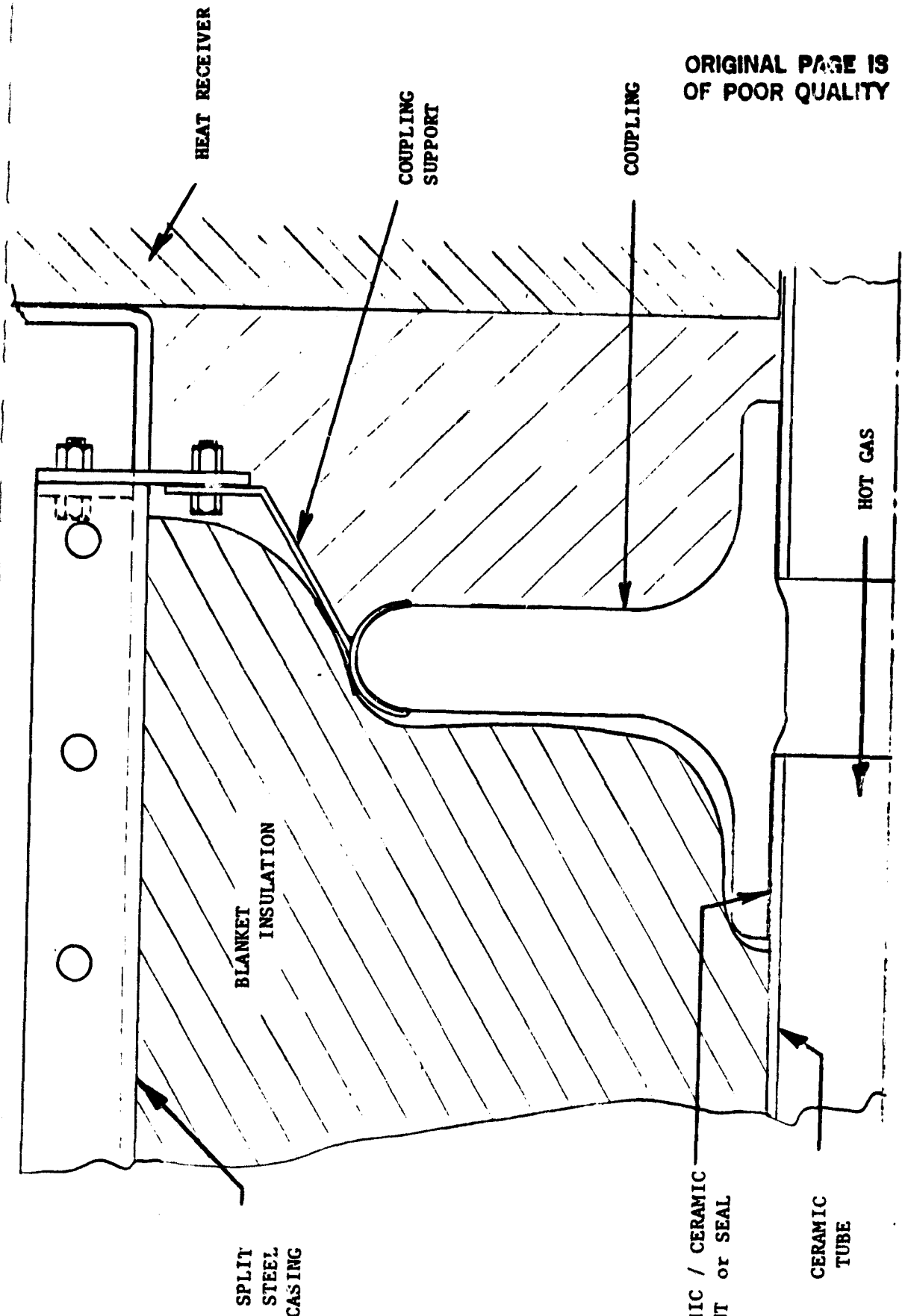

Figure 4-25. Conceptual Connection Method

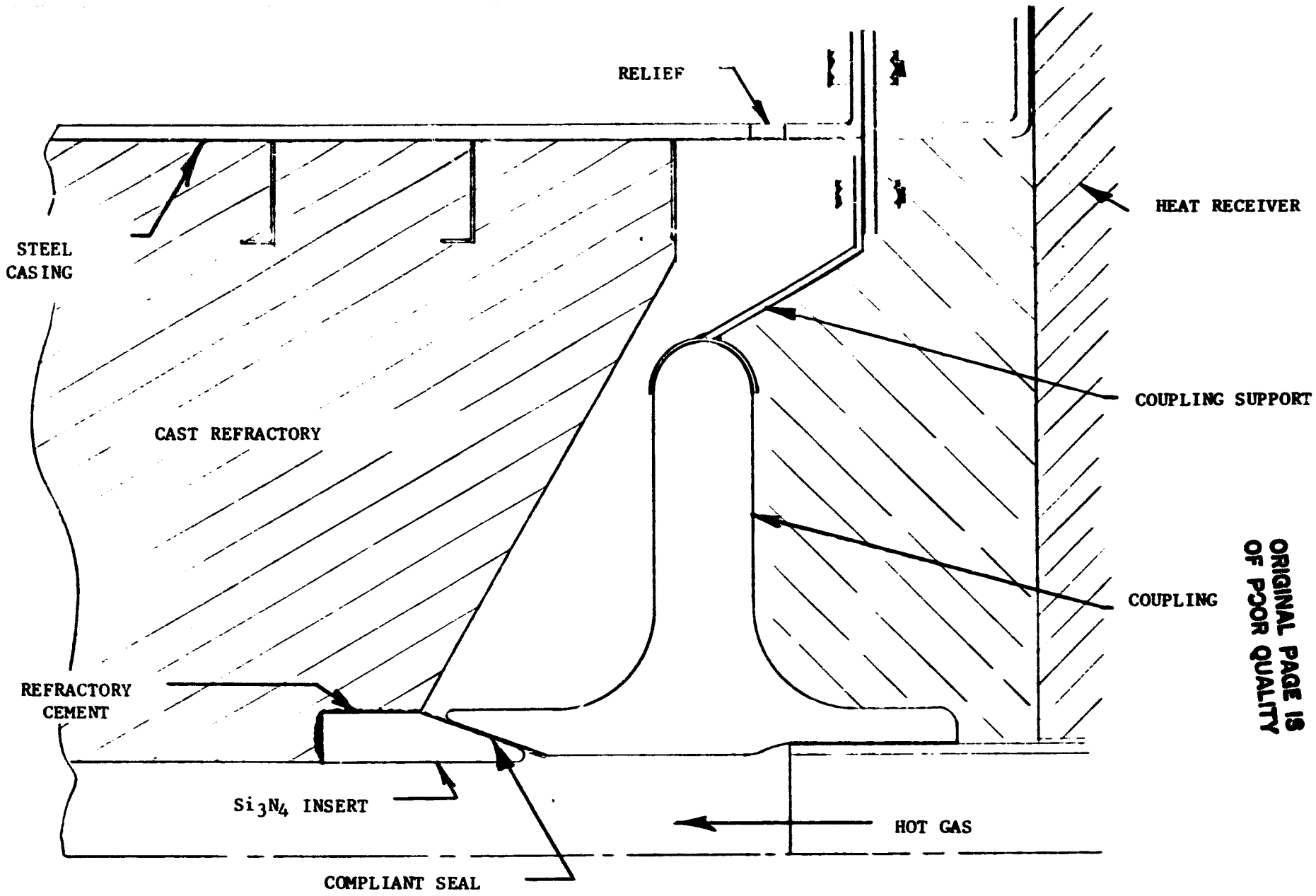

Figure 4-26. Conceptual Connection Method

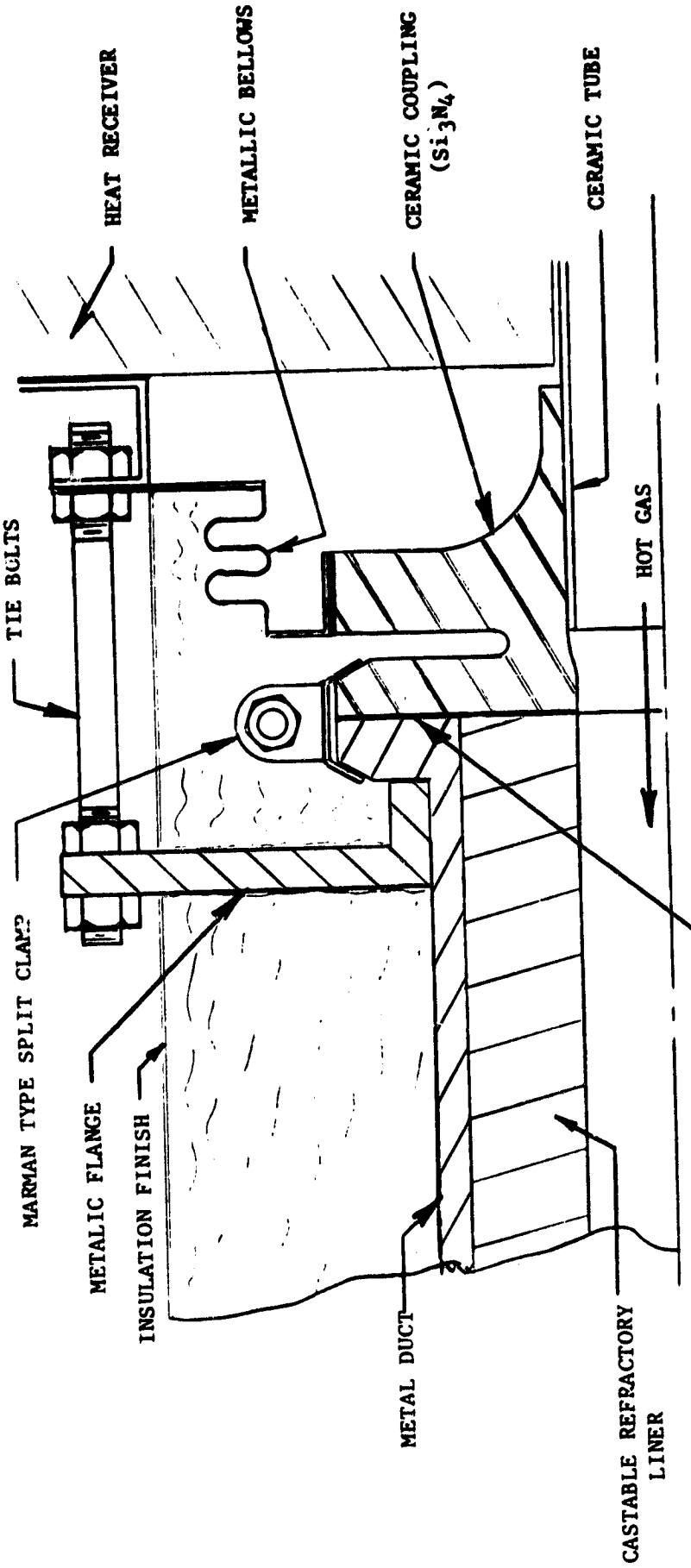

Figure 4-27. Conceptual Connection Method

E. ENGINEERING ANALYSIS

1. Mechanical Design Analysis of Receiver Coil

a. Introduction. The key to the successful operation of the solar receiver is the ability to design a mechanically sound solar receiver coil which can operate at high temperature and pressure. Engineering analysis has been performed on the coil to insure the basic structural integrity of the design through the use of finite element analysis.

b. Computer Analysis. The stress analysis of the receiver coil is accomplished by using the MASS program* developed by the Aircraft Engine Group of the General Electric Company for static and dynamic redundant structures. This program is currently being used to design and develop different aircraft engine components.

The MASS program can be described as an elemental or lumped parameter approach for the analysis of redundant structures. Stresses, loads and deflections are obtained for mechanical loadings (including maneuver), thermal loadings and to a limited extent sinusoidal forcing functions. Finding critical frequencies and mode shapes is another function of the system.

Any solid three dimensional structure can be divided into a large number of geometrically simple elements. If the stiffness matrix of the individual elements can be determined, then the total structure can be analyzed by the matrix method of structural analysis. In the analysis, nodal displacement continuity is demanded from one element to another. Further the structure must follow Hooke's Law and it must be within small deflection theory.

c. Computer Model. The finite element model of the coil is shown in Figure 4-28. Each coil is divided into four 90° tube segments. The coil is modeled in 3-dimensional X-Y-Z system as shown in Figure 4-29 with the coil axis as Y axis and the coil ends are located in the X-Y plane. The connection from the vertical tubes to the helical coil are achieved through appropriate tube bends with a specified center of curvature. The coil end view is shown in Figure 4-30. The coil is divided into 37 segments. The boundary conditions are:

1. The coil ends are fixed:
   a. The linear deflections along X,Y and Z axes are zero.
   b. The rotation about X, Y and Z axes are zero.
2. The coil is subjected to a uniform internal pressure of 3 atmospheres along the length of the coil.

*MASS System-The computer program for General Redundant Structures with Vibratory and General Static Loading, by L. Beitch, Aircraft Engine Division, Cincinnati, Ohio.

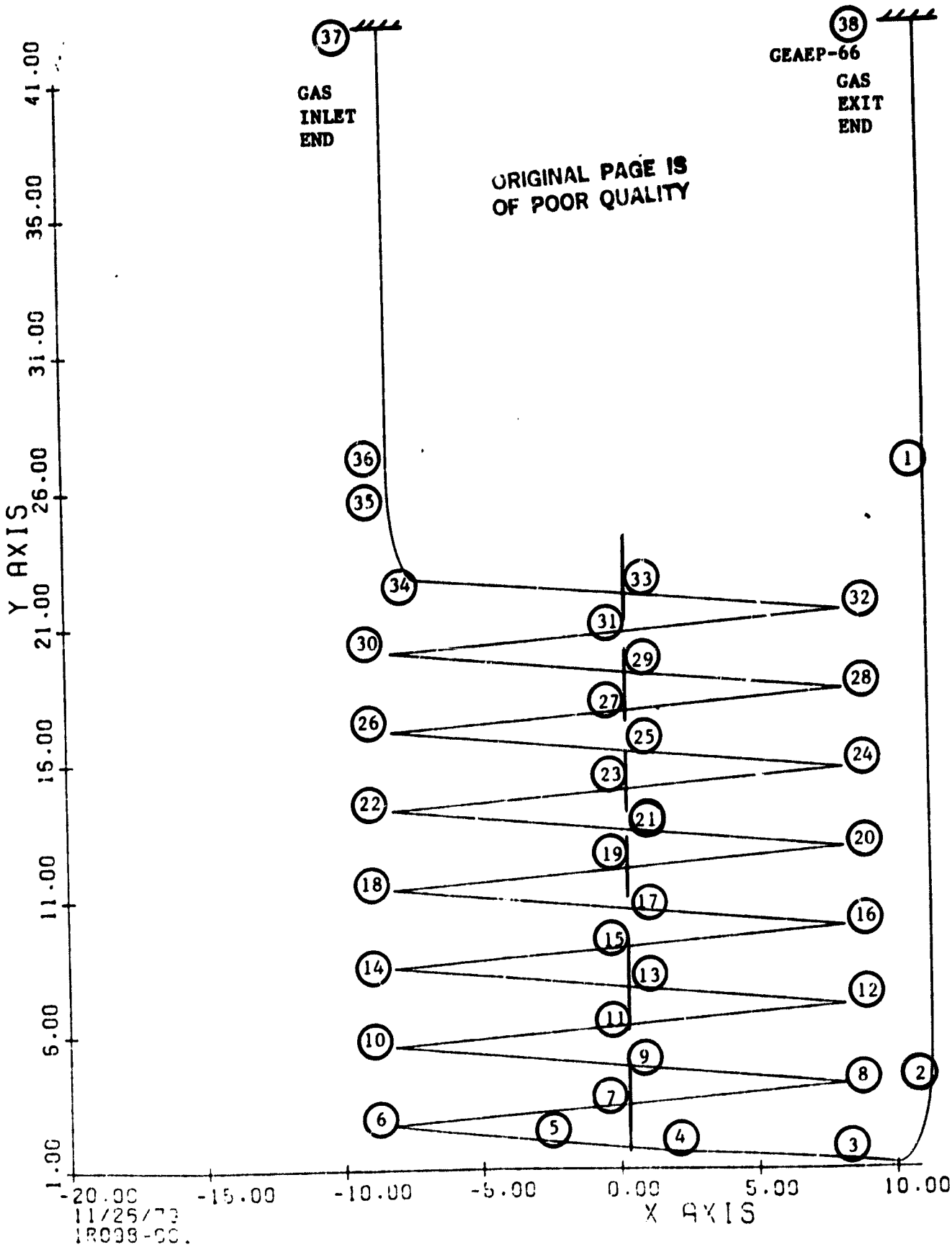

Figure 4-28. Finite Element Model of the Coil

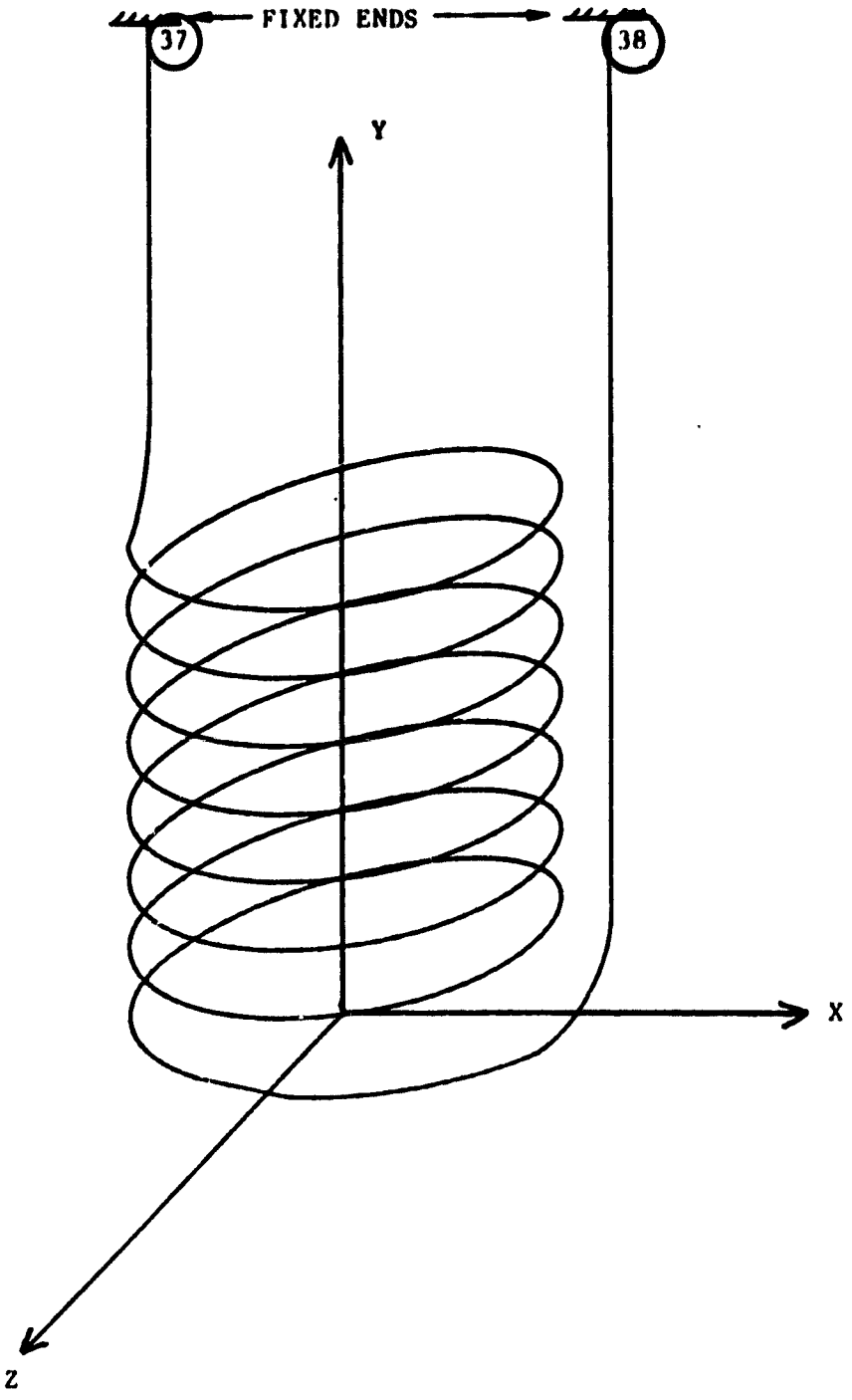

Figure 4-29. Coordinate System for the Coil

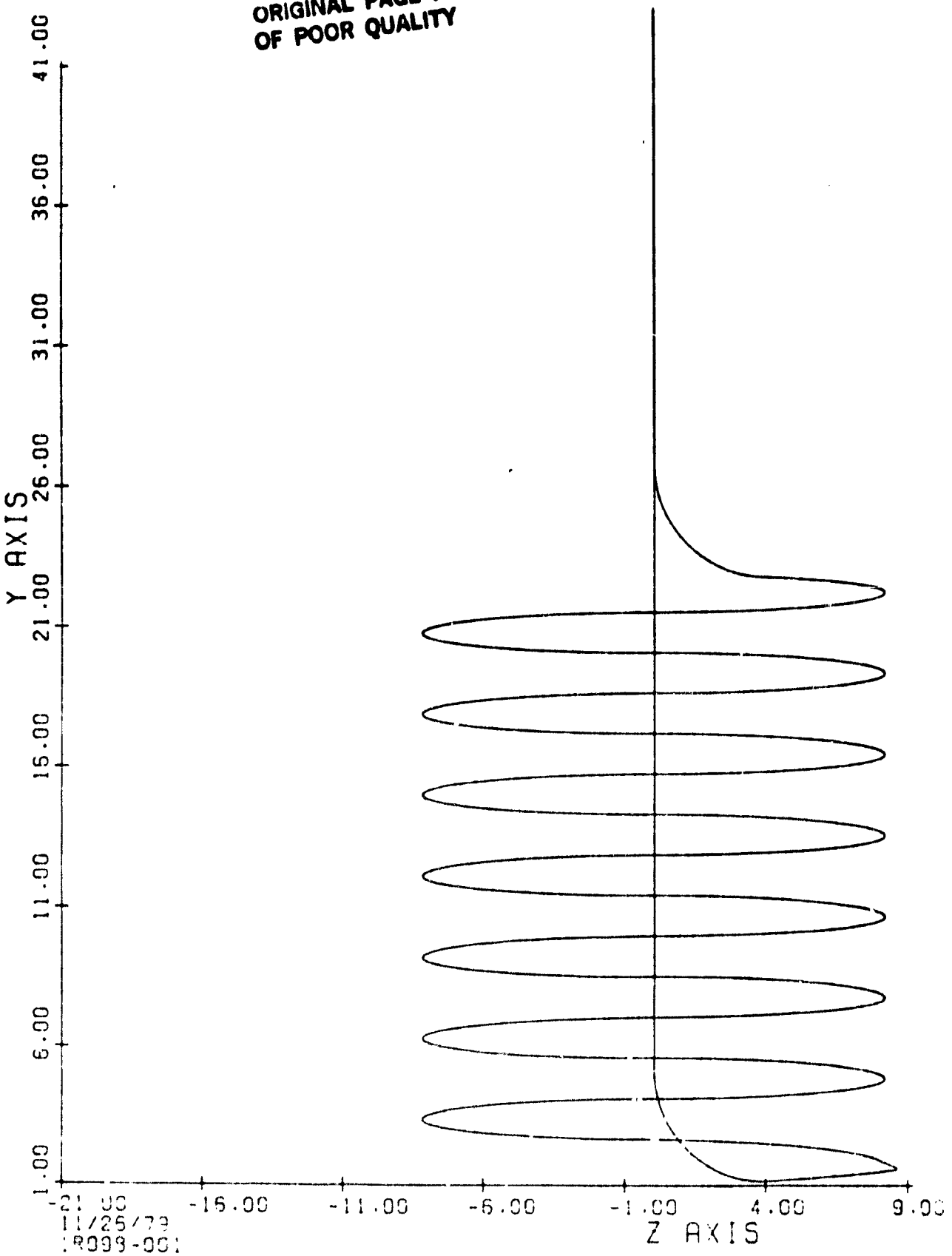

Figure 4-39 Coil End View (Computer Model)

3. The temperature distribution along the length of the coil is shown in Figure 4-31. This information was obtained from the detailed thermal analysis of the receiver.

The physical properties of the coil material used in the program are:

Density = 1.73 kgm/m^3 (0.108 lbs/in^3)
Young's Modulus = 234.4 GPa (34 x 10^6 lbs/in^2)
Shear Modulus = 91.0 GPa (13.2 x 10^6 lbs/in^2)
Thermal Coefficient of Expansion = 3 x $10^{-6}/^oC$ (1.67 x $10^{-6}/^oF$)

d. Results. As the collector tracks the sun, the orientation of the coil axis with respect to the horizontal changes with time. The optimum orientation of the coil in the receiver has to be selected for minimum stress in the coil. The stress analysis is performed for the following cases.

Case 1. Coil vertically hanging down from the supports.

Case 2. The coil ends are fixed at 3 o'clock and 9 o'clock positions so that the gravitational force due to self weight acts in the +Z direction.

Case 3 The coil ends are fixed at 6 o'clock and 12 o'clock positions so that the gravitational force due to self weight acts in the +X direction.

Table 4-7 shows the reaction load and moment and maximum deflection and stresses for all the cases. Case 1 is basically a theoretical study and in practice it does not occur. The stress distribution along the length of the coil for Cases 2 and 3 are shown in Figure 4-32 and 4-33. From a maximum stress point of view, Case 2 is recommended. Further, since the combined stress and reaction moment at support points are approximately the same, the coil support design can be made the same at both ends. For Case 2:

Maximum Combined Stress (local) = 13.87 MPa (2011 psi)
Maximum Radial Expansion = 1.88 mm (0.074 in.)
Maximum Axial Elongation = 4.394 mm (0.172 in.)

The maximum coil stress is less than the allowable stress of 86.18 MPa (12500 psi) and hence it is safe. A computer plot of the superimposed deflection drawing of the coil is shown in Figure 4-34. The coil is fixed at its ends and freely hung inside the hollow cylindrical insulation. Sufficient clearance is given between the coil and the insulation both in the radial direction and at the bottom so that the coil can freely expand and come in contact with the insulation which provides the support to the coil only while it is at the operating temperature. Thus, it is implied that the coil is supported only from its ends when the receiver is cold and sufficient care should be taken that the receiver is not subjected to impact loading and excessive vibration while it is being transported and mounted over the collector.

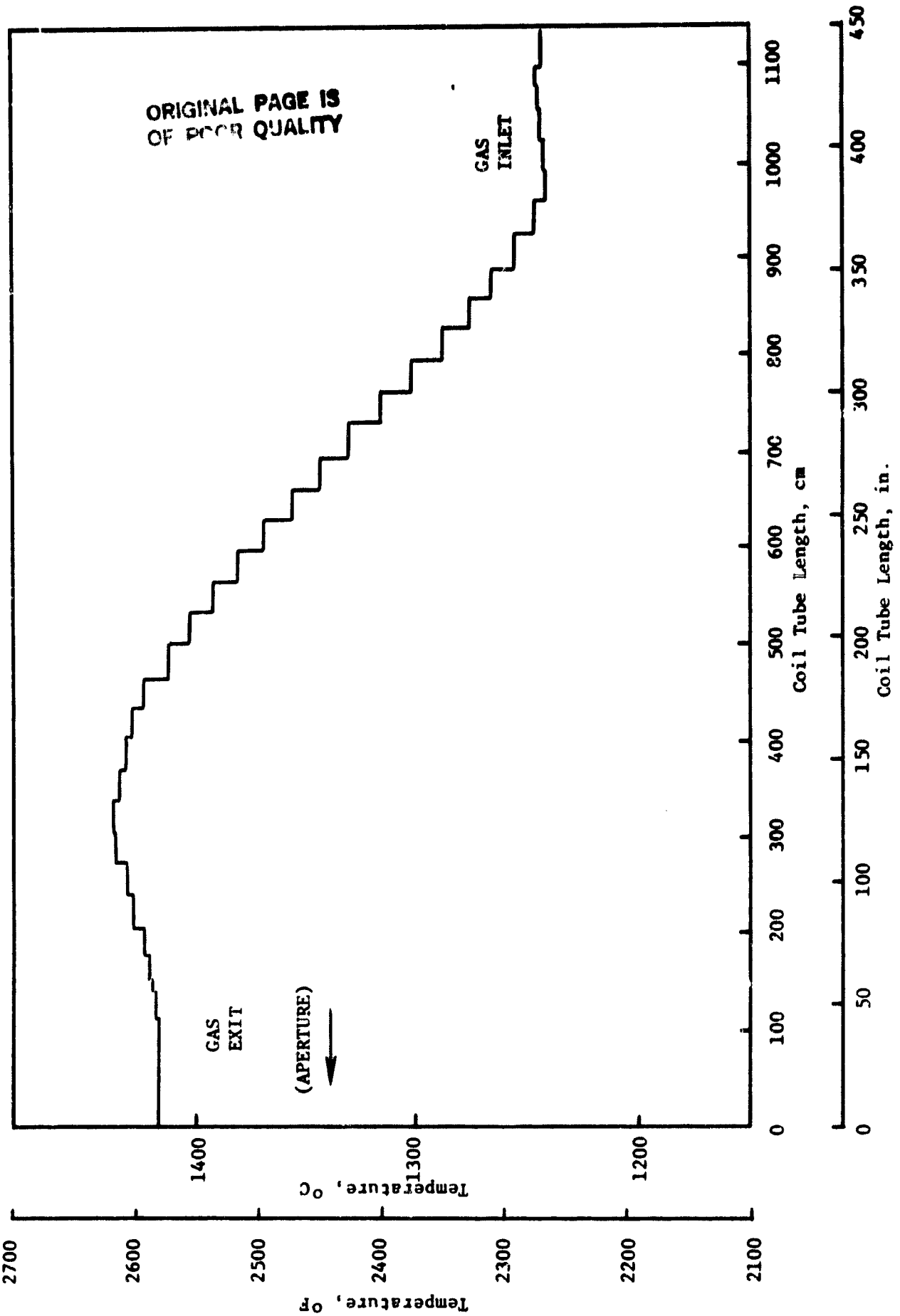

Figure 4-31. Temperature Distribution Along the Length of the Coil.

Table 4-7. Coil Reaction Loads, Combined Stress and Deflection Data

Total Weight = 15.5 kg (34.14 lbs)

	Case 1		Case 2		Case 3	
	kg	lbs	kg	lbs	kg	lbs
X Load (37)*	6.21	13.7	6.44	14.2	-1.77	-3.9
X Load (38)	-6.21	-13.7	-6.44	-14.2	-13.79	-30.4
Y Load (37)	1.90	4.2	1.86	4.1	3.63	8.0
Y Load (38)	-1.90	-4.2	-1.86	-4.1	-3.63	-8.0
Z Load (37)	0.24	0.52	-7.17	-15.8	0.25	0.55
Z Load (38)	-0.24	-0.52	-7.17	-15.8	-0.25	-0.56
	Nom	lb_f-in.	Nom	lb_f-in.	Nom	lb_f-in.
Moment X (37)	-1.39	-12.3	42.1	373.0	-1.68	-14.9
Moment X (38)	1.36	12.0	60.6	536.0	1.48	13.1
Moment Y (37)	-0.21	-1.9	12.3	109.0	-0.80	-7.1
Moment Y (38)	-0.78	-6.9	-14.2	-126.0	-1.32	-11.7
Moment Z (37)	50.4	446.0	51.7	458.0	7.46	66.0
Moment Z (38)	-41.2	-365.0	-42.8	-379.0	-103.0	-911.8
	cm	in.	cm	in.	cm	in.
Max. Radial Expansion**	0.175	0.069	0.188	0.074	0.127	0.050
Max. Axial Elongation	-0.447	-0.176	-0.439	-0.173	-0.450	-0.177
	MPa	psi	MPa	psi	MPa	psi
Max. Combined Stress	11.9	1726.0	13.87	2011.0	16.80	2437.0
Combined Stress (37)	8.38	1216.0	11.06	1604.0	2.37	344.0
Combined Stress (38)	7.04	1021.0	12.34	1790.0	16.80	2437.0

*See Figure 4-28 for location of Nodes 37 and 38.

**See Figure 4-34.

C-2

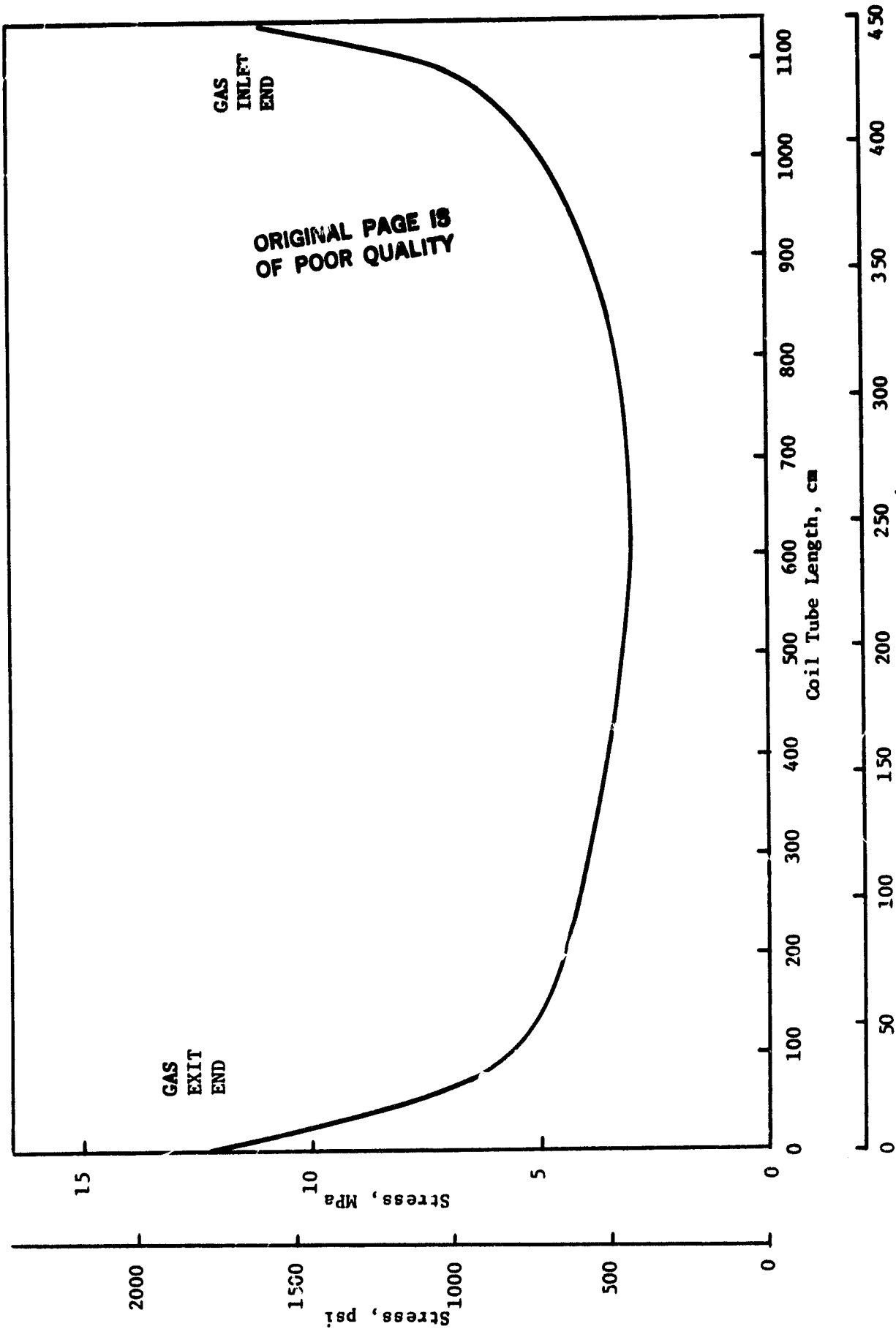

Figure 4-32 Combined Stress Distribution Along the Length of the Coil for Case 2.

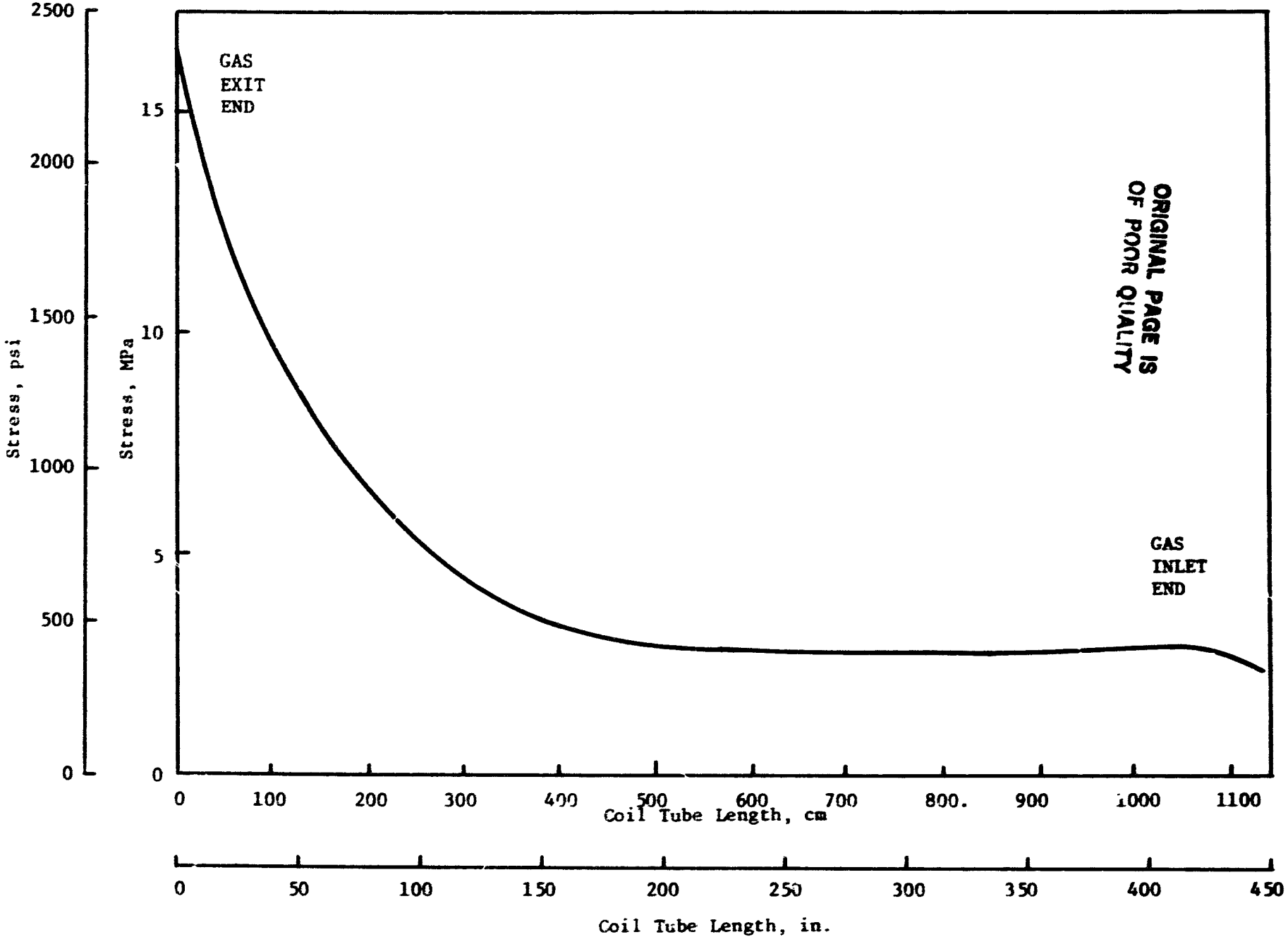

Figure 4-33 Combined Stress Distribution Along the Length of the Coil for Case 3.

ORIGINAL PAGE IS
OF POOR QUALITY

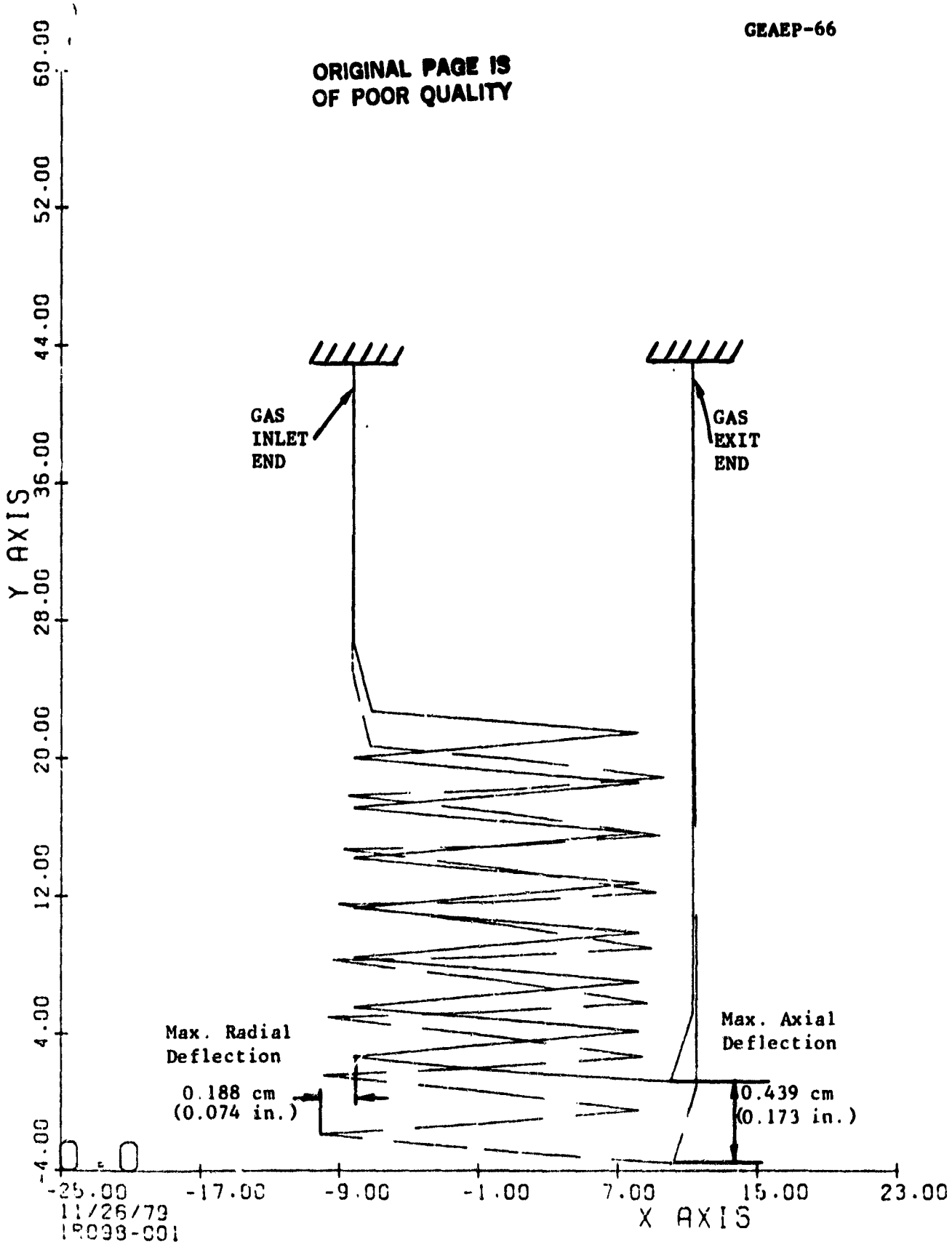

Figure 4-34 Computer Plot of Super Imposed Deflection for Case 2

2. Control System

As in most Brayton system, the heat source (receiver) operational controls are slaved to the overall process control.

System flow is varied so as to provide a scheduled temperature and pressure at turbine inlet, or a scheduled temperature for catalytic reaction applications. Receiver controls will have to detect dangerous conditions and initiate shutdown.

The most severe transient is seen in the loss of flow case starting at full power conditions, with full insolation. The transient analysys (described in Section V-C) shows that some 2-minutes are available before receiver temperatures reach dangerous levels where material damage occurs. It is important that, once detected, the collector tracking system be able to defocus in that time period.

Loss of flow transients will be detected by system sensors (at turbine inlet, etc.) as a loss of pressure transient, and system shutdown (including collector defocusing) initiated.

Similarly, a high air exit temperature that could result in damage to the receiver tubes (and other system components) will be detected by system temperature sensors and air flow increased to lower the exit temperature. If air flow cannot be increased, overtemperature limits will be reached and the collector is defocused.

For normal startup and shutdown, the system controller will vary the flow and inlet pressure to accommodate turbine or process requirements, taking into consideration the rather slow response of the receiver (approx. 15 minutes from ambient to hot temperatures with full insolation and no air flow, and longer with cooling air flow). During startup, inlet air temperature scheduling is important to avoid thermal shock to the hot receiver tubes (if receiver is heated first before flow is started) or the optimum temperature-time schedule chosen if flow is concurrent with insolation to reach steady power operation.

Large leaks in the receiver will result in a pressure drop detected by the system sensors initating shutdown. Small leaks would not be disastrous to the receiver, but would discharge hot gases into the field. Since natural air circulation pumps around 0.0018 kg/sec (0.004 lbs/sec) or 1.7% of design flow of air into the field at close to sleeve temperatures, small leaks of this order would be tolerable, but hard to detect.

In any case, receiver protection can be directly ensured by monitoring sleeve and tube temperatures at several points and activating shutdown mechanisms in case of overtemperature 1538°C (2800°F) for tube, 1649°C (3000°F) for sleeve, leaving a safety margin to allow for control system response time. Thermocouples such as iridium/iridium 60% rhodium 40% or various platinum-rhodium types can be used for temperature measurement in this range.

Receiver controls design needs to be investigated with overall system controls design and operational requirements. The only receiver-initiated actions result from sleeve or tube overtemperature, whereas other problems are detected elsewhere before they can affect the receiver.

A high emphasis on reliability of controls and collector tracking-defocusing capability is needed due to the irreversible damage failure mode of the receiver. The control system design also has to consider the transient response of the receiver (Section V-C) coupled with other system components in assuring adequate, safe rates of control.

F. ADAPTABILITY TO DIRECT CHEMICAL REACTIONS

1. Introduction

There are many reactions possible using high temperature energy. These include the production of fuels, such as hydrogen or methane, the production of chemical feed stocks, such as ammonia or sulphuric acid, and the generation of storable and reversible chemical mixtures, such as reforming steam to form CO and hydrogen.

In order to make efficient use of high temperature energy, it is almost essential to perform the reactions directly in the receiver. The losses and expense of ducting hot gasses from dispersed concentrators to a central chemical plant would cause the economics and efficiency of this type of solar energy to be unacceptable.

In order to perform the reactions directly in the receiver, two items need study. First, since most reactions require a catalyst, the placement and replacement of catalyst must be studied. Second, a reasonably efficient recuperator is needed so that most of the solar energy can be used to drive the reactions and not simply heat the reactants. These are the two areas investigated in this study.

As an example only, and not with the idea that this is the preferred application, the steam reforming reactions were used. This set of reversible reactions is currently used to generate hydrogen, and has been extensively studied for long distance transport of thermal energy between nuclear reactors and users. The two reactions are:

$$CH_4 + H_2O \rightleftharpoons CO + 3H_2; \Delta H = 205 \text{ kJ/mole}$$

$$CH_4 + 2\ H_2O \rightleftharpoons CO_2 + 4H_2; \Delta H = 163 \text{ kJ/mole}$$

The reactions tend to go to the right at high temperature and low pressure. At 30 atmospheres pressure the reaction goes nearly to completion, with approximately 0.5% of the methane unreacted. At 3-8 atmospheres, almost none of the methane remains. Temperatures required are around 1000°C (1830°F). At the 58 kW power level of the conceptual design receiver, about 67 Nm^3/hr of hydrogen would be produced.

2. Catalyst Placement and Replacement

In direct chemical reaction applications, the catalyst can be placed in the receiver tube, either as a pebble-filling or a film coating on the inside walls. The pebble-filled tube will contain enough catalyst to reduce the need for replacement, but results in a much increased pressure drop (that may not be a great problem for this type of application). However, the increased weight of the receiver and the resulting stresses on the tube supports are undesirable.

Catalyst coating of the inside walls of the tube is the preferred technique, and this can be achieved by chemical vapor disposition. Uniform coating of the tube would be hard to achieve, but is not needed in this case. In the case of the steam reforming application, the reaction happens so fast that it is usually heat-rate-limited (rather than catalyst-area-limited). In applications where a larger catalyst area is needed, new inside-finned-tube configurations are possible providing a larger area.

For catalyst replacement, the receiver unit will have to be disassembled in-shop and the receiver coil replaced by a fresh-coated coil. The old coil can then be chemically cleaned and recoated for later use. Replacement rates will depend on the type of application, coating thickness and the receiver duty.

3. Recuperator Heat Exchanger Design

The reformer process gas consisting primarily of steam and methane is preheated by the hot product gasses from the receiver. The chief constituents of the product gasses are carbon dioxide and hydrogen gas formed by the catalytic conversion of the reactants at the pressure of 8 atmospheres and at 1260°C (2300°F). The heat required for the endothermic reaction in the catalyst bed is provided by the solar flux in the receiver. The recuperator heat exchanger provides the heat to increase the gas temperature close to the receiver coil temperature, by recovering the waste heat from the products.

Several concepts can be used for an effective heat exchanger. In fact, most of the heat exchangers that are used in the gas turbine industry are theoretically applicable in this case. However, the limitation exists from the standpoint of suitable high temperature materials. There are five different approaches* to higher temperature heat recovery, some of which will be discussed in the following paragraphs.

a. Coil-Tube Heat Exchanger. Figure 4-35 shows the most promising concept for the heat exchanger design for the process heat application. The products leaving the receiver enter the ceramic heat exchanger coil at 1093°C (2000°F) and exit at 354°C (670°F). The react-

*Basinhis, A., Johnson, J.H., "High Temperature Heat Pipes for Energy Conversion", Tenth IECEC Meeting, Newark, Delaware, August 18-22, 1975.

ORIGINAL PAGE IS
OF POOR QUALITY

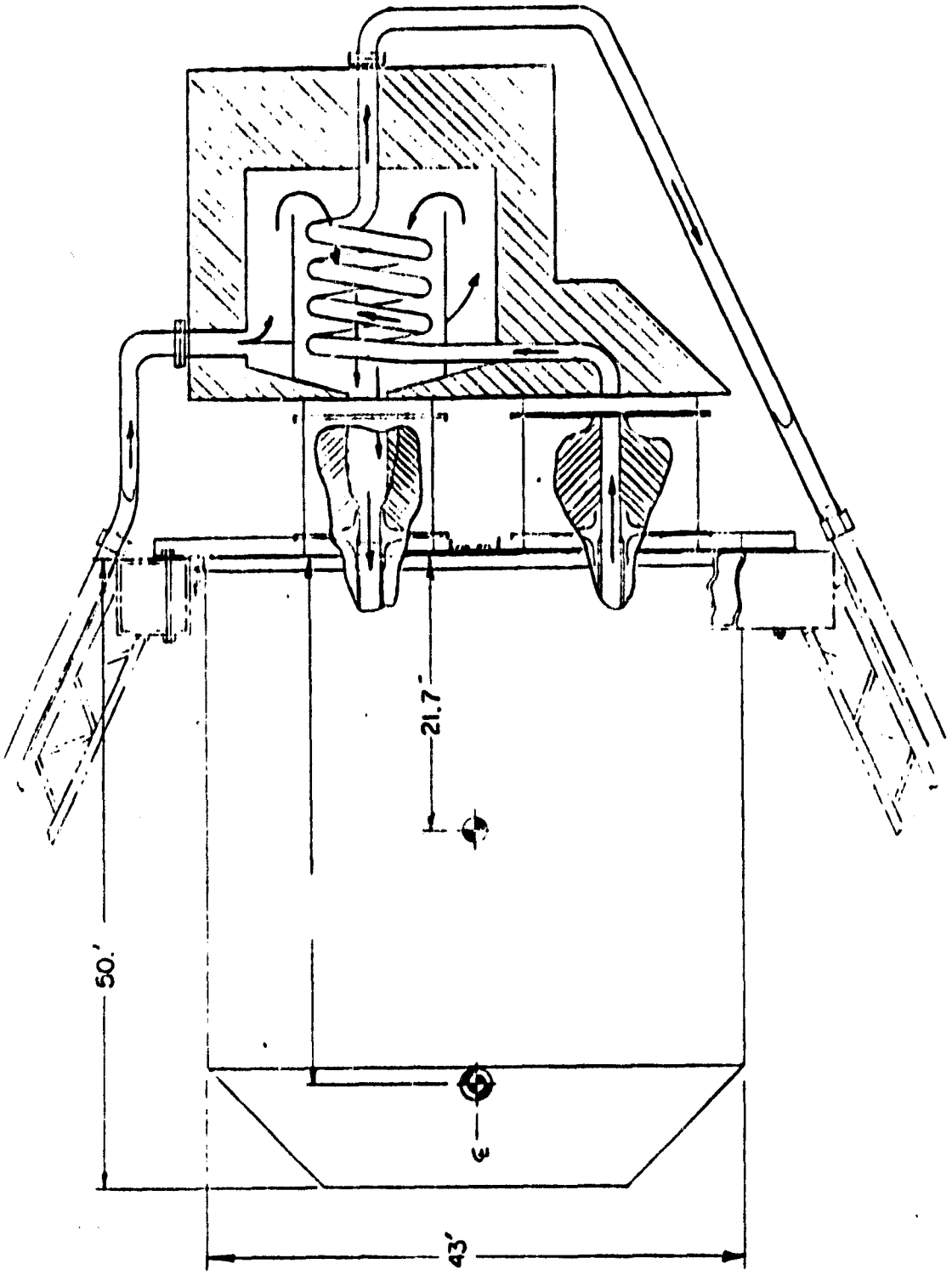

Figure 4-35. Coiled Tube Recuperator Mounted On Receiver

ants enter the annulus of the heat exchanger at 170°C (340°F) and flow across the coil into the receiver at 930°C (1700°F). The sleeve which forms the annulus for the incoming reactants can also be made of ceramic or metal. The high temperature products are contained inside the coil. This type of heat exchanger would be inexpensive on a mass production basis and provides a thermal effectiveness over 0.81 in recovering the heat from the product gasses. The heat transfer mode in the heat exchanger is essentially a combination of radiation and forced-convection from the hot products to the ceramic coils conduction through the tube, and finally a combination of radiation and convection to the incoming reactants. When the temperature differences between the two gas streams become smaller, the heat transfer becomes primarily by convection, as it is at the exit section of the coil.

The length of the heat exchanger tube is estimated to be 3.4 m (11 ft.) in order to heat the incoming reactants to 930°C (1700°F). This concept of the heat exchanger has all the features that made the coil tube receiver concept attractive. It has low installed cost with simple geometry and practically no maintenance requirements.

b. Heat Pipe Heat Exchanger. The second concept for the heat exchanger utilizes heat pipes to transfer the heat from the product gasses to the reactant gasses*. A wide range of materials can be used for the heat pipes using verious working fluids. The heat exchanger consists of several rows of heat pipes arranged either in-line or staggered as in a conventional shell and tube heat exchanger. The heat flows from the hot end to the cold end by the heat pipe cyclic action in a closed container. The working fluid evaporates due to heat addition and condenses due to heat removal. The wick inside the heat pipe pumps the condensate back to the evaporator end by capillary action. The working fluid is selected depending on the operating temperature.

In the application, the first two rows in the hottest range of flow stream will utilize ceramic heat pipes made of β-SiC with a chemically vapor deposited tungsten coating inside the tube. The liner shields the tube from the corrosive liquid metal and also can be used as the wicking medium. The proposed ceramic heat pipes are under development at Los Alamos Scientific Laboratory** in a similar heat recovery application. The next lower temperature heat pipes will consist of stainless steel heat pipes with sodium as the working medium. At still lower temperature ranges, water/stainless steel heat pipes could be used.

The advantages of heat pipe heat exchangers are numerous. Firstly, the product gas inlet temperature and the incoming reactants into the receiver are at the same temperature, thus assuming isothermal catalytic bed temperature. The maximum heat can be transferred by the liquid heat pipes, thus preheating the incoming reactants. Unlike the

*Russell, T.E., "Advanced Energy Programs Class Notes on Industrial Energy Conservation, October 1979.

**Keddy, K.S., Ranken, W.A., "Ceramic Heat Pipes for High Temperature Heat Removal", 18th National Heat Transfer Conference, August 1978, San Diego.

industrial rotary requirements, the heat pipe heat exchanger does not use any moving parts, thus not demanding any external power. Each heat pipe is simple and self contained. The heat pipes are known to operate indefinitely within design temperature range and are permanently sealed. Even if one heat pipe fails, the other existing heat pipes could compensate for the lost heat pipe by transferring more power. The heat exchanger can be made modular allowing inherent compactness and flexibility in the system. The heat pipes operate isothermally with practically negligible temperature and pressure drops. The overall heat transfer coefficients achieved in the heat pipe system are the best compared to other heat exchangers. However, the heat pipe heat exchangers involve moderate installed costs. Table 4-8 shows the representative working fluids and the envelope materials in each temperature range.

c. Shell-Tube Compact Heat Exchanger. This widely used industrial heat exchanger utilizes corrugated plates for the heat transfer surfaces. It provides maximum heat transfer area per unit volume enabling the heat exchanger to be compact. Fairly high heat transfer coefficients can be obtained, but the installed cost involved for this heat exchanger is usually high. The matrix can be made of either ceramics or a metal. Several programs are under contract to develop ceramic regenerators as a part of the automobile gas turbine development program.

Even a conventional shell and tube heat exchanger can be built to be a compact unit. But, a floating head design is required at high temperatures to allow for the thermal expansion of the tube bundle. The design gets to be complicated for high temperature application if it is desired to have separate high and low temperature streams.

d. Heat Wheel Rotary Regenerator. This is similar to the conventional heat exchanger used in automotive gas turbines and large central-station power plants. It consists of a rotating matrix driven by a motor of some kind. Sections of the wheel are alternately heated by the discharge stream and give up their heat to the inlet stream.

Although a successful proven concept for several different applications, it has several disadvantages for this one. These include a relatively high cost and the necessity for an external drive motor.

Table 4-8. Heat Pipe Working Fluids and Container Materials

Temperature Range °C	Capillary Fluid	Container Material
-203 to -160	Nitrogen	Stainless Steel
-60 to 100	Ammonia	Aluminum, Stainless Steel
10 to 130	Methanol	Copper, Stainless Steel
30 to 200	Water	Copper, Stainless Steel
100 to 425	Organic Fluids	Carbon Steel
250 to 650	Mercury	Stainless Steel
500 to 1000	Potassium	Stainless Steel, Nickel
600 to 1200	Sodium	Stainless Steel, Nickel
1000 to 1800	Lithium	Niobium, Tungsten

SECTION V

RECEIVER OPERATION AND PERFORMANCE

A. SPECIAL REQUIREMENTS

One of the advantages of the selected receiver concept is that no special requirements due to orientation or position are imposed on the design. Orientation of the inlet and outlet connections to the receiver have been indicated to be at three and nine o'clock. This was done since stresses in the ceramic tube were a minimum with this arrangement. However, if locations of these connections at twelve and six o' clock are more desirable for some application positioning, connections at these locations are possible.

B. INTERFACE REQUIREMENTS

The interface between solar receiver and concentrator would be at the focal mount support ring (reference Figure 4-2). This ring must be capable of supporting the 234 kg (516 lb.) solar receiver weight plus the weight of any other focal point located equipment (heat exchanger, Brayton machinery, generator, etc.). As indicated in Figure 4-2 the focal mount support ring inside diameter must be approximately 122 cm (48 in.) so that the receiver can be inserted into and olted to the ring.

For the solar receiver alone, wiring from temperature sensors to monitor inlet and outlet gas temperatures plus ceramic material temperatures would be led out through the rear end of the receiver through the support cover to connectors located on the focal mounting ring. If optical type sensors in the plane of the aperture were employed for collector control, the wiring or fiber optics for these units would be routed in a similar manner.

Assuming a heat engine or process heat exchanger were a part of the focal mount located system, additional interface requirements would be imposed on the focal mount support ring. A combination support structure for the solar receiver and heat exchanger/heat engine would most likely be utilized in this case. The support ring would have to be capable of supporting the additional loads and incorporate connectors for additional instrumentation, process lines, etc. See Figure 5-1.

With regard to connections between the solar receiver and process heat exchanger, several types and methods of line insulation are possible as indicated in Figure 4-25, 4-26, and 4-27. With the inlet and outlet ceramic couplings fixed to the solar receiver rear support, thermal expansion of lines leaving these points would require that the process heat exchanger high temperature side be allowed to float with respect to the solar receiver. Provisions for such would, therefore, be designed into the process heat exchanger.

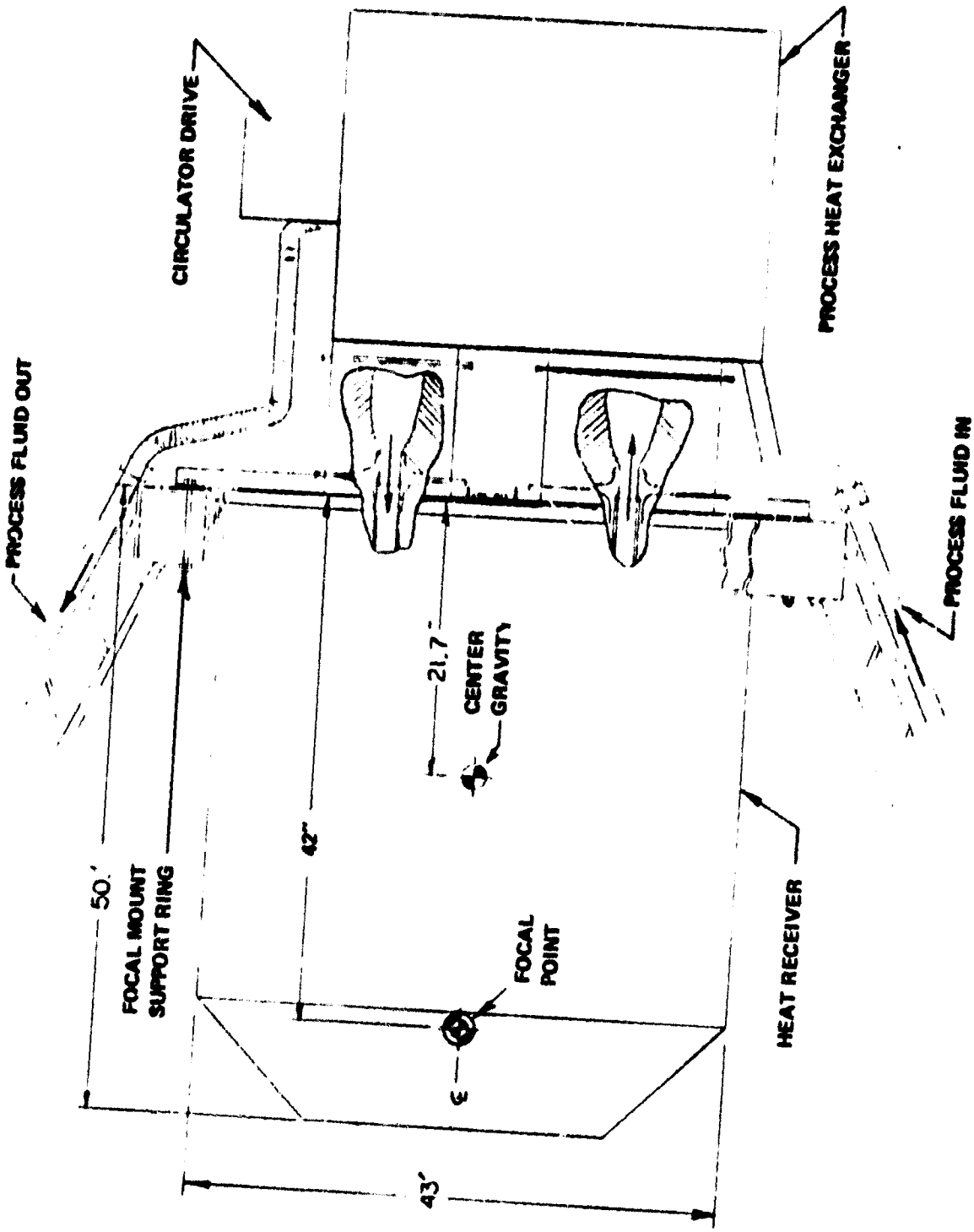

Figure 5-1. Focal Mount System

C. TRANSIENT RESPONSE ANALYSIS

The transient behavior of the receiver is important in the design of system controls and in characterizing system response to input transients (passing cloud cover, etc.). A transient heat transfer program was applied to the receiver model described in Section IV-B and several typical transients were simulated. The program performs a temperature iteration in time using a heat balance calculation similar to the steady-state program described in Section IV-B. Receiver response capability at step inputs from 0-50% and zero to 100% insolation was studied in addition to the loss-of-flow transient and receiver thermal energy storage capability.

1. Loss of Flow Transient

Starting from full power conditions (Section IV-B) with full insolation on the receiver, the program simulated a loss-of-flow transient by cutting the heat removal of the air in the tube. Figure 5-2 shows the temperature response of critical receiver components.

For the abrupt loss-of-flow simulated, the sleeve temperature reaches 1760°C (3200°F) (the limit in air for silicon carbide) in about 200 seconds. Tube temperatures reach 1649°C (3000°F) in 150 seconds, while the top-cap insulation temperature reaches 1760°C (3200°F) in 300 seconds. At these temperatures irreversible material damage starts to occur.

The loss-of-flow transient is perhaps the most severe transient experienced by the receiver in terms of overtemperature exposure (not thermal shock). The results of the analysis indicate that the system controls have at least 2 minutes to respond (basically by defocusing the collector) to prevent receiver damage. The first part of the receiver to see the damage will be the thermal inertia sleeve. (If the sleeve was not present, the tubes would see the damage first and the response time would be much shorter due to the reduced thermal mass of the tubes).

2. Receiver Response From Ambient-No Flow

Receiver response to insolation steps starting from "cold" or ambient temperatures is important in characterizing receiver performance in startup as well as receiver overall temperature-response characteristics. Since the receiver startup flow and temperature schedule is not defined (has to be defined in conjunction with application or prime mover requirements) two simulations were tried:

- Insolation on a cold receiver with no cooling air flow.
- Insolation on a cold receiver with full air flow 0.11 kg/sec (0.244 lbs/sec) at 149°C (300°F) inlet temperature.

The latter simulation was calculated to approximate a possible Brayton-cycle startup condition in the initial stages when the receiver is still cold, and the compressor is operating at full power driven by the generator or a starting motor.

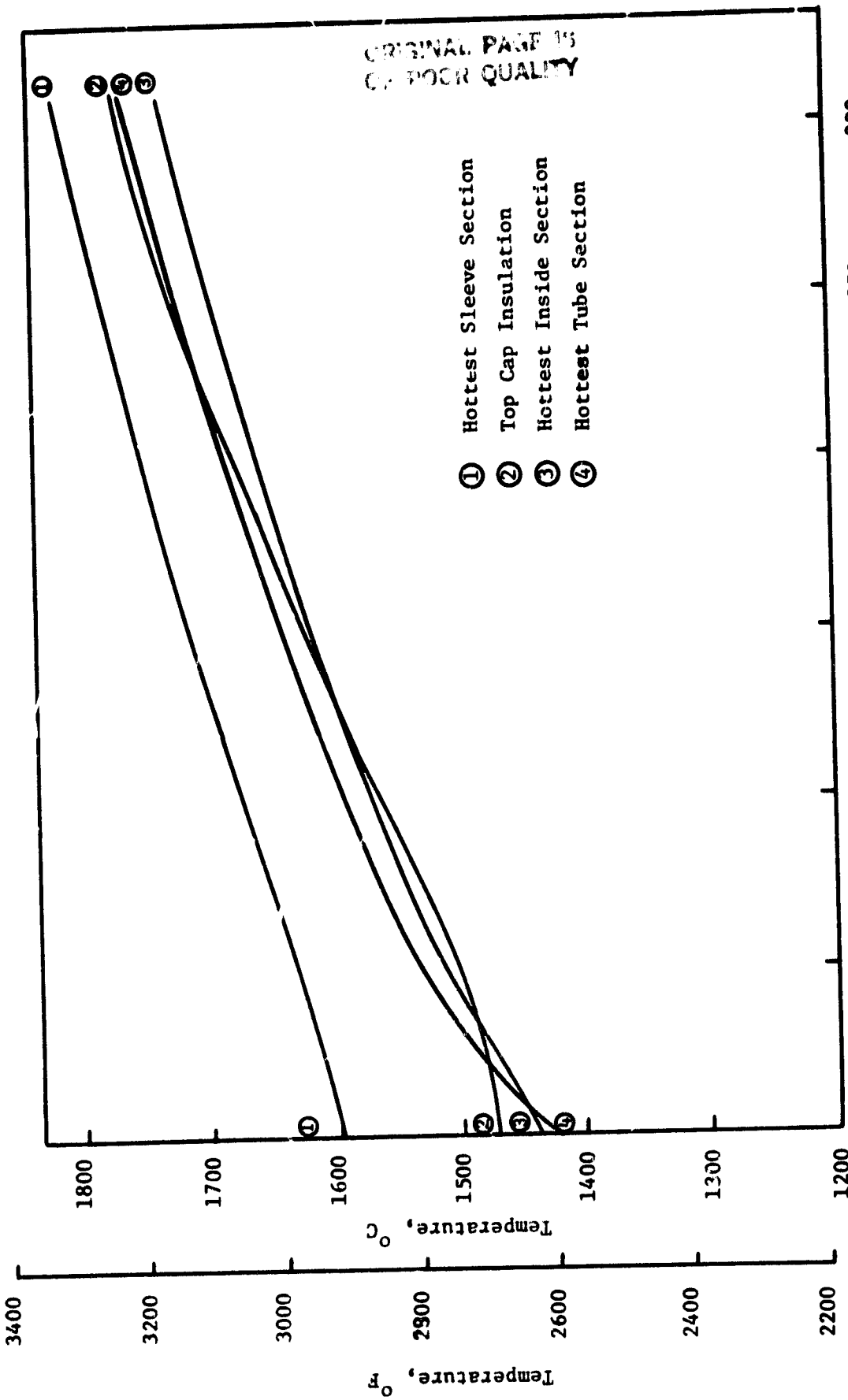

Figure 5-2. Loss of Flow Transient Temperature Response (Start hot, with full insolation)

Figure 5-3 shows the temperature response of critical receiver components to a full (0-100%) insolation step at time 0. The receiver is assumed to be at an ambient 21°C (70°F) before insolation. No cooling flow is assumed. The simulation of the flow case is described in subsequent paragraphs.

Figure 5-4 shows the receiver response (with no cooling flow assumed) to a 0-50% insolation step at time 0, where the insolation is taken as half that of the full power level.

Sleeve, tube and inner insulation surface temperatures reach "hot" values (steadystate power levels) in about 15 minutes for the full-insolation step, and about 30 minutes for the half-insolation step. The plots shown are not typical of startup since it is expected that cooling flow will be started before hot temperatures are reached to prevent thermal shock to the tubes and to allow a smooth transition to power conditions on the Braytoncycle. The results, however, give an order-of-magnitude of the time constants to be encountered in startup.

3. Receiver Response From Ambient-With Flow

Figures 5-5 and 5-6 show receiver temperature response to full-insolation and half insulation steps, respectively, with receiver starting at ambient 21°C (70°F) temperatures and full 0.11 kg/sec (0.22 lbs/sec) flow at an inlet temperature of 149°C (300°F).

After 12.5 minutes, receiver temperatures are still well below "hot" values, which is expected partly due to the very low air inlet temperature. Cooling air flow also slows down receiver response since it causes heat removal before power levels are reached. Again the simulation does not represent an exact startup simulation (to be defined by the system controller) since it is expected that inlet air temperatures will rise (due to the pressure of the recuperator) as the receiver gets hotter. The results, however, are indicative of air heat-pickup transient behavior in startup. After 12.5 minutes, air heat pickup reached approximately 30% of design value with full insolation (compared to 15% for half insolation). These time-constants need to be considered in startup scheduling.

4. Thermal Energy Storage Characteristics

To study the TES capabilities of the receiver, a simulation of insolation cut-off (e.g., passing cloud cover, defocusing, etc.) was done on the receiver starting at full power steady state conditions. Air flow was maintained at full value 0.11 kg/sec (0.244 lbs/sec) with an inlet temperature held at 954°C (1750°F) (design value).

Figure 5-7 shows the temperature response of the receiver including the decaying air exit temperature. Exit temperature is down 111°C (200°F) from design value in about 45 seconds, and down 278°C (500°F) (to 1093°C (2000°F)) in about 150 seconds. The receiver can therefore maintain a good power level for about 2 minutes in case of insolation loss (passing cloud cover, etc.).

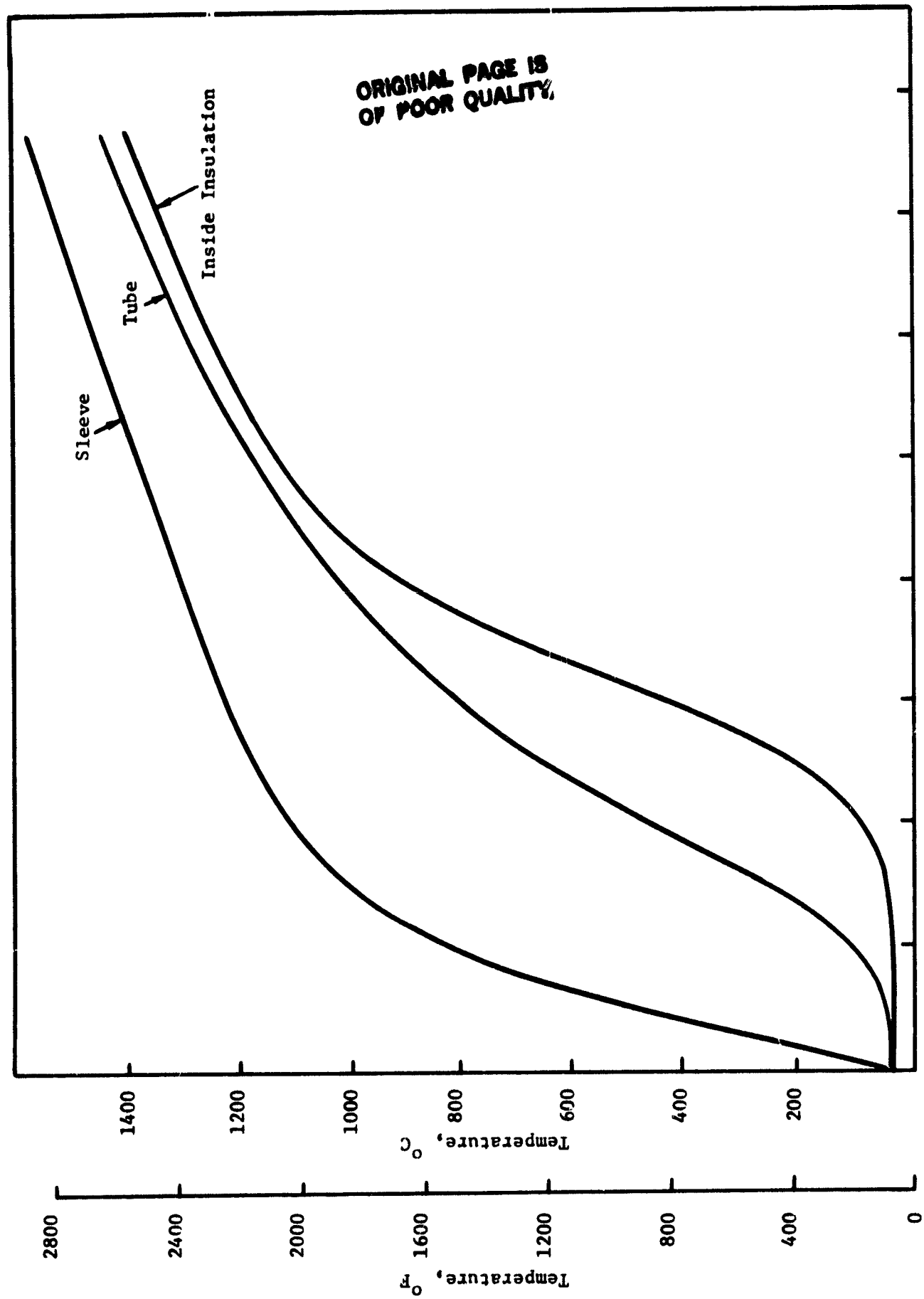

Figure 5-3. Receiver Temperature Response to a Full-Insolation Step from Ambient (No Flow)

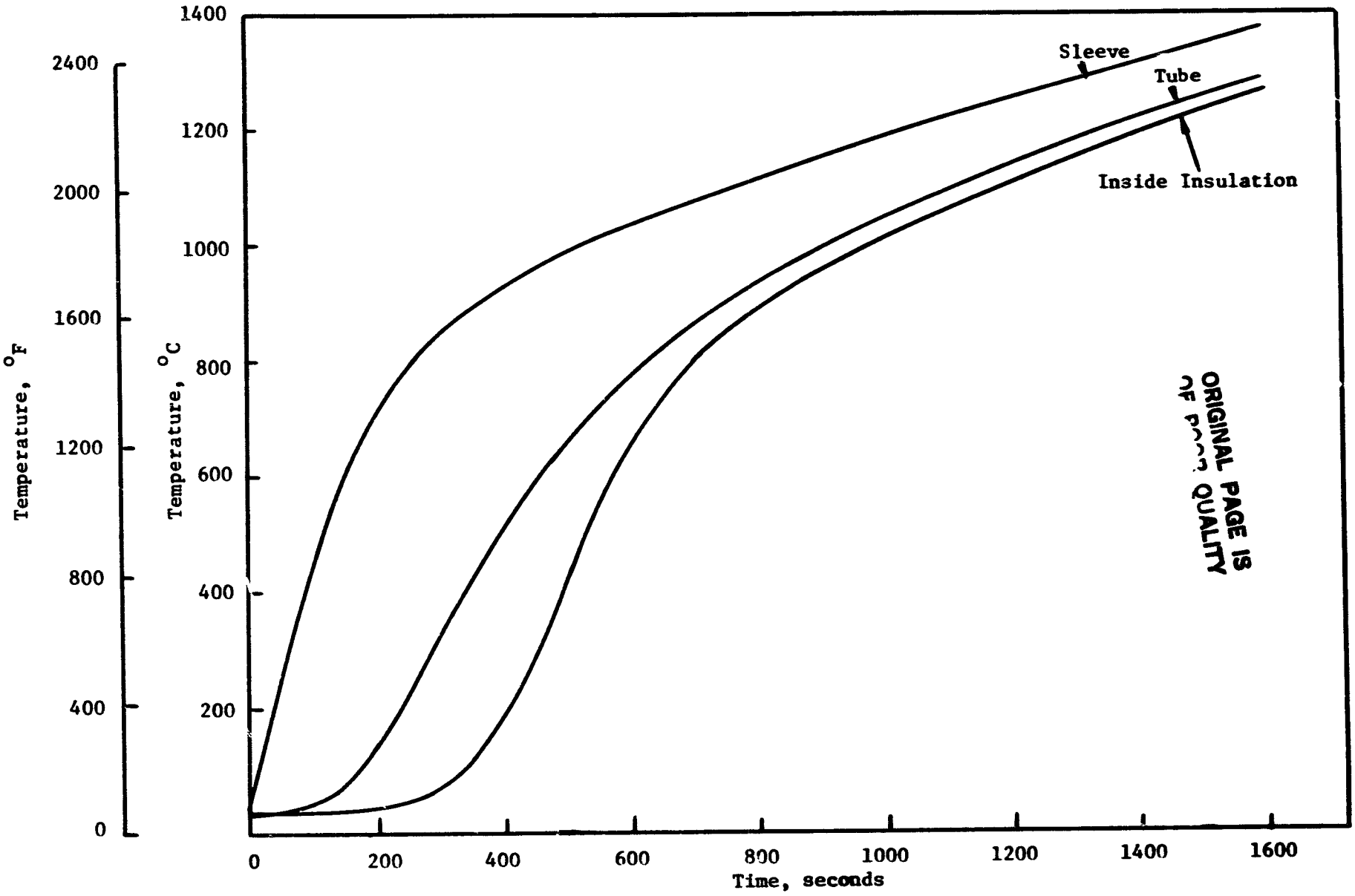

Figure 5-4. Receiver Temperature Response to a Half-Insolation Step from Ambient. (No Flow)

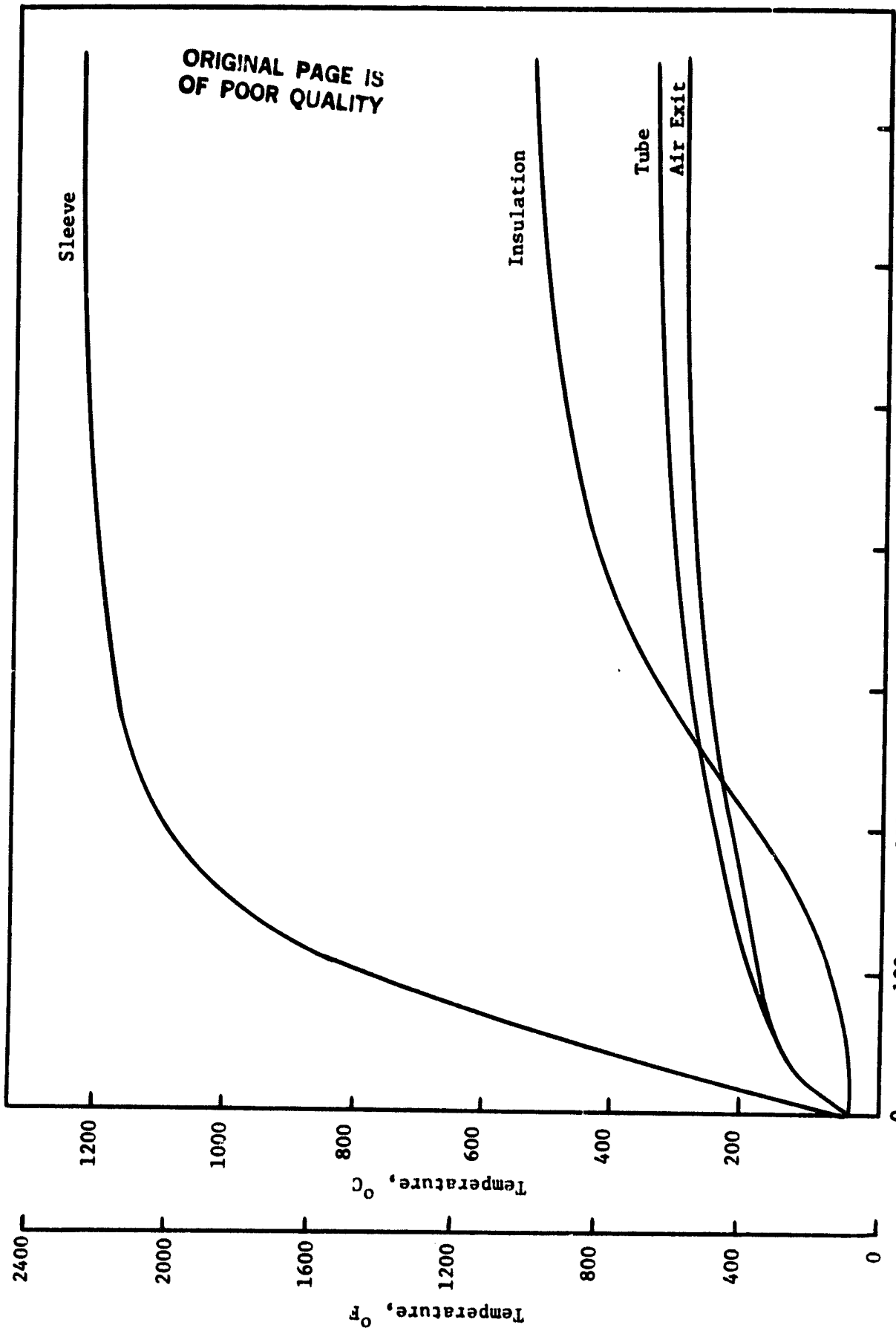

Figure 5-5. Receiver Temperature Response to a Full Insolation Step from Ambient (Full Flow at 149°C Inlet)

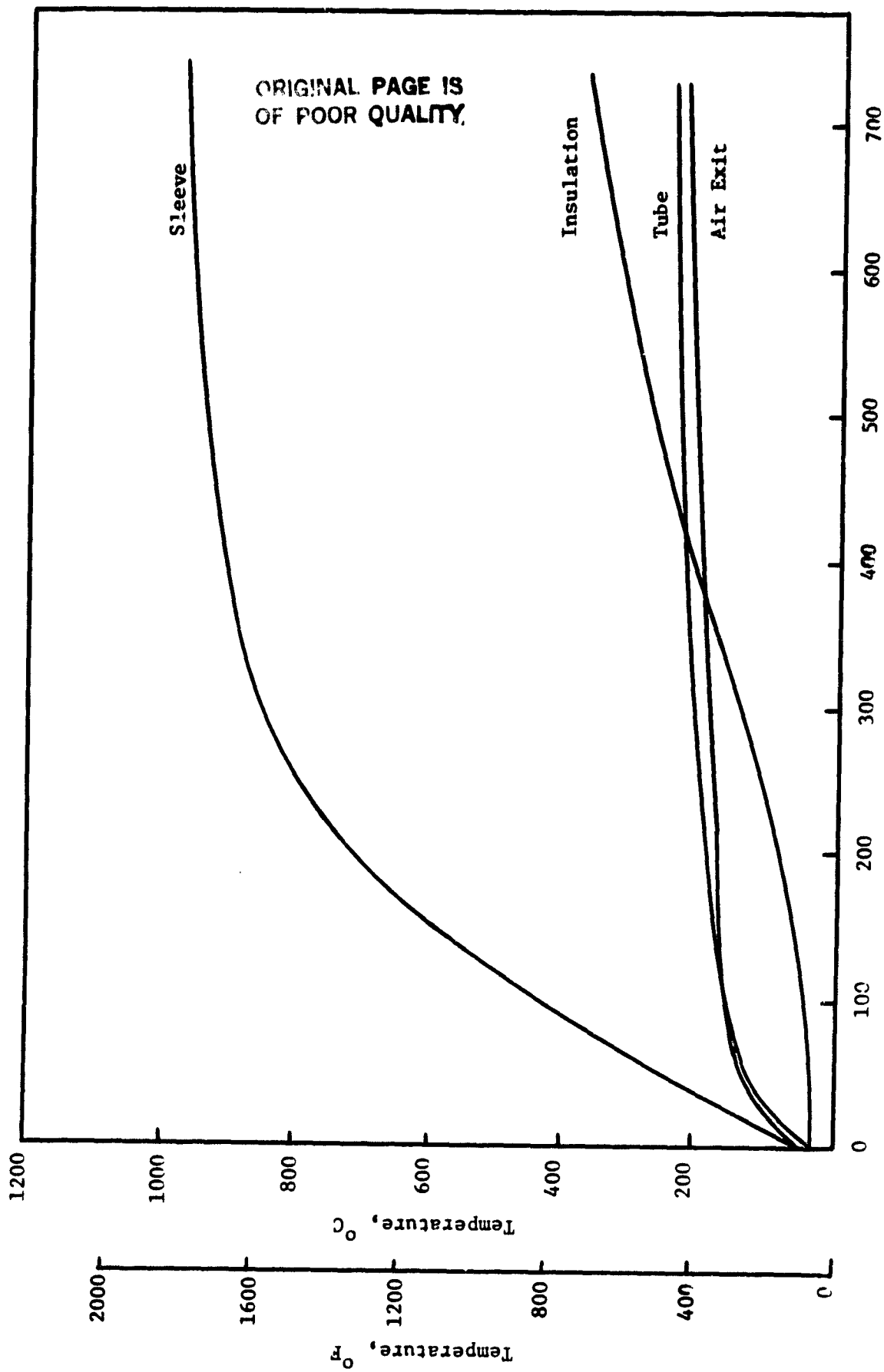

Figure 5-6. Receiver Temperature Response to a Half-Insolation Step From Ambient (Full Flow at 149°C Inlet)

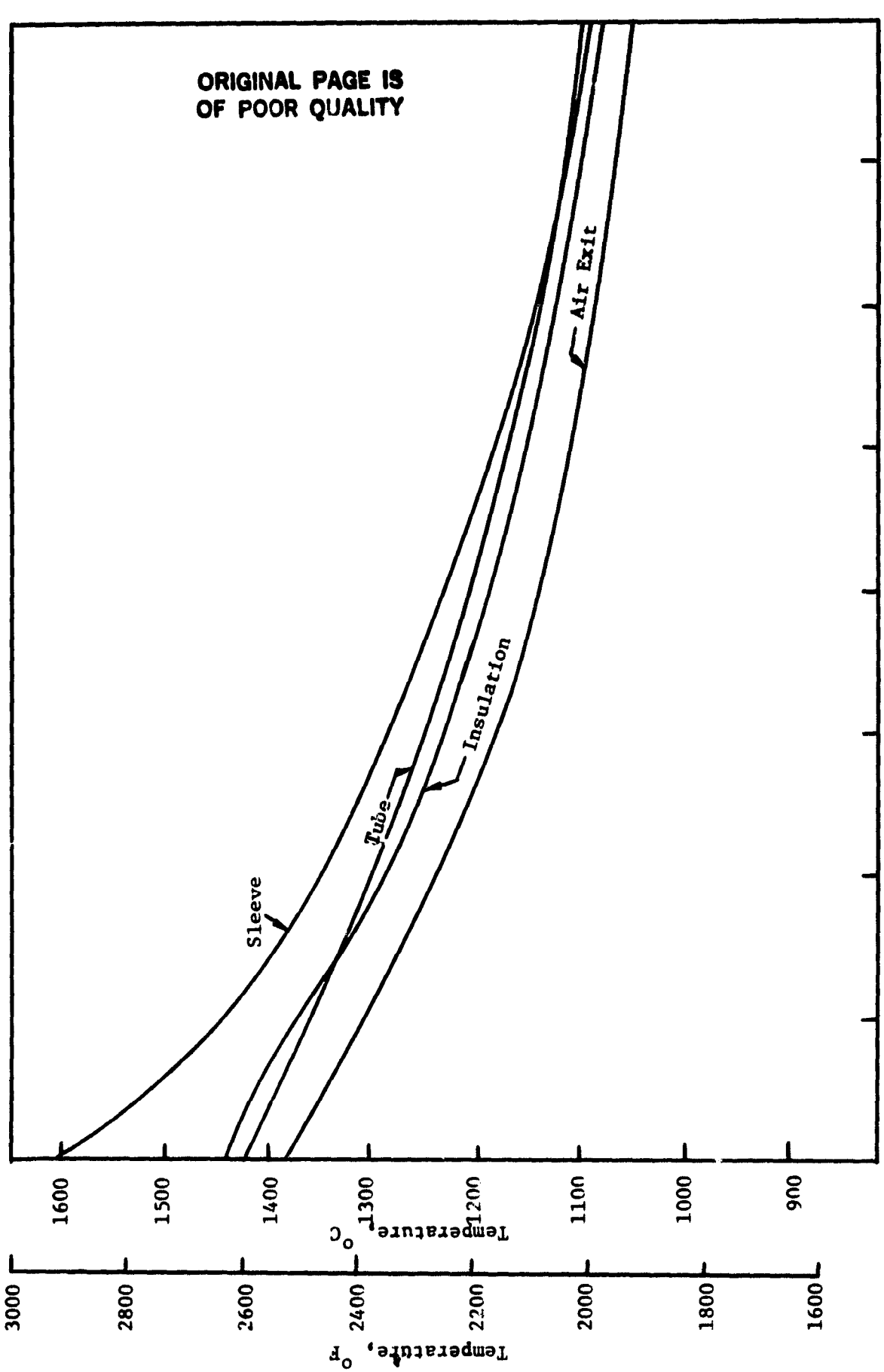

Figure 5-7. Receiver Response to Insolation Cut-off (from full-power temperature). (Full Flow at 954°C Inlet). Shows TES Capability

5. Operational Considerations

The transient response characteristics of the receiver are necessary in control system design for scheduled operational transients (startup and shutdown) as well as emergency response and normal operational transients (passing cloud cover, etc.).

The loss-of-flow analysis indicates the need for fast-defocusing, with a detection and response time limit of about 2 minutes. In the case of overtemperature detection on the sleeve or tubes the response time is reduced depending on the overtemperature set-point.

The slow receiver transient from ambient will dictate the design of the startup flow and temperature sequence. The overall transient response will also be dependent on other system components (regenerator, turbine, etc.) and has to be considered as a whole. Note that the receiver can reach a high power level although much of the insulation is at a low temperature, as long as the insulation inside temperature is high. (The total insulation energy storage capacity is estimated at 40 kW-hr at full-power steady state temperatures, and will take a long time to charge.)

In case of passing cloud cover, the 2-3 minute storage time allowed by the receiver with high exit temperatures provides an adequate capacity for most situations, and enough response time for the control system to react.

Further study of system transients is needed once the application is defined. A dynamic analysis of the interconnected system would be useful in control system specification.

D. SAFETY AND OPERATIONAL CONSIDERATIONS

The solar receiver concept as described herein offers no safety hazards to operating personnel, the general public or the environment. Certain safe operational practices must, however, be followed to prevent damage to the receiver or other system equipment. As with all concentrating type solar receivers, improper concentrator operation can result in the destruction of the solar receiver particularly in the event that the concentrated energy hits the receiver in some spot other than the aperture and remain in this abnormal position for any length of time. A loss of load on the system (i.e., energy not removed from receiver at the proper rate) can also result in damage to the receiver. Therefore, controls to eliminate the possibility of such accidents as described above must be a part of the system.

The solar receiver coil is in a sense a pressure vessel containing gas at high temperatures and relatively low pressure. The volume of gas in the ceramic coil is relatively small so that even a rapid failure of the coil would not result in an explosion of large force which could damage surrounding property or personnel. Assuming the process utilizes air as the heat transfer fluid, no adverse effect on the environment is possible.

Startup or cloud passage could subject the solar receiver, primarily the thermal inertia sleeve to a large thermal shock. Failure of this component could then result in the sun's concentrated rays impinging directly on the solar receiver ceramic coil. A failure of the coil could then result. Since ceramic materials subjected to stresses, whether they be of a mechanical or thermal nature, are very unpredictable only fluids which are not contaminating to the atmosphere should be utilized initially. As operating experience is gained and designs improved for joining and sealing ceramics, the use of high temperature chemical processes involving fluids hazardous to the environment and personnel could be considered.

SECTION VI

PRODUCTION COST ESTIMATE

A. SOLAR RECEIVER COST ESTIMATE

To estimate the mass production cost of the high temperature solar receiver concept as proposed herein the unit was broken down into major components (similar to the Parts List). The material utilized in each component, its weight, unit costs for materials and labor, material and labor costs, and total cost by component were then determined and are indicated in Table 6-1. The overall cost is the sum of the component costs plus assembly of the components into a unit. As indicated in the table, unit costs are based on manufacture of 1000 solar receiver units per year. Estimated costs, based on high production rates, are indicated later in this report.

B DETERMINATION OF UNIT COSTS

The unit material and labor costs indicated in Table 6-1 are the backbone of the overall solar receiver cost and, therefore, the methods and data utilized to obtain these figures require further explanation. Major component costs are examined one at a time as follows:

1. Ceramic Coil

The potential to produce tubing from sintered silicon nitride of almost any diameter, cross-section geometry, or length by extrusion has recently been demonstrated* including sealing and brazing. The low cost production of sintered silicon nitride raw material from materials such as clay and coal (carbon) have been recently reported by Cutler** and his associates at the University of Utah. Thus, both process development and low cost material availability have been demonstrated.

In order to determine the cost of manufacturing sintered silicon nitride tubing the processing sequence must first be examined. The process contains ten (10) distinct operations which are shown in the flow diagram of Figure 6-1. These operations are then listed in Table 6-2 along with the estimated labor time to complete a particular operation. The cost of each operation, based on a labor rate of $7.50 is then computed. Information on labor hours required per operation was obtained from three sources as follows:

---

* Gatti, A., W, Chiu, L. R. McCreight, "Sinterable Si_3N_4 Ceramic Recuperator Materials", NASA-Lewis CRN DEN 3-54, September 1979.

** Lee, J.G., Casa R., and Cutler, I., "Sialon Derived from Clay to Provide an Economical Refractory Material", Indust. Heating, April 1976, pg. 50-53.

Table 6-1. Solar Receiver Cost Estimate

Item	Component Des.	Type Matl.	Wt. Matl. (lbs)	Matl. Unit Cost ($/lb)	Matl. Cost ($)	Lab Unit Cost ($/lb)	Lab Cost ($)	Tot. Cost ($)
1.	Ceramic Coil	Si_3N_4	34	.05	1.70	1.42	48.3	50.00
2.	Thermal Inertia Sleeve	SiC	62	.05	3.10	1.00	62.00	65.10
3.	Insulation (Graded)	Ceramic Fiber	289.1	4.06	1175.	-	-	1175.00
4.	Ceramic Couplings	Si_3N_4	6.0	.05	0.30	2.00	12.00	12.30
5.	Shell & Cover	Painted Steel Sheet	89.5	.30	26.85	1.00	89.50	116.35
6.	Support Structure	Painted Structural	30.0	.30	9.00	1.00	30.00	39.00
7.	Coupling Supports	Hastalloy X	5.5	6.45	35.48	2.00	11.00	46.48
8.	Misc. Hardware	Steel	10.0	2.00	20.00	-	-	20.00
9.	Assembly	-	-	-	-	($24./hr)	200.00	200.00
				Indicated Cost Based on 1000 Units				$1724.23

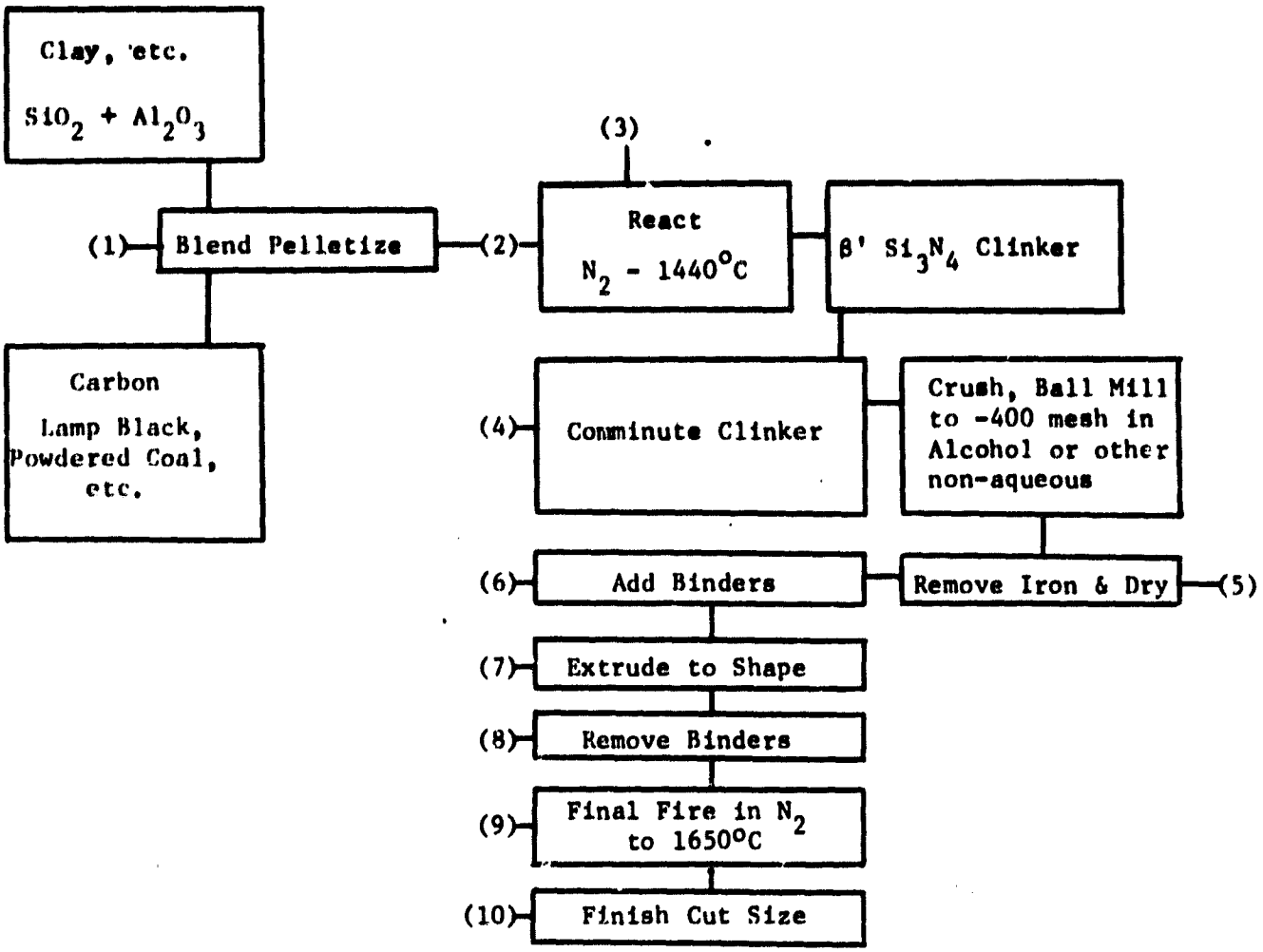

Figure 6-1. Flow Diagram for Low Cost β' Si_3N_4 Materials Which are Non-Strategic and Capable of High Temperature Performance

Table 6-2. Summary-Labor Costs for Sinterable Si_3N_4 Tubing (600 Lb. Batch)

No.	Operation Description	Lab Hrs. Req'd	Cost at $7.50/hr.
1	Blending	0.25	$ 1.88
2	Pelletizing	3.50	26.25
3	Reaction	2.20	16.50
4	Comminute	4.47	33.53
5	Remove Iron	2.00	15.00
6	Add Binders	1.00	7.50
7	Extrude to Shape	2.00	15.00
8	Dewax	2.00	15.00
9	Final Fire	1.25	9.38
10	Finish Cut & Size Ends	4.00	30.00
	TOTALS	22.67	$170.04

C-E Refractories, King of Prussia, PA

Carboloy Product Department, GE Company, Detroit, MI

Locke Insulator Inc., Baltimore, MD

Rough engineering estimates (ROM) were made for operations No. 8 and No. 9 since no similarity existed between those operations and the products produced by these organizations.

Raw materials costs for clay range from $22 to $40 per ton. The latter number was chosen as the most conservative. Cost per pound is $0.02. Coal costs range from $12 to $25 per ton. Using the highest figure, carbon cost per pound is $0.0125. Other sources of carbon, such as lamp black or charcoal, are higher in cost by at least a factor of two. Therefore, being very conservative results in a 1979 raw material cost of approximately $0.045 per pound. The above figures were obtained from the Ceramics Data Book published by The Cahners Publishing Company, 1979.

Referring to Table 6-1 and applying an overhead rate of 500% (quoted by two vendors and including plant equipment, supervision, support, etc.) the cost of sintered silicon nitride (based on a 600 pound batch) is computed as follows:

$$170.04 \times 500\% \div 600 + \$0.05 = \$1.47/\text{pound}$$

One vendor questioned stated that a 300% overhead would be reasonable. This would result in a finished product cost of $0.90 per pound. It is reasonable to assume the cost will be somewhere between the two figures. The more conservative value was used in the cost estimate.

There are two critical areas in the scenario which would need further development. These areas are material processing by means of the Cutler process to produce Si_3N_4 starting materials and extrusion binder systems which would be more readily removed and recycled than the wax-powder mixtures now used.

Present materials produced by Cutler are of a lower quality than those used during our development studies. Producing acceptable raw materials cheaply enough (i.e., $\sim$ 5¢ per pound) is a significant part of this scenario. Si_3N_4 presently available is expensive, the least costly material is still more than $8 per pound.

With low cost materials available, the cost of tubing is almost entirely determined by labor costs. As an example, if the labor costs can be halved, the price of tubing falls to $.71 per pound using the 500% O/H figure.

2. Thermal Inertia Sleeve

Vendors requested to provide cost estimates for the silicon carbide (SiC) sleeve indicated a cost of approximately $2000 to manufacture one or two units. They were unwilling to provide a cost estimate based on one thousand

units. Assuming the costs indicated for the manufacturing of the sintered silicon nitride coil are reasonable there is no reason to believe the silicon carbide sleeve could not be manufactured for approximately the same cost. Due to the simple cylindrical configuration some of the operations should be less expensive. This is reflected in the $1.00/pound rather than $1.42/pound for Si_3N_4 labor estimate. Raw materials would be expected to be the same for both ceramics.

3. Insulation

Insulation costs are based on data obtained from Babcock and Wilcox Company. Their insulation proposal consists of a 2 1/2 inch thick layer of B&W Company 3000 Board insulation surrounding the ceramic coil. This insulation would be in rigidized pieces (two to four pieces). Saffil® fibers are employed and the maximum operating temperatures capability of the insulation is approximately 1649°C (3000°F). As the temperature drops in a radial direction through the insulation, materials of lower temperatures capability are utilized and, therefore, the term graded insulation is employed. At the 1260°C (2300°F) interface, B&W ST Board is used and below 1093°C (2000°F), B&W, 6 lb./ft^3 Kaowool Blanket insulation is used. Based on one thousand units the B&W estimated cost for insulation was $1174. This is $4.06 per pound.

Actually the outer three or four inches of insulation could be fiberglass in place of an equivalent amount of Kaowool insulation. This could result in some cost savings.

4. Other Materials and Labor

Unit costs for materials and labor for the sheet metal casing, structural steel support and superalloy coupling supports are based on engineering estimates from costs incurred in the manufacture of similar items by the GE-AED shop. The assembly hourly labor cost is typical for a technician and includes overhead and G&A.

C. EFFECTS OF PRODUCTION QUANTITY ON UNIT COST

The cost estimates for the 1000th unit was determined to be approximately $1724. It was necessary to project the unit cost at production rates of 10,000, 100,000, and 1,000,000 per year. The technique used involved learning curve theory and was based on the unit cost data given in Table 6-1.

By separating the raw materials out of the insulation package at the same price as that of the silicon nitride and silicon carbide, i.e., $0.05 per pound, the following breakdown of the total cost is made:

Total Labor Cost	$ 453.
Raw Materials	111.
Insulation (w/o Raw Material)	1160.
TOTAL	$1724.

It was observed that much of the cost of the insulation package, in small quantities, is manual labor and assembly. In addition, significant cost improvement can be anticipated during subsequent manufacturing development.

An 80% learning curve was applied to the labor cost and to the insulation package exclusive of raw material. Raw material cost was held constant. Shown below is the estimated cost in mass production.

Number of Parts	Unit Cost
1,000	$1,724
10,000	880
100,000	478
1,000,000	286

Figure 6-2 shows the Unit Cost versus number produced. Note that the cost in large-scale mass production is approximately twice the raw material cost, which is consistant with other studies*.

D. PRODUCTION TOOLING REQUIREMENTS

Capital equipment costs required for production of up to approximately 2000 sintered silicon nitride solar receiver coils per year are indicated in Table 6-3. To increase production above 2000 units per year would require a nitrogen furnace (item No. 9) of Table 6-3 capable of continuous operation. This would increase the cost of item No. 9 to approximately $60,000 or double the cost of the batch-type furnace. The process equipment would then be capable of producing approximately one ceramic coil every hour, or 8760 units per year. The total capital equipment cost would then be approximately $183,000.

Production equipment and facilities presently exist to handle the manufacture of 2000 silicon carbide thermal sleeves per year. Production rates above this figure would require vendors to install additional process equipment.

The insulation material required in the solar receiver construction would be subcontracted to manufacturers engaged in the production of insulation materials.

E. RECEIVER OPERATING LIFE AND MAINTENANCE REQUIREMENTS

The solar receiver conceptual design presented previously in this report has several design features which enhance its operating life. Simplicity in design and fabrication is the key to success and long operating life in any system and it is difficult to see a way in which a simpler design could be

* For Example: Allen, M.M., Larson K.J., and Walker, B.H., "Process Demonstration and Cost Analysis of a Mass Production Forging Technique for Automotive Turbine Wheels, Phase II", Pratt & Whitney Aircraft, COO/2637-1, July 1977.

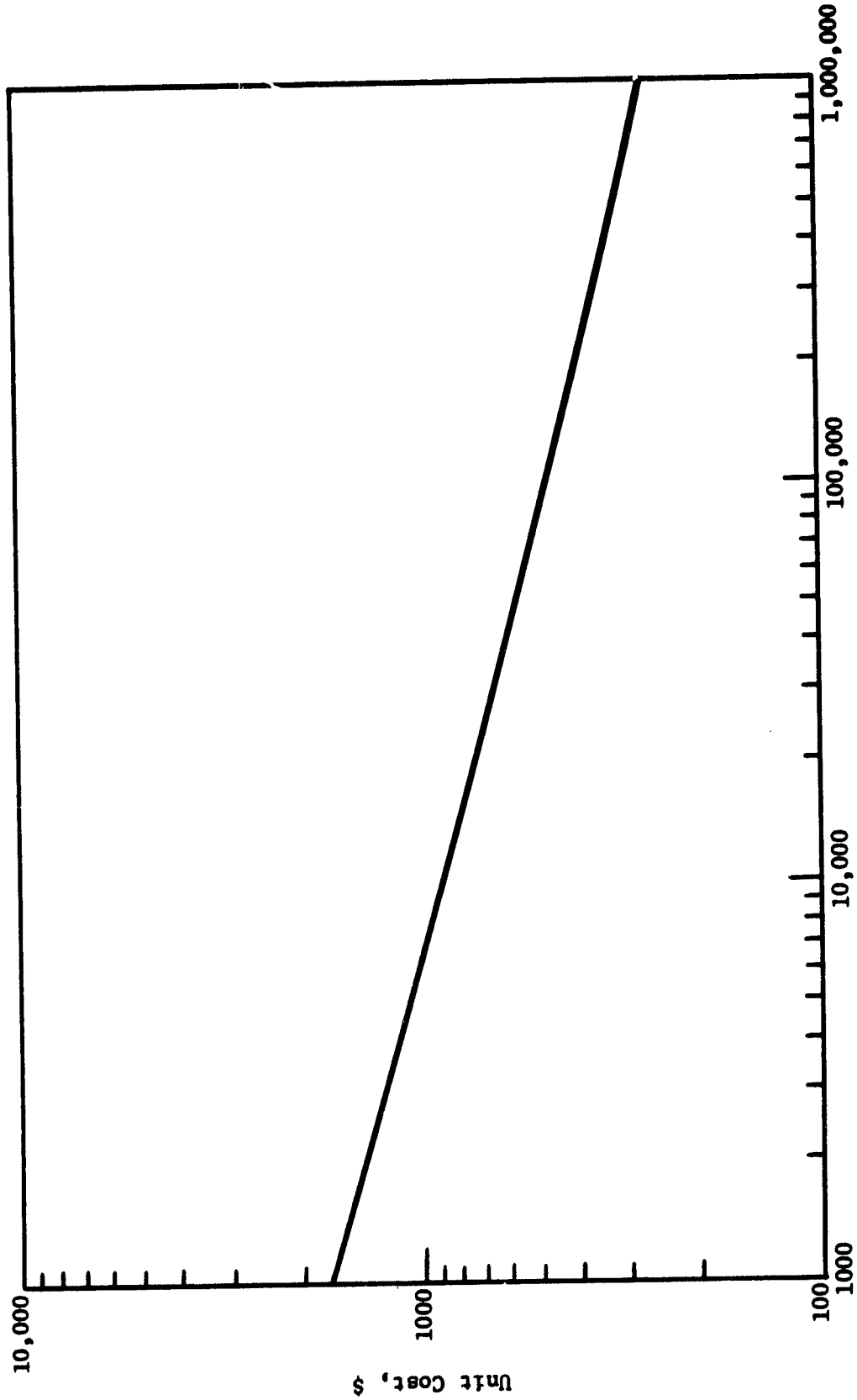

Figure 6-2. Unit Cost in Mass Production

TABLE 6-3 Estimated Capital Equipment Costs
Sintered Silicon Nitride Coil

Item	Description		Cost
1.	Shell Blender		$ 5,000
2.	Pelletizing Press		12,000
3.	Continuous Belt Furnace with Nitrogen Atmosphere		25,000
4.	Jaw Crusher		5,000
5.	Ball Mill		10,000
6.	Magnetic Separator		3,000
7.	Dryer		8,000
8.	Muller		5,000
9.	Extrusion Press		22,000
10.	Oven		10,000
11.	Nitrogen Furnace (Batch - 2 Coils/8 Hr. Shift)		30,000
12.	Diamond Cut-Off Tool		2,000
	Sub Total		137,000
	Freight	1%	1,400
	Installation	10%	13,700
	TOTAL		152,100

produced for a high temperature solar receiver. The coiled ceramic heat exchanger is fixed only at its inlet and outlet connections allowing freedom for thermal expansion in all directions from these fixed points. To further protect the heat exchanger, a ceramic sleeve is utilized as a thermal damper between the concentrated rays of the sun and the ceramic coil. This sleeve moderates the thermal shocks possible during startup and after cloud passage and should greatly increase the life of the coiled ceramic heat exchanger. No parallel arrangement of tubes requiring many ceramic joints is required, in fact, no joints whatever exist in the coiled tube which could result in fluid leaks.

Maintenance requirements for the solar receiver portion of the focal mounted system should be minimal. The receiver casing weather seals must be kept tight to prevent the entry of water or other foreign material into the insulation. Weathering of the outer steel casing will require painting from time to time. Since there are no moving parts, no lubrication at periodic intervals is necessary. In the event of a break in the ceramic coil it is expected that the complete solar receiver would be removed from the focal mount ring and a replacement unit installed at the site overhaul shop. No routine replacement of the coil or thermal sleeve is contemplated. Only periodic inspection to insure that the thermal sleeves have not cracked or cracks in the ceramic coil do not exist appears necessary.

SECTION VII

CONCLUSIONS

As a result of this conceptual design study, the following conclusions are made concerning high temperature solar thermal receivers:

1. Of all the concepts evaluated, the one using a helical coiled silicon nitride tube is the most attractive for high temperature service. It showed good efficiency, high temperature capability, low pressure drop, and a potential for low cost in mass production. It is a simple design with few parts which should lead to easy replacement of parts and low maintenence costs.

2. The matrix (honeycomb) concept was very attractive at lower temperatures. Although the requirement of a fused silica window limits the temperature capability of this concept, where it can be used it shows excellent performance and the potential for low cost in mass production.

3. No new materials development are required for the helical coiled tube concept. Only the size of the coiled tube requires fabrication process development. The materials and processes are presently available. The rest of the design is made out of commercially available materials.

4. Detailed thermal analysis confirms the parametric analysis. A finite element 2-dimensional thermal analysis gave results for temperatures and heat losses in good agreement with the parametric analysis. For the Brayton cycle design point an efficiency of 62% was achieved with a 2 milliradian slope error concentrator. Peak temperatures were well below material limits.

5. Stress analysis of the coiled tube showed that a large factor of safety exists. A finite element stress analysis showed that the coil could be hard mounted to the support structure and operate safely in all operating positions. Deflections due to pressure and temperature were small.

6. Transient thermal analysis showed that the helical coil designs could operate sucessfully over a wide range of conditions. Analysis of the loss-of-flow condition showed that up to 2 minutes would be available to defocus the concentrator before damage would occur. The thermal inertia sleeve takes the initial thermal shock and protects the coiled tube. Enough thermal inertia exists to allow several minutes of operation during cloud cover.

7. The conceptual design is adaptable to direct chemical reactions. A small amount of effort showed that several ways of placing catalysts in the receiver were both possible and practical. Several recuperator designs were identified which could provide the necessary thermal energy recovery.

8. Low cost in mass production is achievable. Cost estimates of $300-400 per unit at a production rate of 200,000 to 1,000,000 per year appears reasonable. The basic designs and materials of construction lead to a naturally low cost receiver.

SECTION VIII

RECOMMENDATIONS

The following reommendations follow logically from the conclusions of the study.

1. It is recommended that a feasibility demonstration of the fabricability of the silicon nitride helical coil be performed. This component is the only one which is not commercially available. The materials and processes are developed, but not for the specific size and shape required. A sucessful demonstration, using existing facilities, will provide the necessary proof that the concept is viable.

2. Subject to a successful demonstration of fabricability of the helical coiled tube, a full size receiver should be designed, built, and tested. With confidence in the fabricability of the helix, a program leading to a full size receiver appears to have no barriers. This would provide the technology for the use of high temperature solar energy in economic and efficient fashions.

APPENDIX A

THE MATERIALS AND FABRICATION PROCESS FOR A HIGH TEMPERATURE SOLAR THERMAL RECEIVER

(Contract 955455)

L. R. McCreight
General Electric Company
Philadelphia, Pa. 19101

Introduction

One of the most promising concepts for the design of a high temperature solar receiver depends upon the capability to extrude and shape a ceramic tube into a helical coil. Figure 1 shows a concept for a high temperature solar thermal receiver which uses a large coiled ceramic tube as the key heat exchanger element between the solar energy and the gas to be heated. The size and complexity of this part put its fabrication beyond the current state of the art but within the range of development capabilities. This memo was prepared to fully discuss the materials and especially the fabricating process for this program.

While there are several oxide, carbide, and nitride ceramic materials capable of resisting the high temperatures and some of the related aspects for service as a solar receiver, the best choices for consideration are between the silicon carbides and silicon nitrides. Either family of material can probably be satisfactorily used in this program although some particular chemical environment may dictate choosing one over the other. However, if all other aspects are equal, the silicon nitrides have certain properties which make them the material of choice. These are a lower thermal expansion coefficient and a lower modules of elasticity

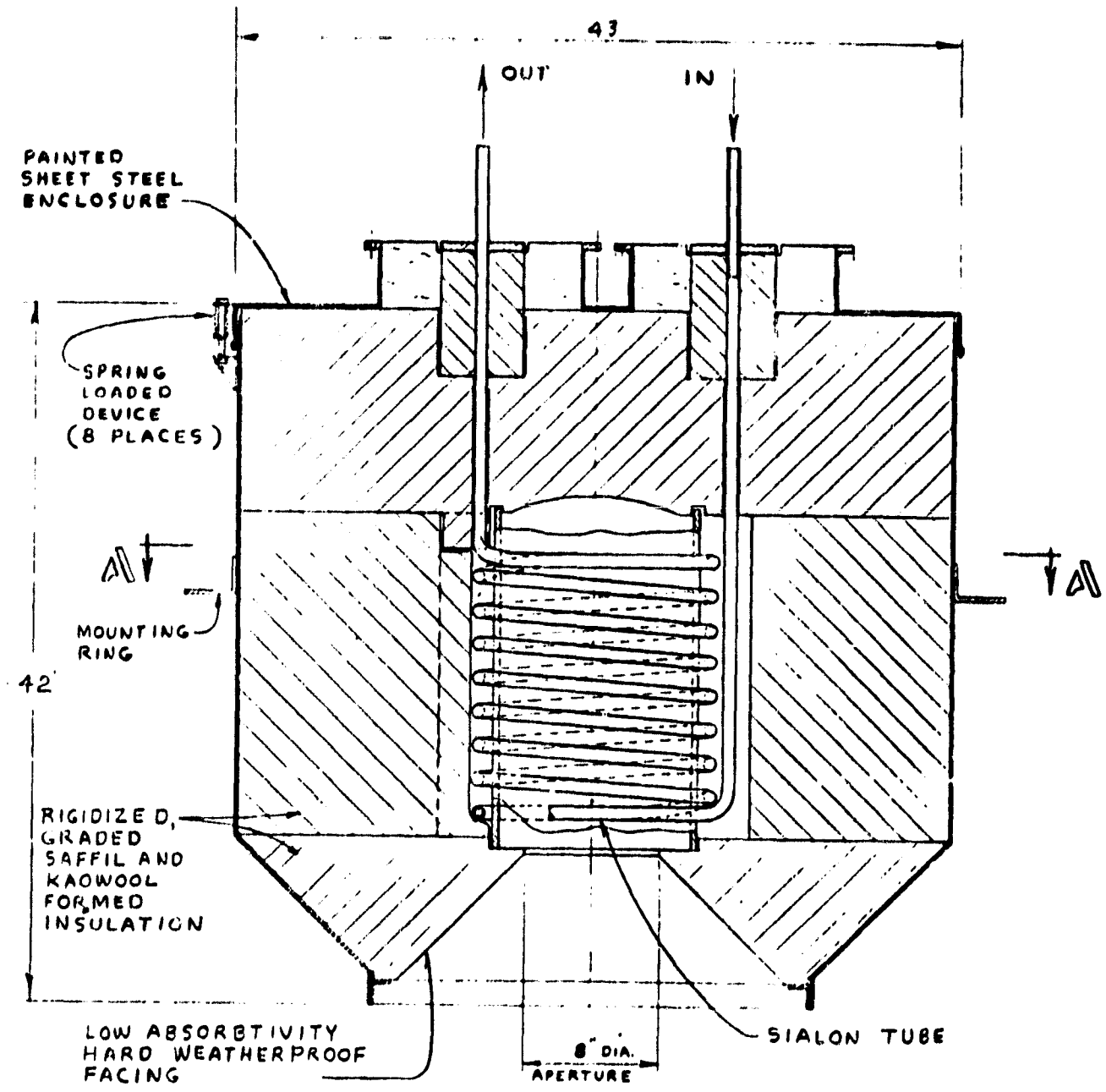

Figure 1. High Temperature Solar Heat Receiver

as compared to the silicon carbides. While silicon carbide has a higher thermal conductivity it is still generally more thermal shock sensitive than the silicon nitrides. In the case of the older and better established silicon carbides, several compositions and methods of fabricating are available, while until recently only hot pressing and reaction bonding were available for silicon nitrides. Now that essentially all of the standard ceramic processes are available for silicon nitrides (largely through our recent work) they can be more widely applied.

Our work has been aimed at initially making the so called sialons (which are named by using the symbols for the four major chemical ingredients; Si, Al, O, and N) using about a 50-50 mixture of Si_3N_4 and Al_2O_3-AlN. Subsequent compositions have been prepared with as high as 94-95% Si_3N_4. These are processed with our own high purity silicon nitride grinding media to avoid the contamination which is common to other grades of silicon nitride and by all of the common ceramic forming techniques. Some of the properties, compositions and examples of these materials are shown in Figures 2, 3 4 and Table 1. It is our opinion and therefore recommendation that the sintered silicon nitrides be emphasized in this program at this time. The final choice of material may be dictated by chemical reactions or other considerations and indeed any of several materials may ultimately be needed to handle the range of applications. Meanwhile the processing and fabrication requirements to successfully demonstrate the concept should be undertaken with a material which offers the most chance of success.

Extrusion is the process of choice for fabricating thousands of tons per year of many products in each of the three general classes of materials: ceramics, metals, and plastics. General criteria for choosing extrusion include: large length to cross section dimensions, generally hollow and/or

Table 1. Physical Properties of Some GE-SSL Sinterable Si_3N_4 Compositions

Designation	Composition in w/o before processing			Modulus of Rupture(a)		Density gm/cc	Young's Modulus
	Si_3N_4	Al_2O_3	AlN	Room T	1370°C		
GE-102	40	60	15	60,000 psi	24,000 psi	3.07	31.6×10^6 psi
GE-128	66	24	10.0	50,000 psi	27,500 psi	3.10	36.4×10^6 psi
GE 129(b)	88.7	8.0	3.3	50,000 psi	Not Tested	3.10	37.4×10^6 psi
GE 130(b)	94.5	4	1.5	50,000 psi	Not Tested	2.96	Not Tested

(a) Best values

(b) Determined by P. Land, AFML, to be published

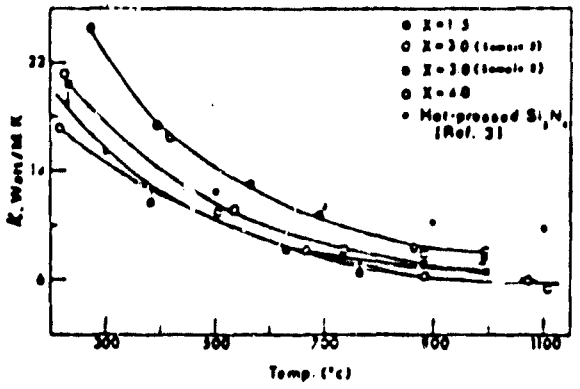

Figure 2. Thermal Conductivity of Hot Pressed Silicon Nitride and Selected $Si_{6-x}Al_xO_xN_{8-x}$ where x=1.5, 3 and 4 after Rao, Kokhtev and Lockman, "Electrical and Thermal Conductivities of Sialon Ceramics," Dept. of Materials Science and Eng., Univ. of Florida, Gainsville, Fla. 32611

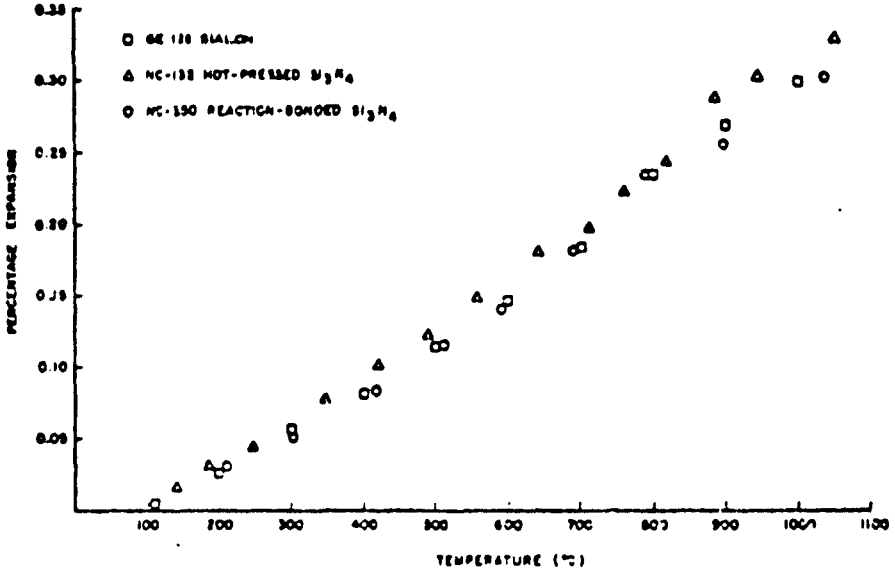

Figure 3. Thermal Expansion of GE-128 Sialon, Hot Pressed and Reaction Bonded Silicon Nitride

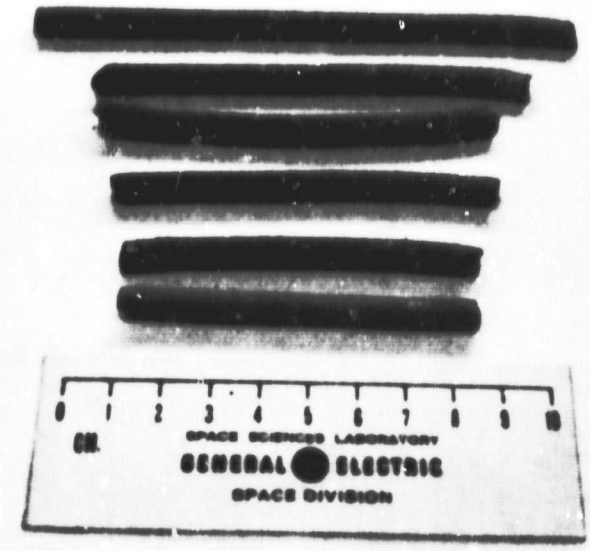

Extruded Tubing

Injection Molded Turbine Blade

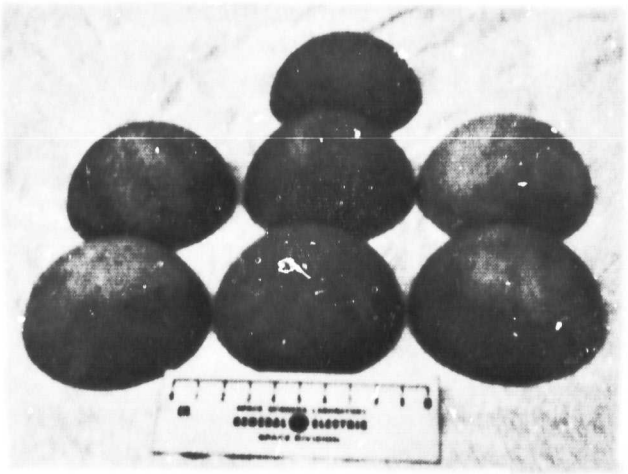

Slip-Cast Radome Shape

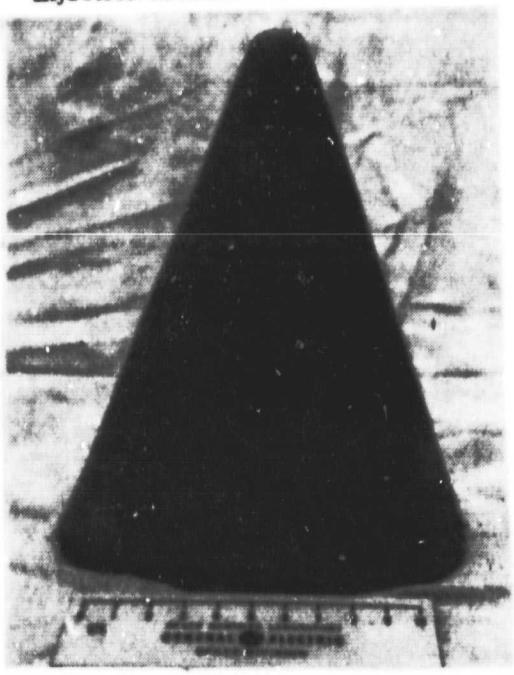

Jiggered Radome Shape

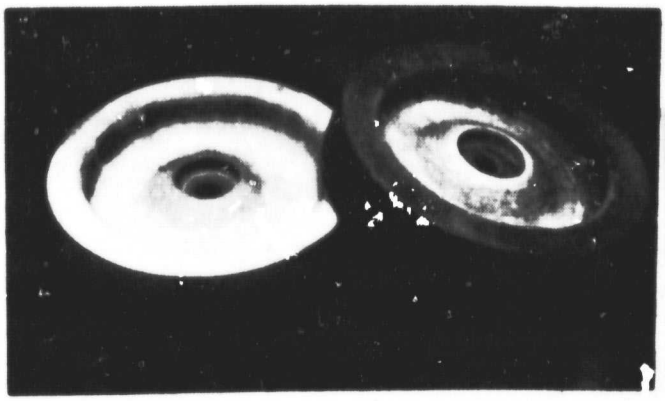

Hydro-pressed Piston Caps for 5-1/2" Dia. Diesel Engine Pistons

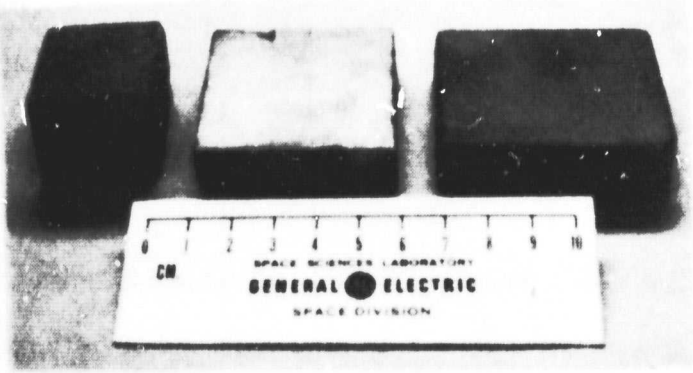

Pressed Block Shapes

Figure 4. Examples of Various Fabricated Shapes of Sinterable Si_3N_4

complex shapes having symmetry about at least one axis and, of course, a suitable relationship among the temperature, viscosity and pressure characteristics of the materials. In a few cases there are alternate forming methods available. Usually extrusion is less expensive, although it also usually produces somewhat less precise dimensions.

Among the common products made by this technique are: tubing, architectual trim such as of stainless steel, aluminum, and plastics, insulation on heavy wire and cable, common brick, sewer pipe, chimney liners, and furnace and thermocouple tubes. Machinery for extruding the heavy clay products (e.g. brick, sewer pipe and tile) are illustrated in Table 2 from the J. C. Steele & Sons, Inc. In addition there are many less common products and many variations of the basic process. Some examples of these include: a combination of extrusion and pulling on the product called pultrusion, some (but not all) glass drawing operations to make both simple sheet or tube shapes as well as more intricate shapes, and ceramic heat exchanger cores (that will be discussed in greater detail later) which in one process start with an extruded sheet which is then embossed with spacer legs followed by winding into a roll during which the spacers are bonded to the previous layer.

It should be mentioned that some of these products are produced in intermittent or batch operations and others are (or can be) in essentially continuous operation for up to several years. The resulting products can therefore be extremely long or cut to short lengths depending upon the end use, or shipping, or handling requirements. Wire and cable insulation, bricks, and glass tubing are among the examples of the long continuous extrusion processes even though the end products are cut (on the fly) to various lengths for handling etc, reasons. Some of these are illustrated

TABLE 2

PLUGGING AND DEAIRING EXTRUSION MACHINES

Separate Drive Machines

Pug Sealers and Extruders separately mounted in any of three different arrangements. Separate control of input just about eliminates over-filling of vacuum chamber. This advantage becomes tremendous during product changes. When extruding pipe, only the auger needs to start and stop. Pugging is more uniform with pug sealer running continuously. Total power required is divided.

	MODEL (Gearing)	CAPACITY U.S. BRICK PER HOUR	PRODUCT	POWER & MOTORS RECOMMENDED	AUGER SIZE & POINT DIAMETERS	PUG TUB SIZE & VOLUME	WEIGHT LENGTH TUB HEIGHT
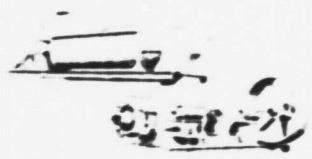	**50F** *Gearing Ex (A) P/S (A)	10M-17M	Brick Hollow Tile Drain Tile Pellets Sewer Pipe	EX. 150/200 HP P/S. 100/125 HP Both 720/750/ 900 RPM	16", 17" & (13") (11½"), 12", 14" & 16"	30" Dia. x 11'5" 64 cu. ft.	34,500 lbs. In-line 25'9" Ht. 10' Rtl. 18'10" Ht. 8'10"
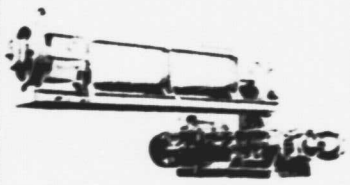	**75AD** *Gearing Ex (B) P/S (B) P/S (B)	15M-22M	Brick Hollow Tile Drain Tile Pellets Sewer Pipe	EX. 200/300 HP P/S. 150/200 HP Both to 1200 RPM	17" 14" & 16"	33" Dia. x 12' 81 cu. ft.	46,300 lbs. In-line 28'2" Ht. 10'3" Rtl. 16'10" Ht. 9'1"
	75AS *Gearing Ex (C) P/S (B) NOT SHOWN	15M-22M	Sewer Pipe plus brick and tile	EX. 200/250 HP (300) 720/750 RPM P/S. Same as AD	17" 14" & 16"	33" Dia. x 12' 81 cu. ft.	45,500 lbs. In-line 26'5" Ht. 11'1" Rtl. 16'9" Ht. 9'1"
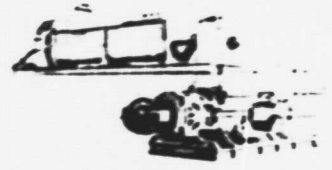	**90A/B** *Gearing 90AD Ex (B) 90BD P/S(B) 90BDV P/S(B)	18M-30M	Sewer Pipe Brick Hollow Tile Drain Tile Pellets	EX. 200/400 HP P/S to 300 HP BDV P/S to 300 HP	19¼" 18" (16")	36" Dia. x 13'6" 109 cu. ft.	71,100 lbs. In-line 31'10" Ht. 11'2" Rtl. 17'10" Ht. 9'10"

in Figures 5 and 6. More detailed discussion of some examples of these products are presented later in this memo.

Finally, a few caveats should be mentioned. In general, a more or less uniform cross section of material should be maintained in extrusion. It also helps to have symmetry about all axes of the cross section. There are certain limitations on the relationships among wall thickness, overall cross sectional size, and the radius to which the product can be later formed for any given material composition and condition. In general these caveats add up to indicating that extrusion is somewhat of an art which depends very strongly upon the skill and experiences of the designers and operators to make products successfully.

The preceding comments are broad, general, and based generally on less sophisticated materials and products than are needed here. They, along with our other knowledge of ceramics, lead us however to recommend a simple helical coil design for the solar receiver. Such a design should permit ease of fabrication, longer life, and lower cost than more complex designs. The primary design is therefore briefly reviewed next followed by some discussion of the current state of the art in the area of modern engineering ceramics. With some development effort, it appears likely that the current state of the art can be extended for making the tubes. Primary development effort is needed to achieve the size and shape of the desired helical coil and not to achieve the basic materials or processes which has already been accomplished.

Application to the High Temperature Solar Receiver

The proposed concept (No. 1) of a single helical coil of sintered silicon nitride (sialon) is a simple elegant design which has many virtues for the desired application. It minimizes joints, notches, small radii,

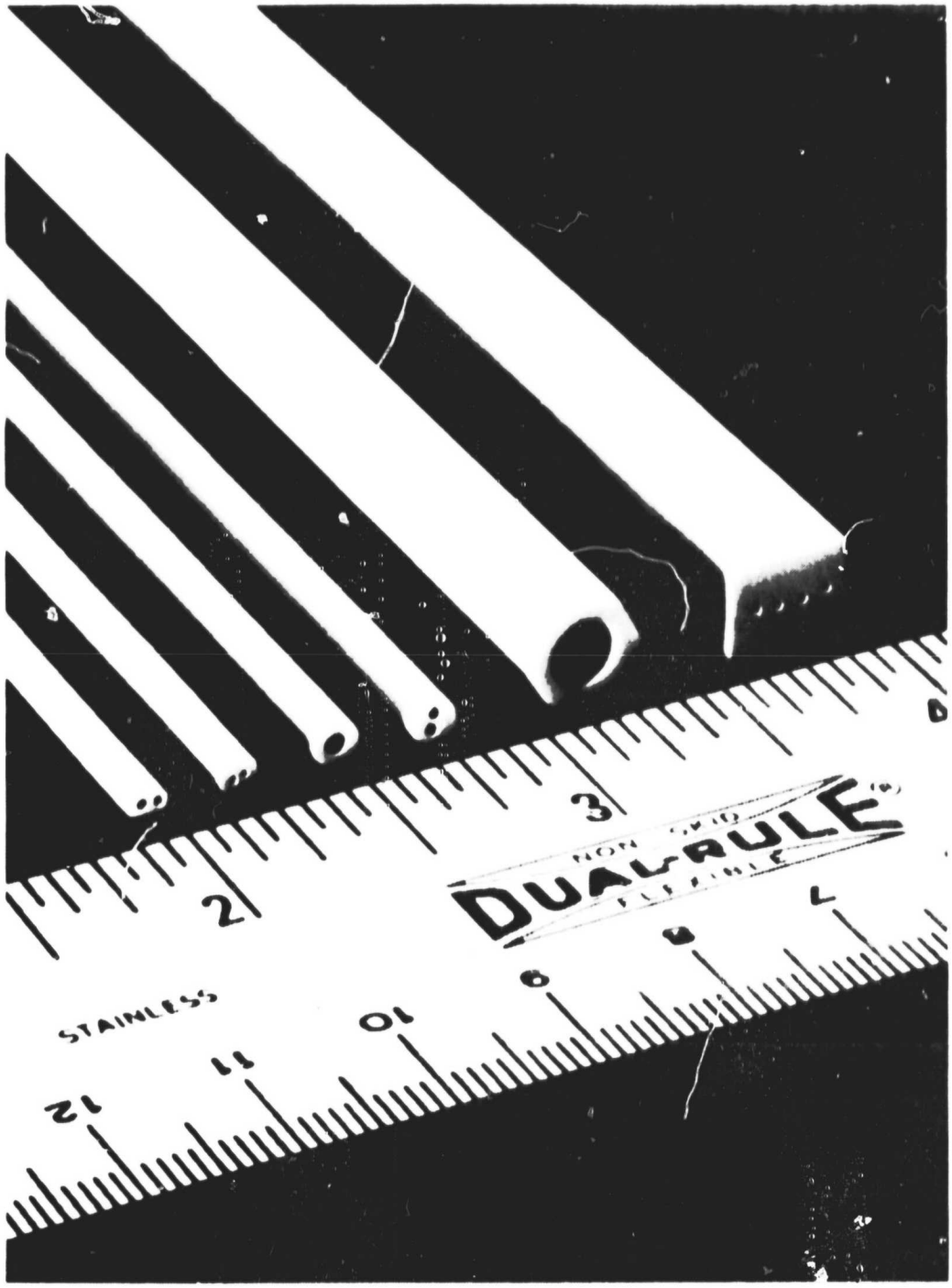

Figure 5. Extruded Thermocouple Tubing, Courtesy Coors Porcelain Co.

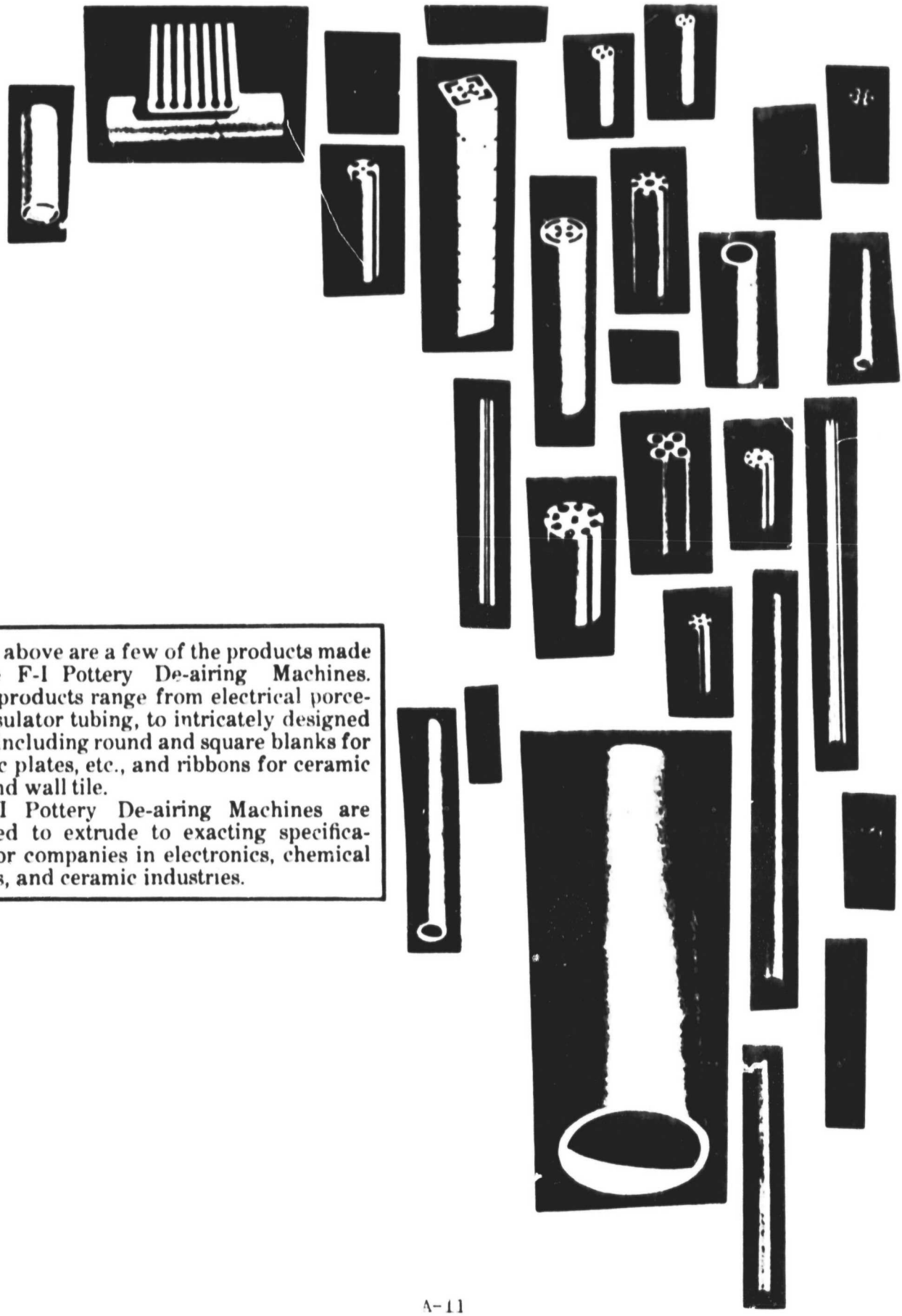

Shown above are a few of the products made by the F-I Pottery De-airing Machines. These products range from electrical porcelain insulator tubing, to intricately designed pieces including round and square blanks for ceramic plates, etc., and ribbons for ceramic floor and wall tile.
The F-I Pottery De-airing Machines are designed to extrude to exacting specifications for companies in electronics, chemical plastics, and ceramic industries.

Figure 6. Various Extruded Ceramic Shapes, Courtesy Patel International Div. of Plymouth Locomotive Works

etc. while providing freedom to expand and accommodate stresses which in many other designs would probably prove detrimental or even catastrophic for ceramic materials.

The obvious fabrication process is to extrude the silicon nitride powder, mixed with about an equal volume of organic binders, as a tubular shape, as was done on a small scale as shown in Figure 7. This would be done while the mixture is warm enough to provide ease of both extrusion and formability to coil the tubing into the desired helical shape on a mandrel, as illustrated in Figure 8. After cooling (and perhaps also drying) the internal mandrel would be removed and some external supports placed to hold the helix for firing while also permitting it to shrink the usual 15%-25%, as shown on Figure 9.

A typical size of product needed for this application requires on the order of fifty feet of two inch tubing wound into approximately an 18 inch diameter by three foot long helix. It is not the material or process but achieving this set of dimensions while maintaining the necessary properties which is beyond the state of the art.

State of the Art

Some examples of the state of the art, to be described here, suggest that a foundation exists on which to develop the necessary skills to produce the desired large helical tube.

1. Lucalox lamp tubes. These tubes are extruded continuously of very high quality alumina with about a 3/8" dia. and about 30 mil walls as shown in Figure 10. They are cut into 30" lengths for firing and later cut to about 5" lengths for use in very high efficiency lamps. In the lamps, they serve as pressure vessels for sodium vapor at temperatures to about 1250-1300° C. The demonstrated long life (15,000 + hours)

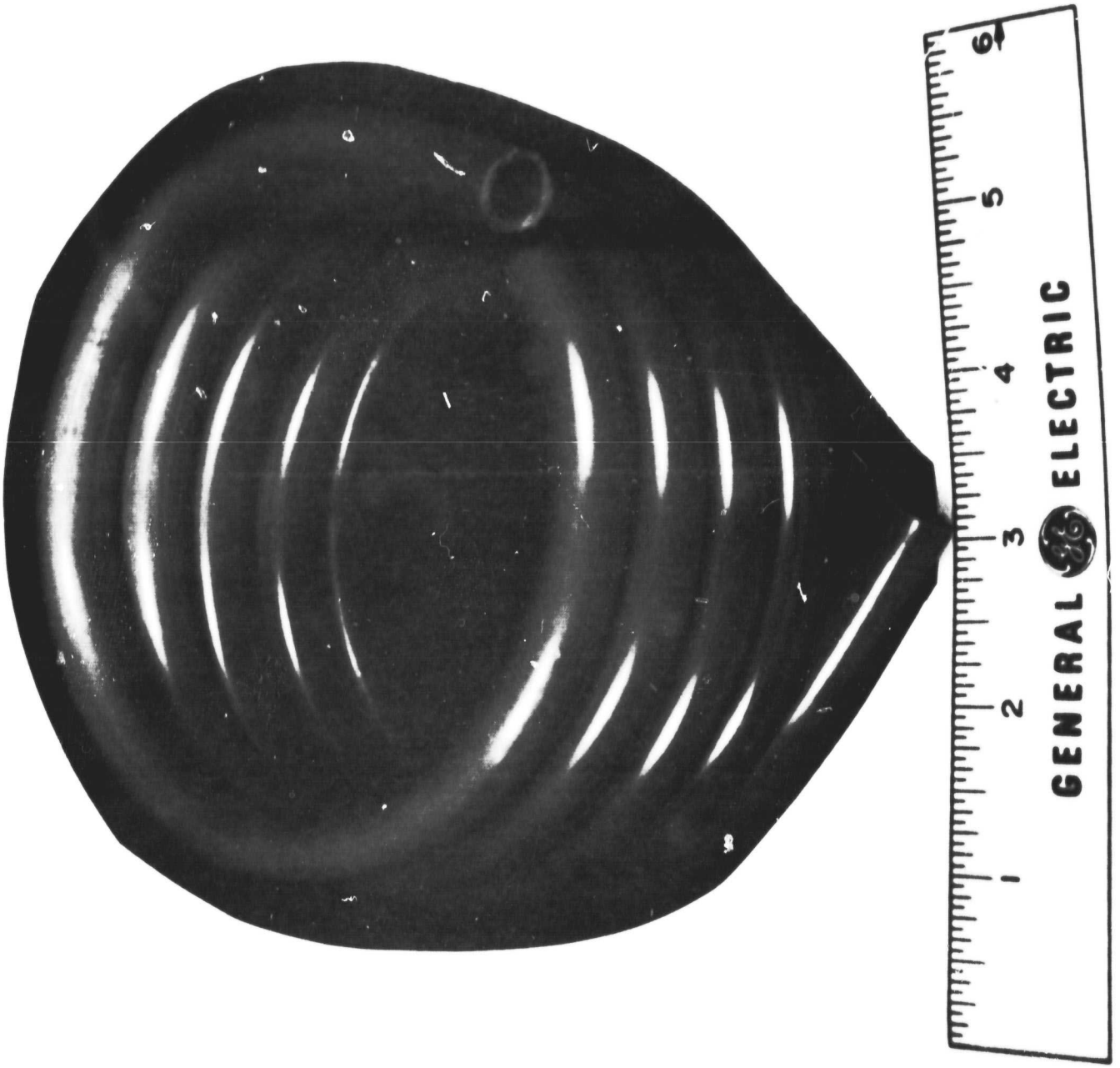

Figure 7. Sintered Silicon Nitride Tubing as Extruded with about 50% Wax Binder.

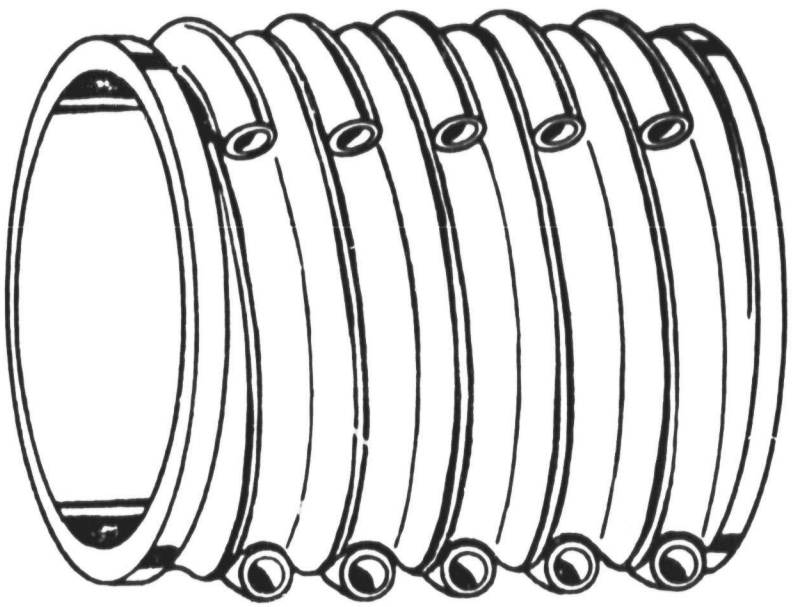

Figure 8. Schematic Arrangement of Mandrel for Winding Soft Extruded Tubing into a Helical Coil. The Mandrel would be Segmented to Permit its Removal

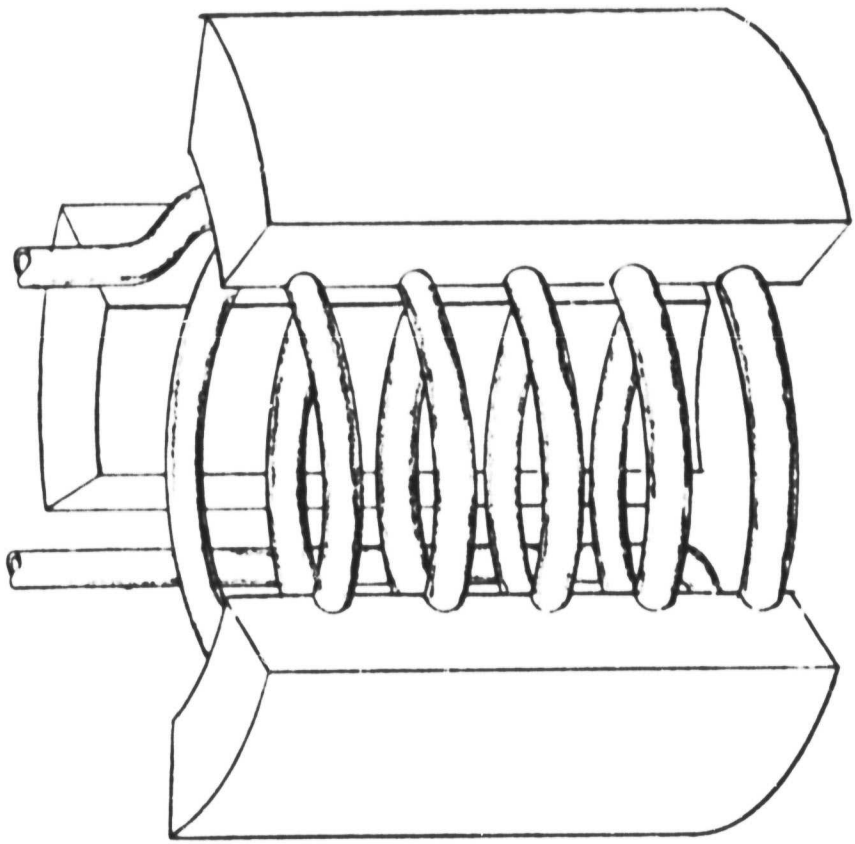

Figure 9. A Method for Supporting the Coil During Firing Is Suggested in This Figure. The Supports Would Be Made of Graphite with Deep Enough Slots to Permit Shrinkage of the Tube While Still Supporting it.

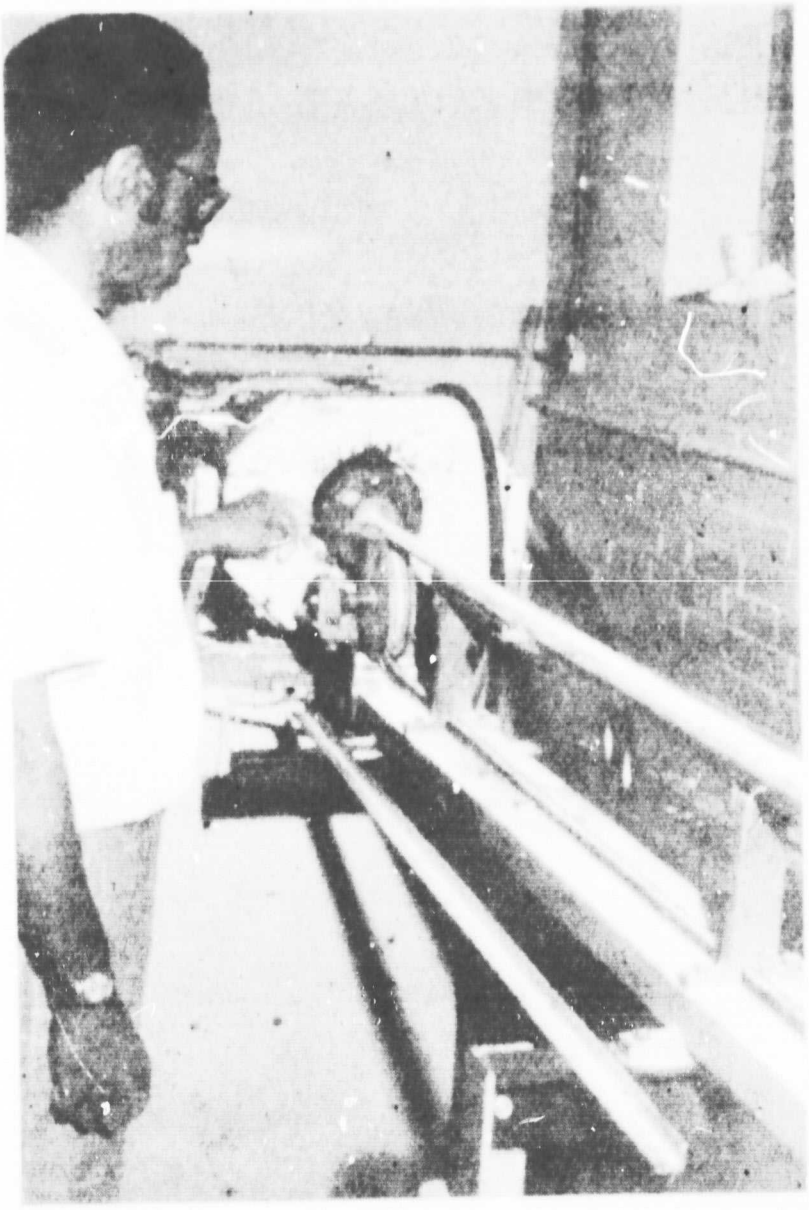

Figure 10. Extrusion of Lucalox(R) Tubing.

of demanding service with a very high degree of reliability certainly qualifies them for listing as an application of a modern engineering ceramic material and process.

2. Ceramic Regenerator Heat Exchanger Cores. Several processes are used to make these cores including: extrusion, extrusion followed by calendaring and/or embossing and by an impregnated paper process (ala corrugated paper) which is now less favored. A quadrant of a heat exchanger and several views related to the processing and resultant products as shown as Figures 11-15. In the Coors process, long strips (typically 1300' for an 18" wheel and 2600' for an 25" wheel) or organically bonded ceramic powders are formed into a tightly wrapped helical wheel so as to provide many small (500-1000/sq in.) gas passages parallel to the axis of the wheel. The wheels are typically about 18-28" dia x 2-3" thick (or long) for automobile gas turbine applications. Materials are primarily low expansion oxides such as beta spodumene and cordierite which are lithium aluminum silicate and magnesium aluminum silicate, respectively. The heat exchanger wheels are fired to around 1400° C then finished machined and fitted with a ring gear to drive them. This heat exchanger is then an extremely important component for recovering waste heat in industrial applications and for possible gas turbine powered autos. In the latter application, a goal for the life of the heat exchanger is 3500 hours at a nominal 30 rpm with as much as 1000° F temperature differential across it. This calculates to over 6×10^6 thermal cycles and life tests have already indicated that over 10,000 hours or about 18×10^6 cycles are possible. Our role over the past four years on this field has been to develop more corrosion resistant materials

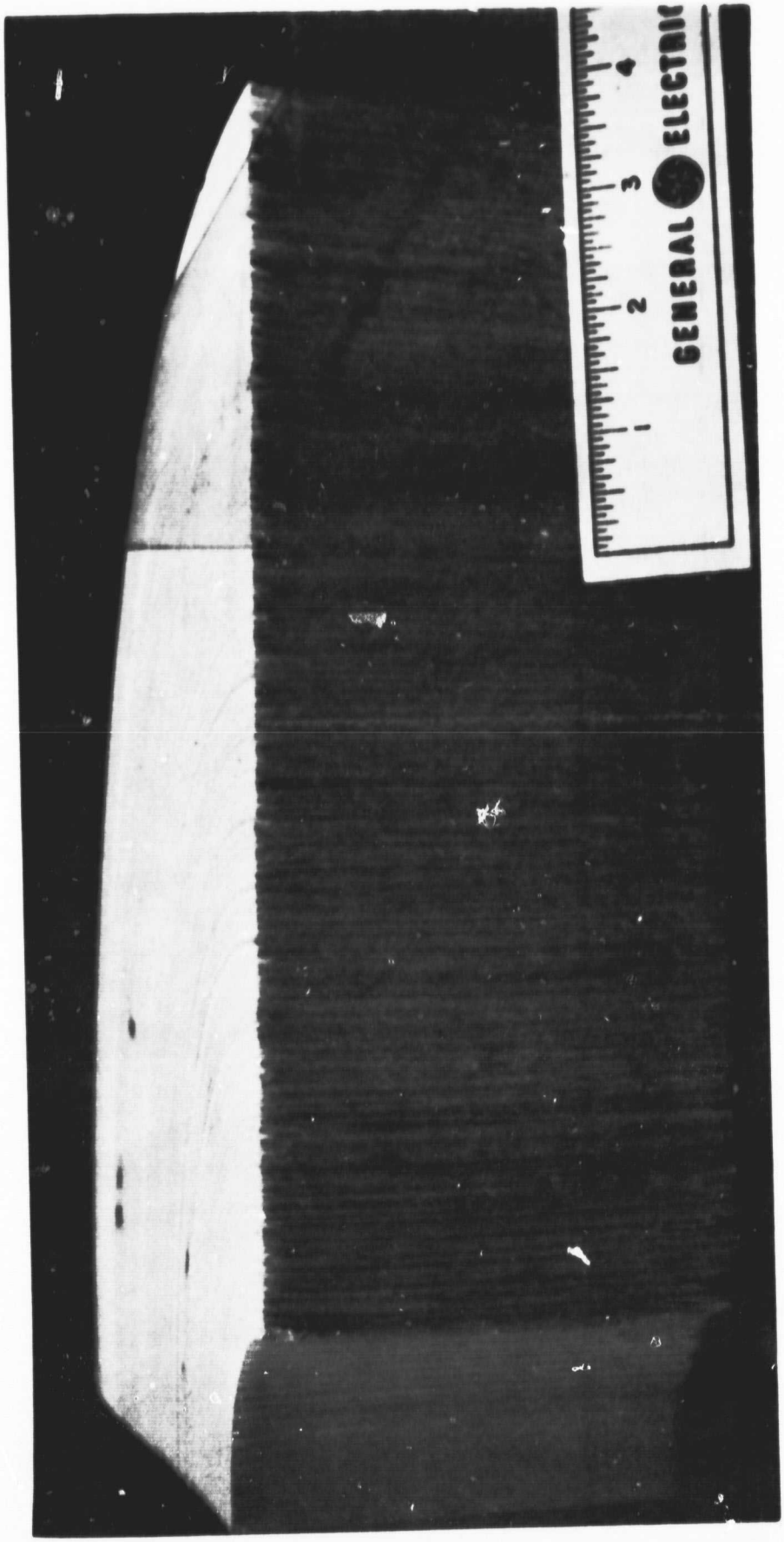

Figure 11. Untrimmed Quadrant of an Automotive Gas Turbine Heat Exchanger Core Made of GE Developed Materials by Coors Porcelain Co., using the Process Illustrated in Figure 12 to Provide the Cross Section Illustrated in Figure 13.

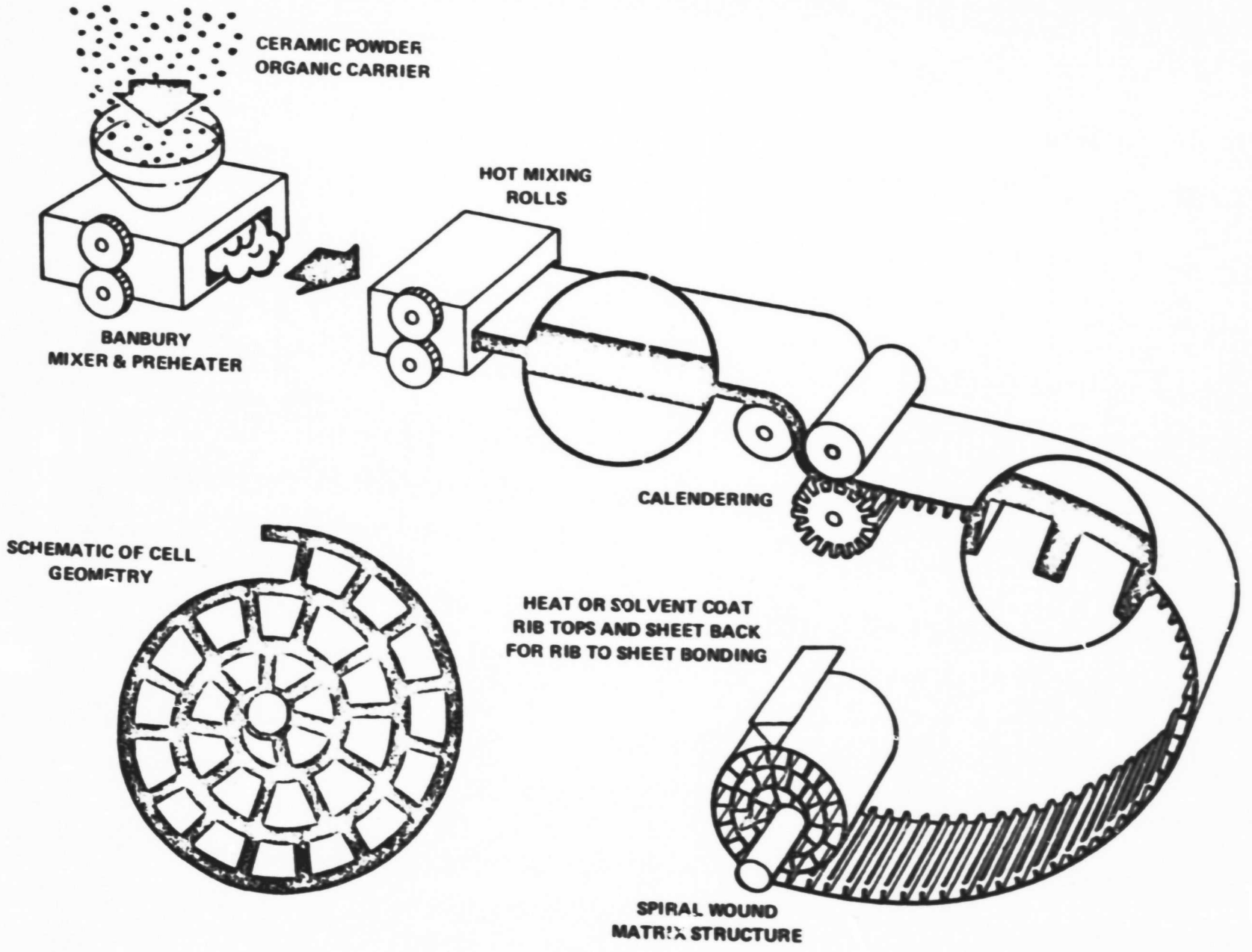

Figure 12. Typical Extrusion and Embossing Operation for Making Honeycomb Ceramics by Coors Porcelain Co. to make Products Illustrated in Figures 11 and 13.

Figure 13. Enlarged Cross Section of Honeycomb

ORIGINAL PAGE
BLACK AND WHITE PHOTOGRAPH

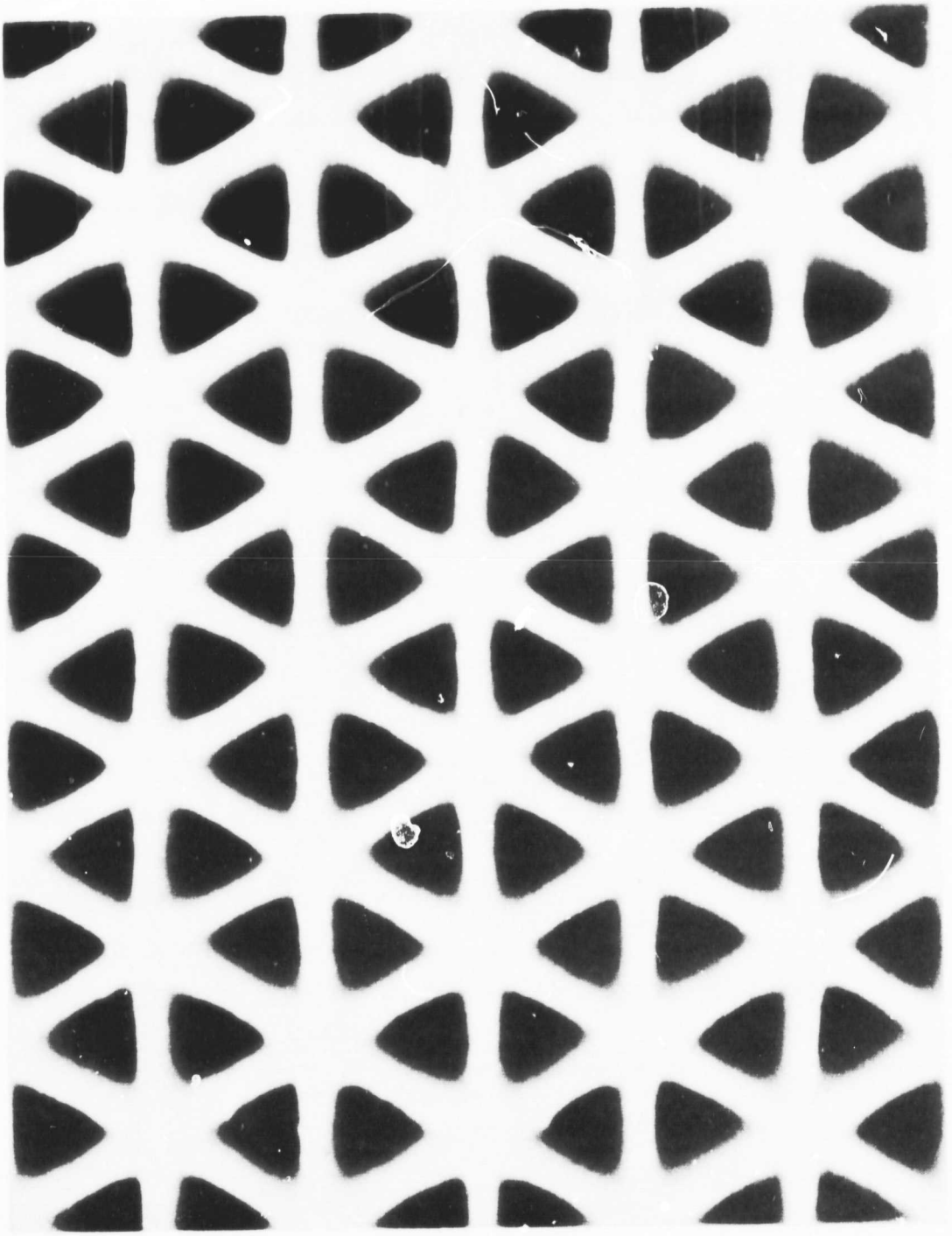

Figure 14. GE 3200 NGK-Extruded Fired at 1200°C (12X)

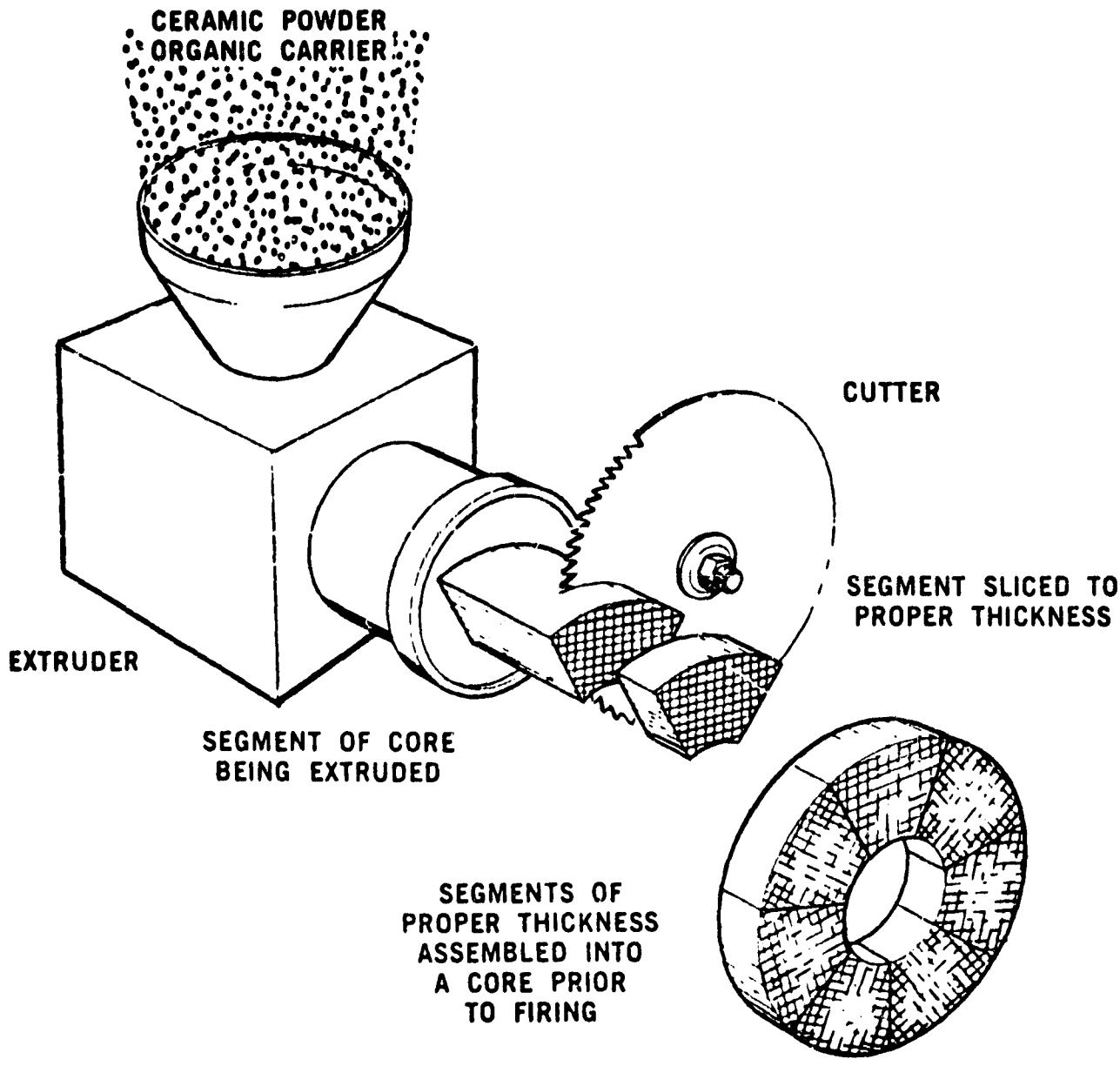

Figure 15. Typical Extrusion Operation for Making Honeycomb Ceramics

applications, some typical products from Norton Co. which are at the limits of the current state of the art are: (1) tubes having up to a 6" diameter by about 100" length and (2) combustors about 12-14" dia. x 30" long with one end closed. In more complex units smaller dimensions have been fabricated for example, a 30" high heat exchanger consisting of 10 - 1" dia. partially finned "U" tubes connected to 2 - 4" dia. plenum tubes. Efforts are underway to make larger parts and to develop both mechanical and chemical (braze) bonds for assembling large components.

A ceramic recuperator development, Phase I program has just been completed in our laboratory for NASA-Lewis.* It was aimed at demonstrating the initial feasibility of fabricating a recuperator for an advanced Stirling cycle powered auto. The recuperator is to recover waste heat at 1370°C (2500°F) and to be made of our sintered silicon nitride in a configuration illustrated in Figures 16 & 17. The initial design of the small exhaust gas tubes was triangular as indicated in Figure 16. This was later changed for case of fabrication to the more rectangular shape shown in Figure 17 along with some of the design parameters for this recuperator. This program was unfortunately cancelled for the convenience of the government during the first phase but it was sufficiently complete to indicate that (1) the tubes can be extruded and fired (2) they can be assembled into modules using a glass brazing material and (3) that the basic silicon nitride materials are resistant to corrosion by some salt and sulfur compounds associated with automotive operations. A final presentation was recently made at NASA-Lewis and a final report is in preparation.

*Ceramic Recupertor Fabrication Technology, Contract DEN 3-54 for NASA-Lewis Research Center

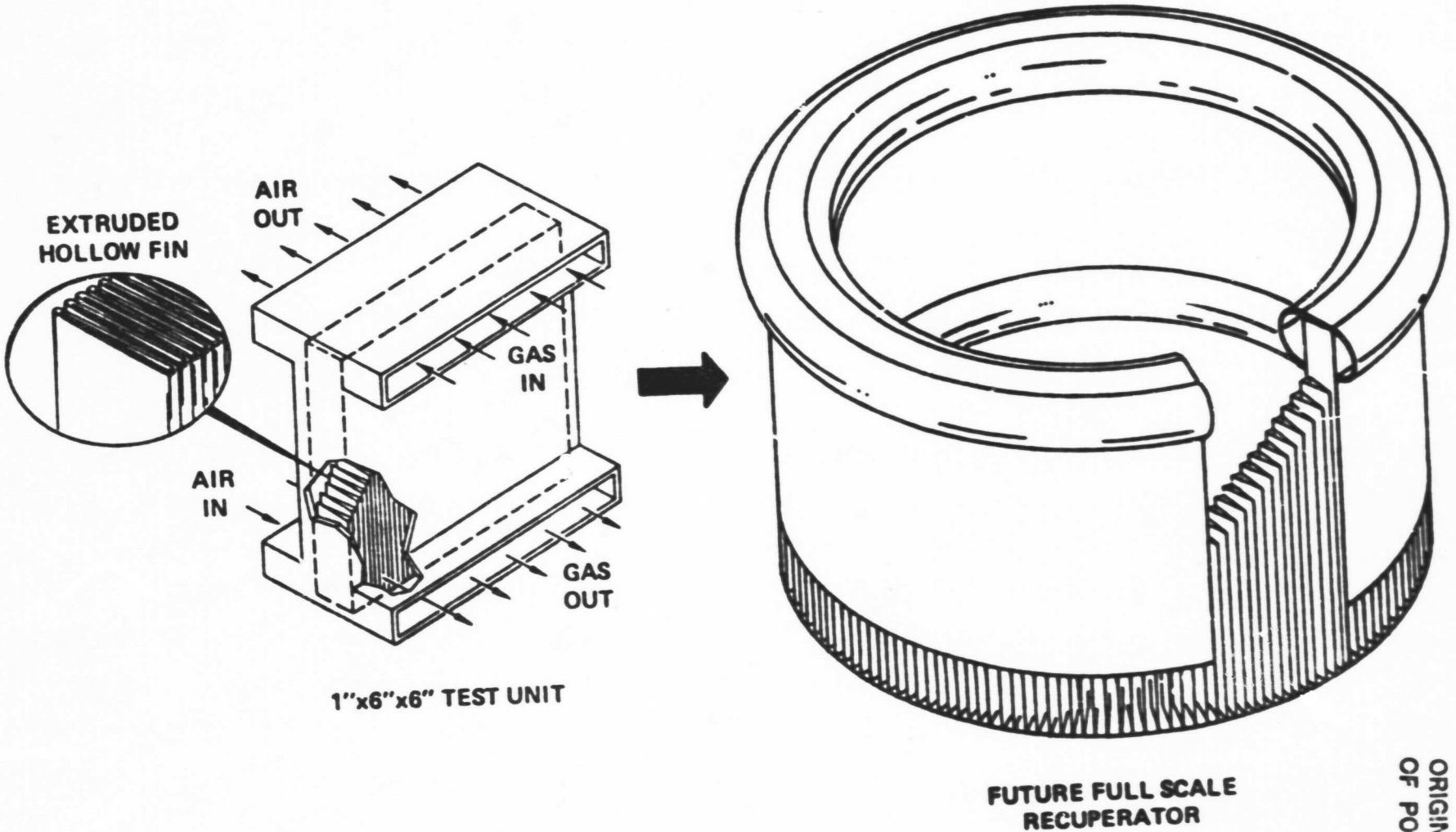

Figure 16. Sintered Silicon Nitride Recuperator Component Module, and Future Full Scale Design Concept.

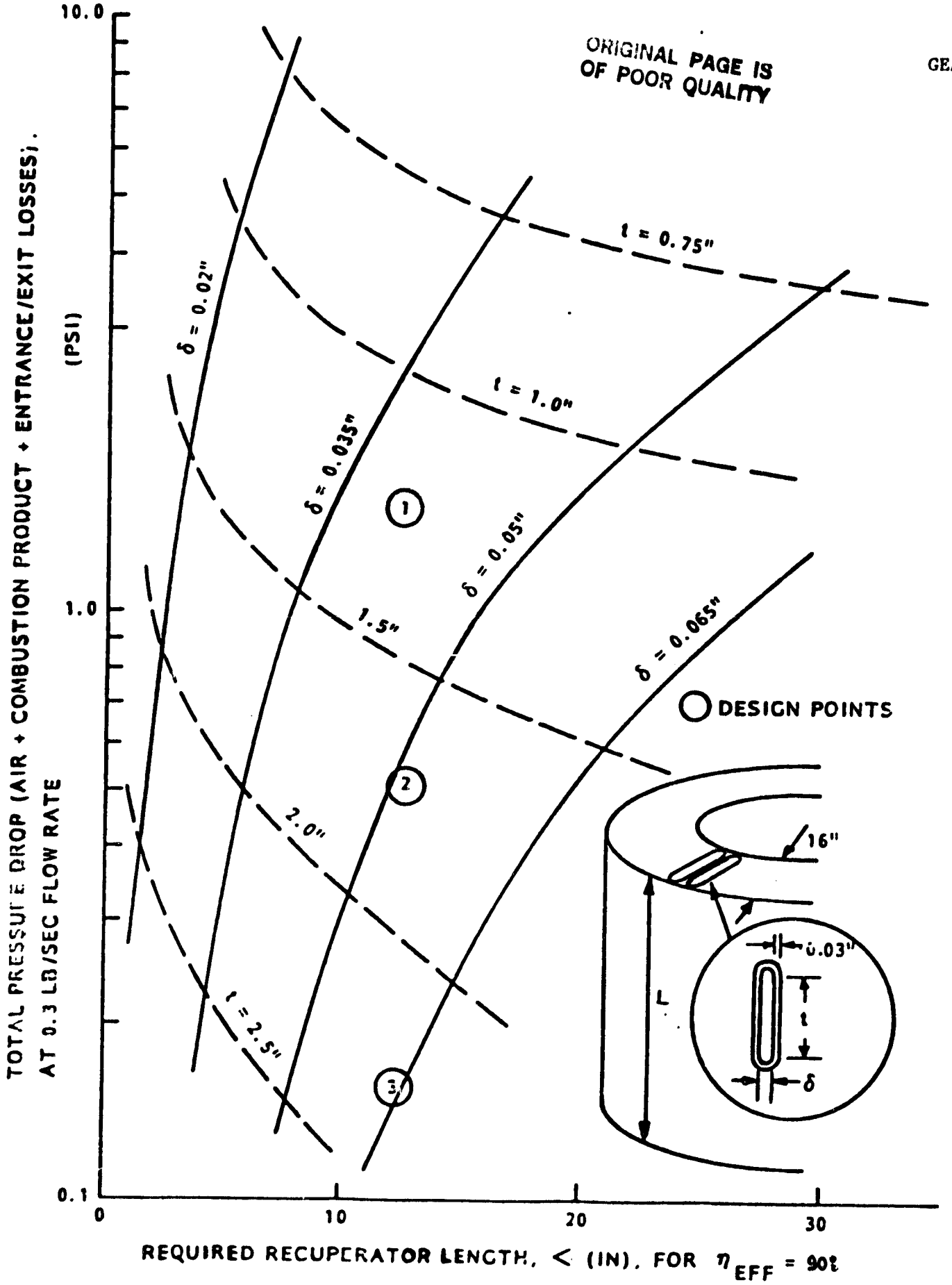

Figure 17. The Final Design of Exhaust Gas Tubing (Except for a Mid-Span Web) is shown Along with Some Design Parameters

Conclusions

The state of the art for making large helical coils of ceramic tubing does not yet include the sizes of interest to this program. It is furthermore, possibly a subjective matter of opinion as to the feasibility of accomplishing the task. It is then the author's opinion that with suitable development effort the goal can be accomplished and that it is well worth doing as compared with alternate approaches. His opinion is also supported by experienced senior technical personnel at four of the leading producers of these products (Norton Co., Coors Porcelain Co., and the Quartz and Chemical Department and the Carboloy Department of General Electric Co.

It appears that an acceptable definitive proof of concept will have to come from experimental demonstrations of the materials and processes for the design being proposed rather than simply from opinions. One way of proving the feasibility of this concept is a multi-step series of demonstrations and tests of the product be carried out over about a 12 - 18 month time period as follows:

1. Extrude several 10' lengths of 1/2" sialon tubing and form them into 6" dia. x 6" high helical coils for processing studies. In parallel make some additional similar but shorter tubes for mechanical testing and for joining development and tests.

2. Upon successful completion of the above work, scale up the fabrication tests to make several 20-25' lengths of 1" dia. thin wall sialon tubing into 12-15" dia. x 12-15" high helical coils primarily for processing studies but to include mechanical testing and general characteristics.

3. Finally scale up the process to the final size of helical coil chosen for the program for a demonstration of feasibility and for final proof of concept tests.